Stratigraphic and tectonic framework of Late Cretaceous and Paleogene strata of southern Aotea Basin, northwest New Zealand

by

Callum Skinner

A thesis submitted to Victoria University of Wellington
in partial fulfilment of requirements for the degree of
Master of Science in Petroleum Geoscience

School of Geography, Environment and Earth Science

Victoria University of Wellington
2019

Abstract

Seismic reflection data reveal thick sediment sequences of Late Cretaceous to Paleogene age in the region northwest of Taranaki Basin. A new stratigraphic framework for latest Cretaceous and Paleogene strata is created based on stacking patterns and stratal termination relationships of seismic reflectors. Sequence-bounding reflectors are tied to petroleum exploration wells, including recently-drilled Romney-1, to assign age and paleoenvironment interpretation. I identify the following sequences: (1) a late Haumurian to Teurian (68 – 56 Ma) aggradational shelf sequence, with at least two regressional events linked to eustatic sea-level falls; (2) a diachronous deepening of the basin that progressed from north to south during the late Waipawan to Heretaungan (53 – 46 Ma); (3) small-scale volcanism at the southern boundary with Taranaki Basin is contemporaneous with this deepening; (4) a prograding delta on Challenger Plateau during the Porangan to Runangan (46 – 35 Ma) that is evidence for tectonic uplift of the basin margins; and (5) an onlapping sequence from latest Runangan to present (35 – 0 Ma) that indicates Challenger Plateau subsided 1,300 m. A revised set of paleogeography maps and generalised stratigraphic chart summarise these observations. The Eocene phase (52-46 Ma) of tectonic subsidence and diffuse volcanism is one of the earliest signs of tectonic activity associated with development of the Cenozoic plate boundary through New Zealand. Petroleum system analysis reveals that southern Aotea Basin is prospective for petroleum exploration, with 3 plays identified in the Late Haumurian to Teurian (79 – 56 Ma) strata, in spite of Romney-1 proving unsuccessful.

Acknowledgements

I would like to acknowledge and thank Rupert Sutherland for his guidance, patience and invaluable reviewing of this thesis. Hannu Seebeck and Damian Orr for their useful discussions and feedback. Aleksandr Beliaev for his technical support. The Ministry of Business, Innovation and Employment for access to the '2018 Block Offer Data Pack'. Seisware for the provision of an academic license. Sarah Lomas and Jeannette Walker for the flexibility in employment to undertake this thesis. But mostly I would like to thank my wife, Dana, for her unwavering support and encouragement, and my daughter, Imogen, for being a happy, chatty baby who (mostly) slept well at night.

Contents

List of Figures

List of Tables

1 Introduction

A major reorganisation of tectonic plates and their motion occurred in the western Pacific during the Early to Middle Eocene: Hawaii-Emperor bend (O'Connor et al., 2013), Izu-Bonin-Mariana subduction initiation (Arculus et al., 2015, Ishizuka et al., 2011), and cessation of Tasman seafloor spreading (Gaina et al., 1998). In New Zealand, there is limited evidence for this reorganisation. Rifting of Emerald Basin south of New Zealand initiated at ~45 Ma (Sutherland, 1995), and contraction and uplift in Reinga Basin started at ~39 Ma (Bache et al., 2012b, Sutherland, 2019). During initiation of the Australia-Pacific plate boundary, the pole of rotation for the Australia-Pacific plate boundary was located near North Island, explaining the low tectonic rate and spatial transition from rifting to convergence (King, 2000b, Sutherland, 1995). Aotea Basin is northwest of North Island beneath the New Caledonia Trough (Exon et al., 2007). Using high quality regional 2D seismic reflection data and the recently drilled Romney-1 exploration well, I construct a Late Cretaceous and Paleogene stratigraphy and document signals of initiation and evolution of Tonga-Kermadec subduction.

Taranaki Basin has a long history of petroleum exploration and exploitation. In 1864 the first petroleum well, Alpha-1, was drilled on the New Plymouth foreshore. Offshore exploration in 1969 led to discovery of the Maui gas-condensate field (Skinner, 2008). As deep-water drilling technology advanced, interest in adjacent basins increased and seismic reflection data were acquired, followed by drilling of Waka Nui-1 (1998) and Romney-1 (2015) exploration wells. The southern Aotea Basin and its margins are now covered by ~28,000 line km of high quality 2D seismic reflection data, and penetrated by five petroleum wells (Figure 1).

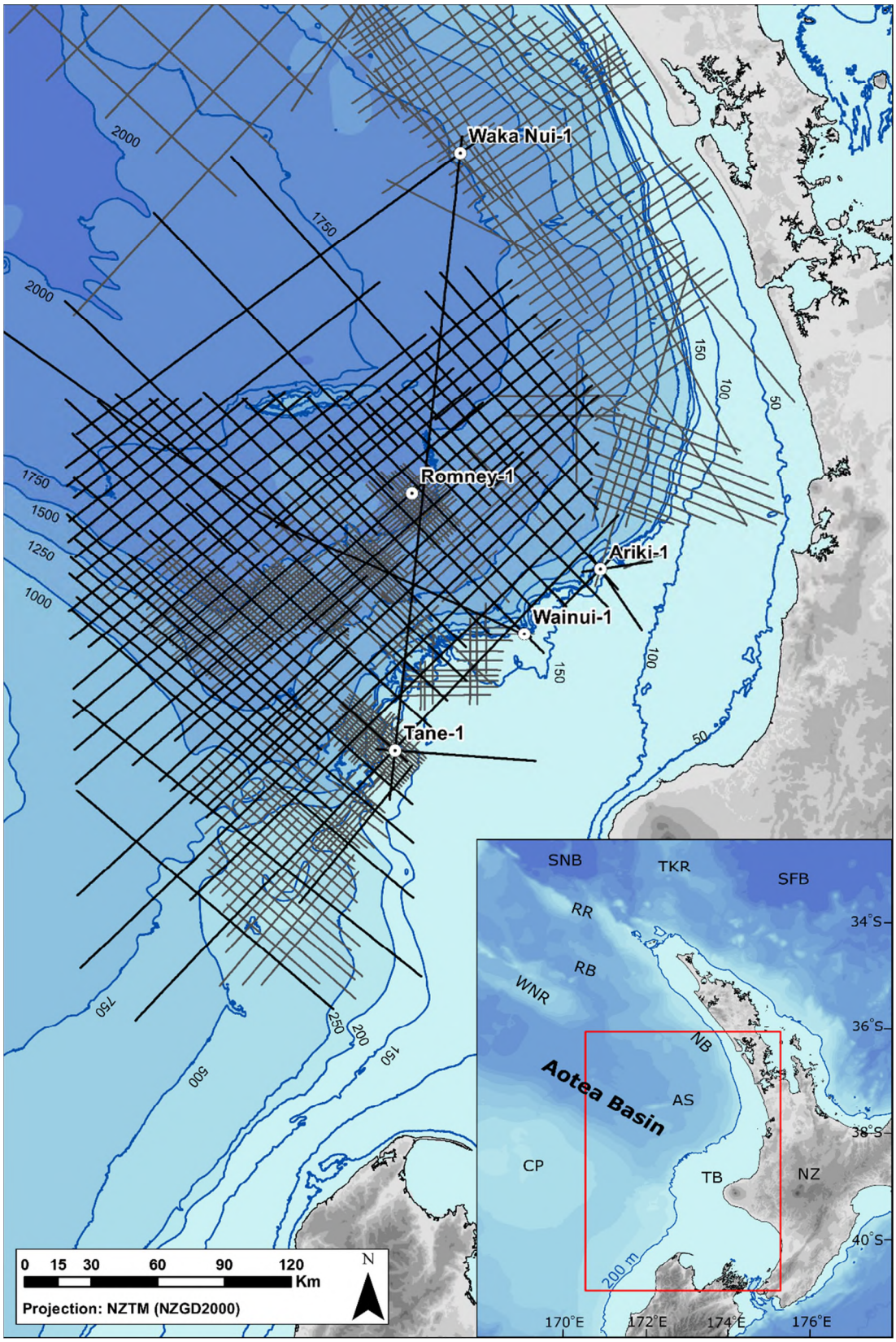

Figure 1. *Aotea Basin bathymetric map (Mitchell et al., 2012), along with data used for this study, and insert showing relationship of study area to northwest New Zealand. Seismic lines are shown as black (interpreted) and grey (available) lines. Petroleum wells are represented by black and white circles. Insert: 200 m contour represents shelf break. AS. Aotea Seamount, CP. Challenger Plateau, NB. Northland Basin, NZ. New Zealand, TB. Taranaki Basin, TKR. Three Kings Ridge, RB. Reinga Basin, RR. Reinga Ridge, SFB. South Fiji Basin, SNB. South Norfolk Basin, WNR. West Norfolk Ridge.*

The study area is west of North Island, New Zealand, and covers ~85,000 km^2 that includes southern Aotea Basin and the western margins of Taranaki and Northland basins, and the northern flank of Challenger Plateau (Figure 1). The Cretaceous to Holocene sedimentary sequence in Aotea, Northland and Taranaki basins represents a first-order transgressive to regressive megasequence (King, 2000a, King and Thrasher, 1996, Mortimer et al., 2014, Baur et al., 2014, Bache et al., 2012a, Bache et al., 2012b). Southern Aotea Basin has been referred to as "Deepwater Taranaki" (Uruski, 2007, Uruski and Wood, 1991, King and Thrasher, 1996, Strogen et al., 2017), but I adopt the definition of Aotea Basin provided by Exon et al. (2007) and Collot et al. (2009). For the sake of brevity, southern Aotea Basin will simply be referred to as Aotea Basin in this thesis.

I construct a hierarchal seismic stratigraphic framework, based on reflector stacking patterns and terminations, using principles of Vail et al. (1977), Mitchum Jr and Vail (1977), Neal and Abreu (2009), Catuneanu et al. (2011), and Allen and Allen (2013). Sequence-bounding reflectors are tied to five petroleum exploration wells, which I reanalyse: check-shot data, lithology, biostratigraphy, and wireline geophysical logs. The integration of seismic reflector interpretation with age and paleoenvironmental data from wells, is used to construct a general stratigraphic chart and paleogeographic maps from latest Cretaceous to earliest Miocene. I also present a petroleum systems assessment.

2 Geologic Setting

2.1 Introduction

The Cretaceous to Holocene sedimentary sequence in Aotea, Reinga, Northland and Taranaki basins records five tectonic phases that affected northwest Zealandia: rifting, passive margin transgression, plate boundary initiation, drowning, and regressive prograding shelf (King, 2000a, King and Thrasher, 1996, Mortimer et al., 2014, Baur et al., 2014, Bache et al., 2012a, Bache et al., 2012b, Isaac, 1994). Appendix 1 contains a copy of the New Zealand Geological Timescale, it is this timescale by Raine et al. (2015) that is referenced throughout this thesis.

2.2 Basement

Acoustic basement in Aotea, Reinga and Taranaki basins, consist of Palaeozoic to Mesozoic volcanic and sedimentary terranes associated with subduction along the Gondwana margin and Median Batholith plutons (Mortimer, 2004, Mortimer et al., 2014, King and Thrasher, 1996, Bache et al., 2014). The variability of the basement is demonstrated by Sutherland (1999) using magnetic data and by penetration of basement by wells Waka Nui-1, Ariki-1, Wainui-1 and Tane-1, which sampled Murihiku Supergroup, Brook Street Volcanics, Takaka Terrane, and Separation Point Batholith, respectively (SBPT, 1984, SBPT, 1982, SBPT, 1977, Milne and Quick, 1999).

2.3 Rifting

Subduction along the Gondwana eastern margin halted between 105 – 100 Ma (Davy et al., 2008, Matthews et al., 2012). The cessation in subduction was followed by widespread rifting across northwest Zealandia, resulted in formation of northwest striking grabens and half-grabens that are recognised in seismic reflection data at the base of Aotea Basin (Collot et al., 2009, Strogen et al., 2017, Uruski and Wood, 1991), Reinga Basin (Bache et al., 2012b,

Herzer et al., 1997) and Taranaki Basin (King and Thrasher, 1996, Strogen et al., 2017). Te Ranga-1

penetrated this sequence along the eastern margin of Taranaki Basin, and found it to consist of Ngaterian (99 – 92 Ma) coal measures (King and Thrasher, 1996). The syn-rift sequence hasn't been intersected in Reinga Basin, but is inferred to consist of the same aged coal measures (Herzer et al., 1997).

Romney-1 terminated in the syn-rift sequence in Aotea Basin, consisting of Teratan to Piripauan (90.5 – 83.6 Ma) marginal to shallow water marine facies (Strogen et al., 2017). Seismic data indicate the syn-rift sequence includes a further 1 – 1.5 s two-way-time (TWT) thick prograding clinoform shelf sequence that have not been penetrated (Sutherland et al., 2010, Uruski, 2007, Uruski and Warburton, 2010, Collot et al., 2009, Strogen et al., 2017) .

Widespread northwest striking rifting ceased in the Early Haumurian (83 Ma), in northwest Zealandia (Laird, 1993, Strogen et al., 2017, Mortimer et al., 2014).

2.4 Passive margin transgression

Opening of the Tasman Sea in the Early Haumurian (83 Ma) led to northwest Zealandia becoming a passive margin (Sutherland, 1999, Gaina et al., 1998). Thermal subsidence was manifest as a transgressive sequence of fluvial to shallow marine to shelfal environments, and finally bathyal sediments were deposited (Herzer et al., 1997, Uruski and Warburton, 2010, King and Thrasher, 1996, Bache et al., 2012a). Transgression progressed from north and west to south and east, and led to outboard areas of Taranaki and Aotea basins experiencing bathyal environments from the Early Eocene (56 Ma) (King and Thrasher, 1996, Strogen et al., 2017, Arnot and Bland, 2016).

2.5 Plate boundary initiation

A reconfiguration of plate motion in the southwest Pacific and initiation of the Australia-Pacific plate boundary during the Porangan stage (45 – 43 Ma), in northwest Zealandia led to convergent deformation and in south Zealandia led to rifting of the Emerald Basin (Sutherland et al., 2017, Sutherland, 1995, Wood et al., 1996).

Plate convergence and subsequent subduction are inferred to have progressed from north to south during the middle to late Eocene (Baur et al., 2014, Sutherland et al., 2017). Obduction of ophiolitic nappes in New Caledonia at 44 – 34 Ma, is evidence of convergence (Aitchison et al., 1995, Collot et al., 2009). In Reinga Basin, contraction of strata and uplift of Reinga and West Norfolk ridges occurred after 48 – 43 Ma and before 36 – 30 Ma (Bache et al., 2012b, Sutherland et al., 2017). Bache et al. (2012a), show that deformation in Reinga Basin decreased in intensity from north to south. In Taranaki Basin, the Taranaki Fault System initiates along ~400 km of strike in the Bortonian (43 – 40 Ma), and is considered to be an antithetic thrust fault to the subducting Pacific Plate in the Tonga-Kermadec subduction zone (Stagpoole and Nicol, 2008). However, in Taranaki Basin only minor compression is recognised in latest Eocene strata as growth on the Mania, Kapuni, Stratford, and Inglewood structures (King and Thrasher, 1996, King, 2000b). Sutherland (1995) demonstrated that the pole of rotation for the Pacific Plate was proximal to Taranaki Basin, hence, minimal deformation occurred. In Aotea Basin, evidence for late Eocene folding or slumping is described by (Uruski, 2008) and Baur et al. (2014), but is only visible on one seismic line (DTB01-04).

2.6 Drowning

The Oligocene sequence in Taranaki Basin, is marked by a basal unconformity absent of latest Eocene and Early Oligocene (34 – 27 Ma) strata, and a change from clastic fluvial and shallow marine facies to carbonate rich mudstones and limestones deposited in a bathyal environment (King and Thrasher, 1996). Stern and Holt (1994) show through paleobathymetric curves that platform subsidence occurred in the Waitakian to early Otaian (25 – 18 Ma) in southern Taranaki Basin. In Reinga Basin, subsidence of wave cut platforms on Reinga Ridge and West Norfolk Ridge have subsided > 1 km since the Runangan (36 – 34 Ma) (Bache et al., 2012a, Bache et al., 2012b, Sutherland et al., 2017). In Aotea Basin, an unconformity from 43 – 27 Ma was identified by Collot et al. (2009), and Baur et al. (2014) model >1 km of platform subsidence since this time.

2.7 Regressive prograding shelf

The Australia-Pacific plate boundary propagated southward as subduction of the Pacific plate under proto North Island connected with dextral transpression along the Alpine fault through proto South Island during the late Oligocene (King, 2000b). Convergence led to emplacement of the Northland Allochthon (Herzer, 1995, Isaac, 1994).

During the Miocene, convergence across major crustal faults, e.g. Taranaki Fault and Alpine Fault, led to uplift and erosion of the hinterland (King and Thrasher, 1996, King, 2000b, Stagpoole and Nicol, 2008). The products of this erosion were deposited in southern Taranaki Basin initially and, have prograded north and west to form the present-day shelf (King and Thrasher, 1996, King, 2000b).

3 Seismic

3.1 Data

3.1.1 Introduction

All reflection 2D seismic data were sourced from the Ministry of Business, Innovation and Employment's 'Online Exploration Database' and the '2018 Block Offer Data Pack' (www.nzpam.govt.nz). These data were loaded into the seismic interpretation package Seisware^{TM} 10.0, for quality control (QC) and interpretation.

Seismic reflector profiles from ten multi-channel 2D seismic surveys, totalling ~28,800 line km and covering ~85,000 km^2 in the study area (Figure 1) were used in the interpretation. Table 1 summarises the general acquisition parameters of these seismic surveys.

Table 1 *Summary of the acquisition parameters, polarity, and bulk shift of the 2D seismic surveys used in this study.*

Survey	Year	Line km	Streamer Length (m)	Fold	Record Length (ms)	Polarity	Bulk Shift (ms)
CNL95a	1995	5275	6020	98	8192	SEG Normal	25
CNL95b	1995	163	6020	98	8192	SEG Normal	0
UNCLOS-177 (TL1)	1996	1090	3000	30	16000	SEG Normal	0
ASTROLABE (DTB01)	2001	6600	6000	120	8000	SEG Normal	0
CEN05	2005	2620	6000	120	6000	SEG Normal	0
HOKI07	2007	900	6100	120	6114	SEG Normal	0
STRATUS-2D	2008	810	7950	106	12000	SEG Normal	45
DTB08	2009	4800	10050	134	10000	SEG Reverse	0
ATB10	2010	4740	8000	160	8192	SEG Normal	0
MER10	2010	1820	8000	160	8192	SEG Normal	0

3.1.2 Polarity

The polarity of the data set is predominantly Society of Exploration Geophysics (SEG) Normal (zero phase): an interface with positive impedance contrast is displayed as a positive peak (Figure 2). Table 1 lists polarity of the surveys used in this study.

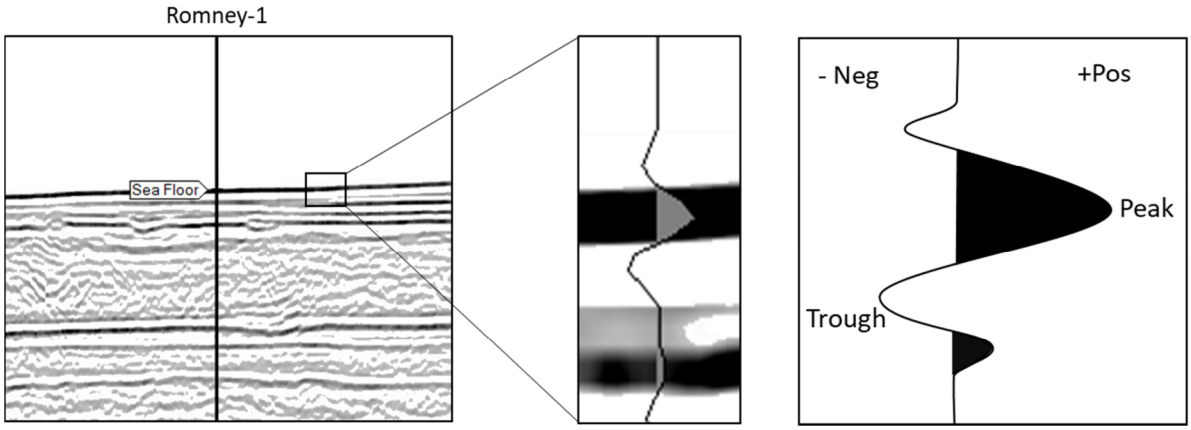

Figure 2 *Polarity of seismic data A) Screen shot of DTB01-18 at Romney-1. B) Magnified seabed reflector with wiggle trace overlay. C) Cartoon annotating positive and negative amplitude, in the case of SEG Normal this is seen as a peak (black infilled) and trough (white infilled), respectively.*

3.1.3 Mis-ties

The seabed was the first reflector interpreted in order to QC the data for mis-ties (internally and between seismic surveys). All seismic surveys were found to be internally consistent, however, CNL95a and STRATUS-2D seismic surveys were found to mis-tie with adjacent seismic surveys and required a bulk shift of 25 milli seconds (ms) and 45 ms, respectively (Table 1).

3.1.4 Quality

All seismic survey data are considered to be of good to high quality with coherent reflectors to 5 s two-way-time (TWT) or deeper and the ability to interpret arbitrary lines across multiple seismic surveys with ease (Figure 3).

3.1.5 Nomenclature

Each seismic reflector and unit have been assigned a three-part code to identify it e.g. T-AOT-1. Part one identifies if the reflector represents the top (T) or base (B) of a unit; and a prefix of U is used to identify a seismic unit. Part two identifies that the seismic reflector or

unit is from Aotea Basin (AOT). Part three identifies the seismic unit (1 - 4) or sub-unit (e.g. 1a).

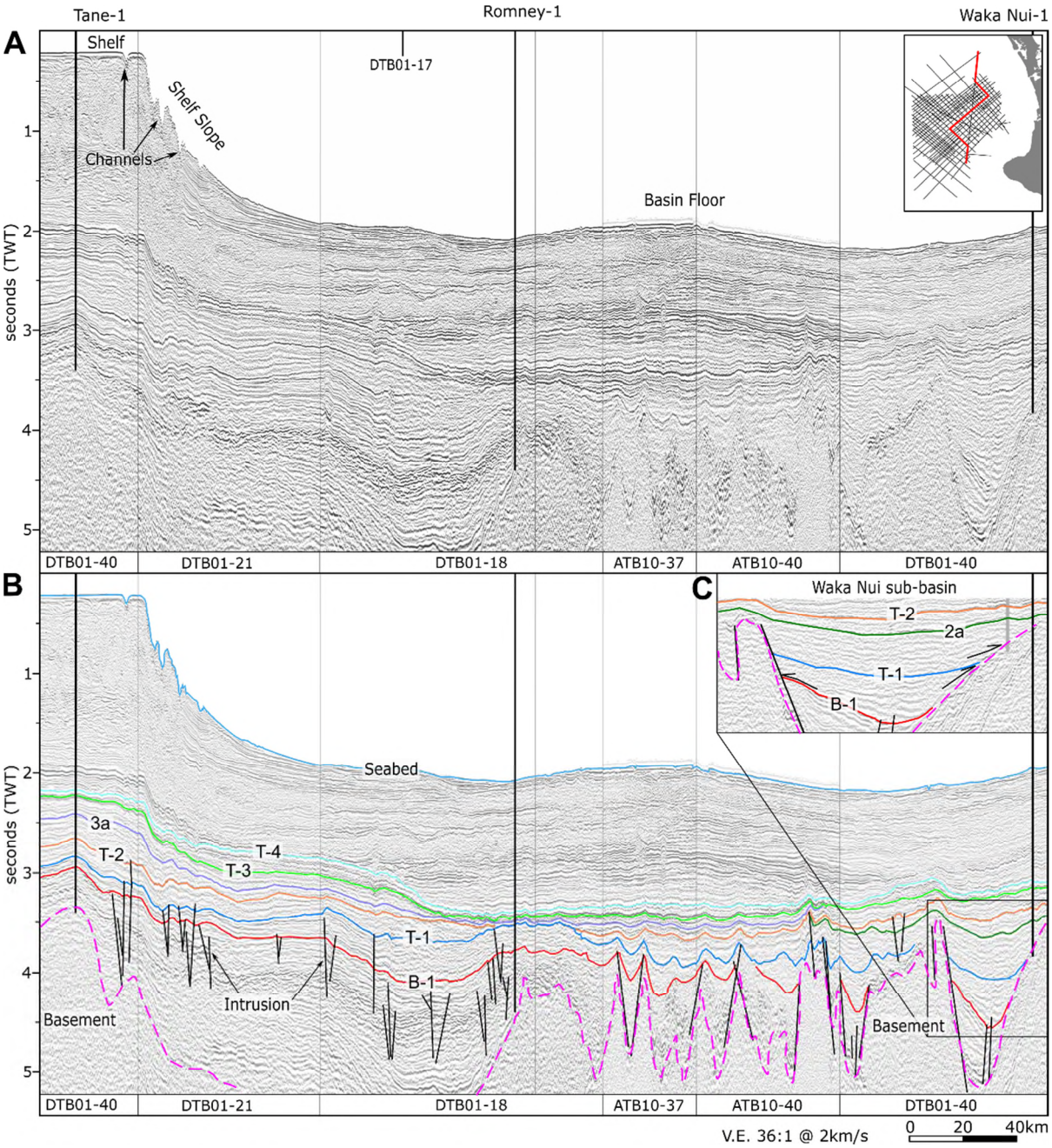

Figure 3 *Uninterpreted (A) and interpreted (B) composite seismic profile DTB01-40-21-18-ATB10-37-40-DTB01-14. Reflectors: seabed (blue), T-AOT-4 (cyan), T-AOT-3 (light green), T-AOT-3a (purple), T-AOT-2 (orange), T-AOT-2a (dark green), T-AOT-1 (blue), B-AOT-1 (red), and Basement (magenta). Insert (C) showing onlap reflector terminations in Waka Nui sub-basin.*

3.2 Seismic reflector and unit descriptions

3.2.1 Introduction

Seismic sequence stratigraphy is the recognition and interpretation of sequences of seismic reflectors based on their geometry and stratal termination relationships (Van Wagoner et al., 1987, Mitchum Jr and Vail, 1977, Mitchum Jr et al., 1977, Vail et al., 1977, Catuneanu et al., 2011, Allen and Allen, 2013). Seismic reflection data (Figure 1) were interpreted to define and map significant reflectors, both basin-wide and geographically restricted, over the time-period of interest i.e. Late Cretaceous to earliest Miocene strata.

Each bounding reflector was picked based on its relationship to terminations of overlying (onlap and downlap) and underlying (truncation and toplap) reflectors, following the principles described by Mitchum Jr et al. (1977) (Figure 4). Termination relationships and the geometry of intervening reflectors were used to recognise and define depositional sequence boundaries, and infer likely facies types (Allen and Allen, 2013). Onlap, downlap, and toplap are interpreted as non-depositional hiatuses or condensed sections, and truncation can indicate either erosional hiatus or structural disruption (Vail et al., 1977). In addition, offlap (Figure 4) is an important stratal stacking pattern to recognise, as it is interpreted to represent forced regression with proximal subaerial/wave base unconformities (Catuneanu et al., 2009). Figure 5 shows the units that were mapped across Aotea Basin, and Figure 6 shows the mapped extent and depth in TWT of unit bounding reflectors.

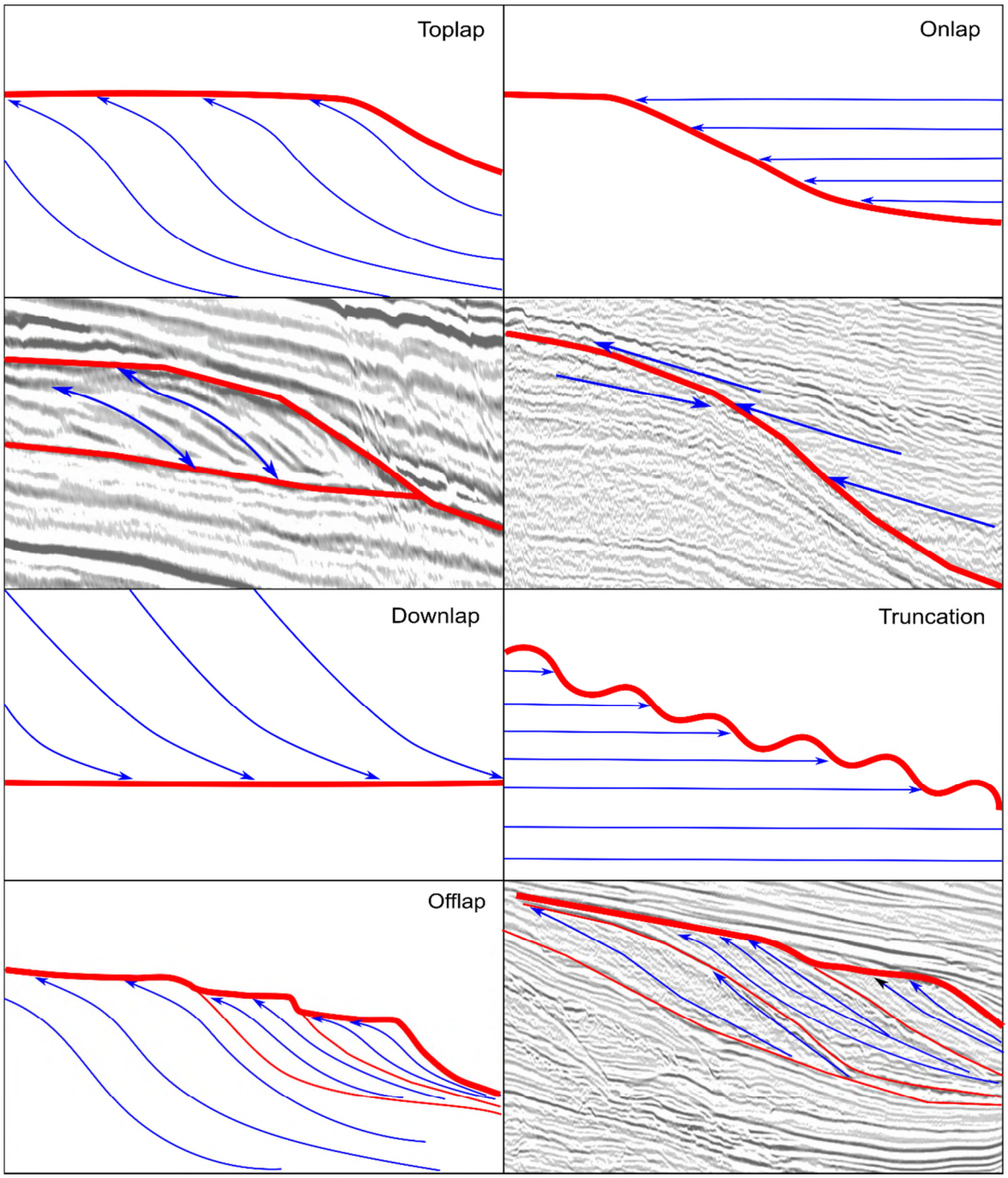

Figure 4. *Seismic reflectors were interpreted to be significant horizons (red) based on their relationship to stratal terminations (blue arrow) of overlying or underlying strata, or a combination of these (Mitchum Jr and Vail (1977) and Catuneanu et al. (2009)). The seismic data examples are from this study.*

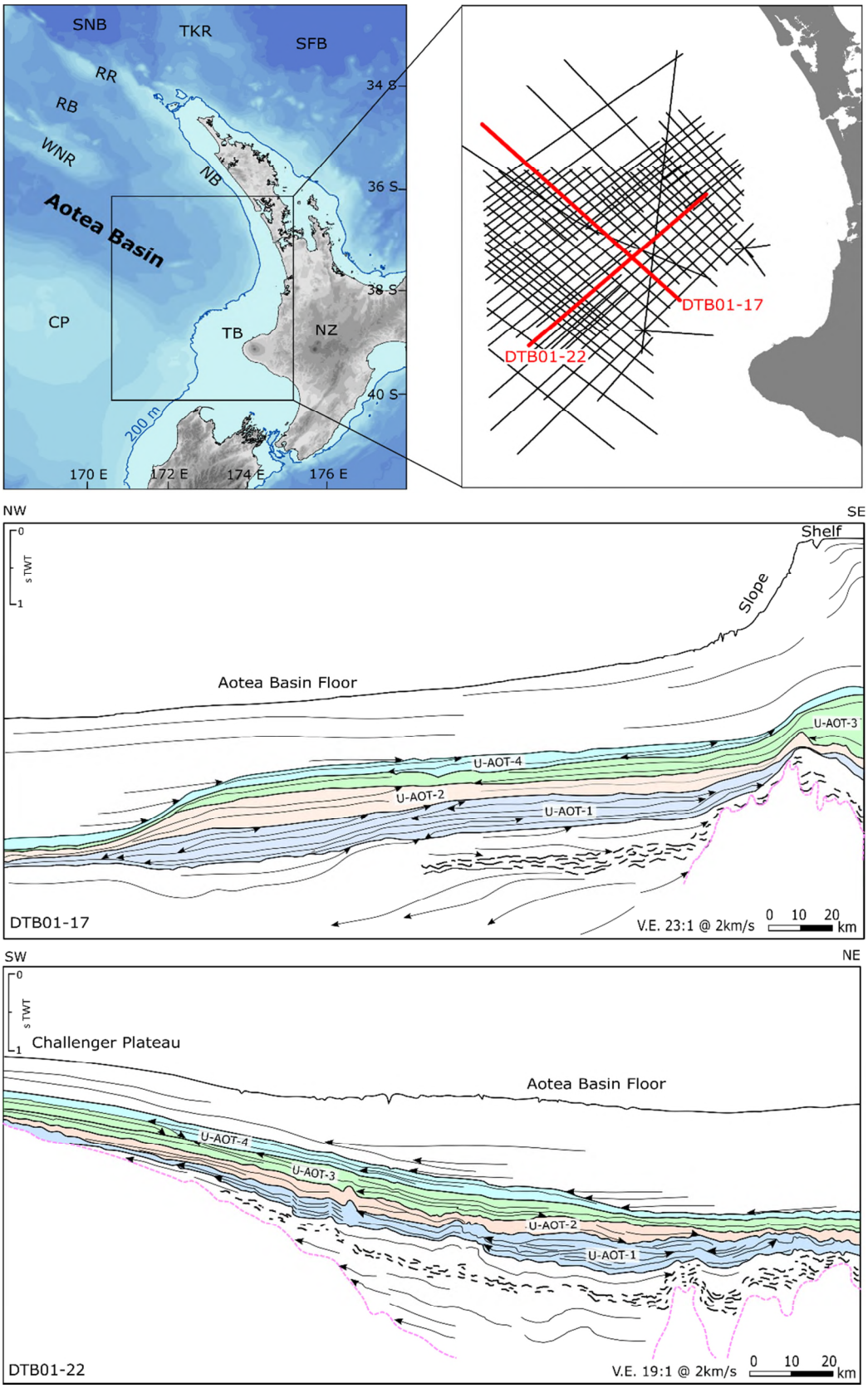

Figure 5 *Top left: bathymetric map of northwest New Zealand with all major physiographic features labelled. Top right: map showing seismic data interpreted in this study with the cross-sections highlighted in red. Upper cross-section: DTB01-17 is a strike line that runs down the axis of Aotea Basin from the shelf to bathyal depths. Lower cross-section: DTB01-22 is a dip line that runs from Challenger Plateau (mid bathyal) towards the Northland Basin (bathyal)*

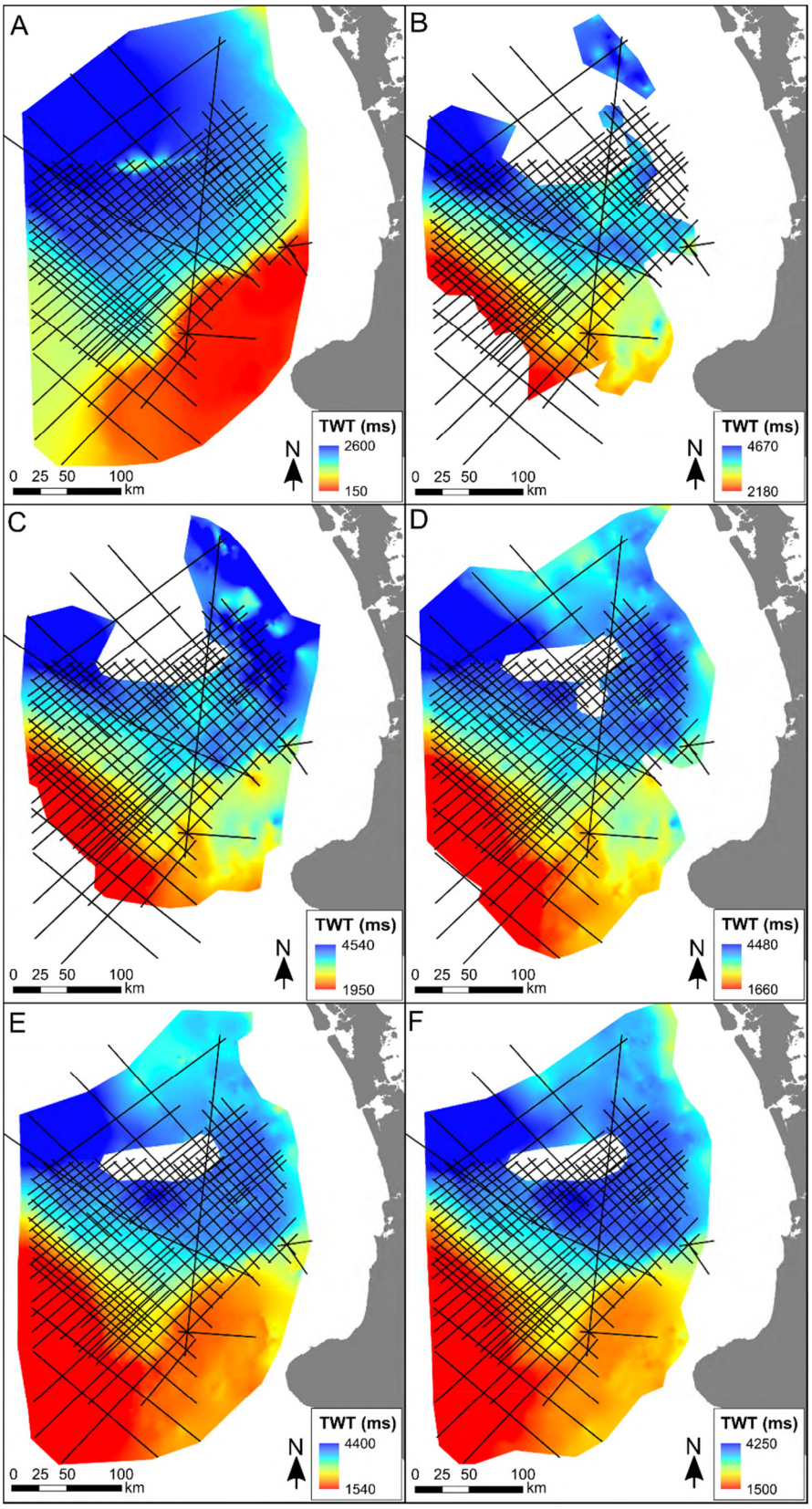

Figure 6 *Distribution of seismic reflectors (A) Seabed, (B) B-AOT-1, (C) T-AOT-1, (D) T-AOT-2, (E) T-AOT-3, and (F) T-AOT-4 shown as gridded surfaces in two-way time (TWT) milli seconds (ms).*

3.2.2 Seabed

The seabed (upper blue horizon in Figure 7) is a continuous high-amplitude positive polarity reflector, that ranges in depth from 150 to 2600 ms TWT (100 – 1,700 m) in the study area (Figure 6A & 7). A seismic velocity of 1,500 m/s for sea water was used to convert two-way time to depth for the following seabed observations. In the eastern part of the study area, the shelf (<200 m depth), seabed is sub-horizontal, dips ~ 0.15° to the northwest, and underlying strata are continuous and sub-parallel. The shelf slope seabed (200 – 1000 m) has a dip of 2 – 3° and is incised by northwest trending channels up to ~3,500 m wide and ~250 m deep (Figure 3). Reflectors just below the seabed have similar dip and patterns of channel incision. In the western part of the study area, the basin floor (>1000 m depth), seabed has a dip of ~ 0.4°, and truncates underlying sub-parallel strata (Figure 7). The basin floor is incised by the same northwest trending channel system seen on the slope, but channels have reduced width and depth: maximum ~1200 m and ~120 m, respectively (Figure 8).

3.2.3 U-AOT-1 reflectors

B-AOT-1 (red horizon in Figure 7) is mapped as a moderate- to high-amplitude continuous positive polarity reflector, that ranges in depth from 2,180 ms TWT in the Challenger Plateau region, to 2,930 ms TWT in the shelf region, to 4,670 ms TWT in the northwest of Aotea Basin (Figures 1 & 6B). Along the flank of Challenger Plateau, B-AOT-1 onlaps basement and is in turn onlapped by overlying strata (Figure 8). The onlap relationships cause the reflector to become discontinuous in some places (Figure 8). In the northwest of the study area, B-AOT-1 is downlapped by overlying strata (Figure 9). Beneath the present-day slope and shelf, B-AOT-1 is onlapped by overlying strata (Figure 7). In the north of the study area, near Waka Nui-1, B-AOT-1 is an angular unconformity that is onlapped by overlying strata and terminates against basement as an onlap (Figure 3C).

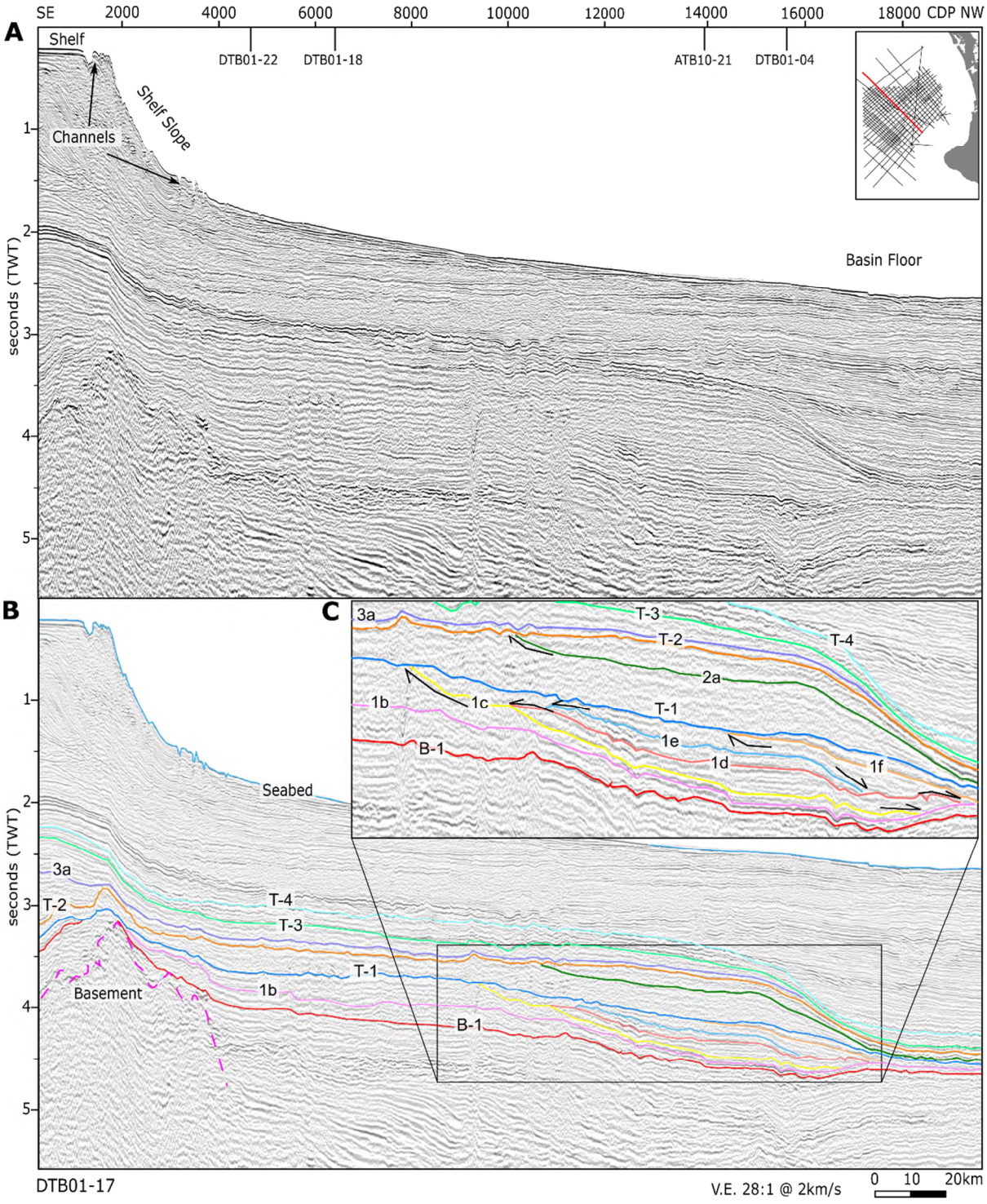

Figure 7 *Uninterpreted (A), interpreted (B), and insert (C) seismic profile DTB01-17: a strike line that runs down the axis of Aotea Basin. Reflectors: seabed (blue), T-AOT-4 (cyan), T-AOT-3 (light green), T-AOT-3a (purple), T-AOT-2 (orange), T-AOT-2a (dark green), T-AOT-1 (blue), T-AOT-1f (light orange), T-AOT-1e (light blue), T-AOT-1d (coral), T-AOT-1c (yellow), T-AOT-1b (pink), B-AOT-1 (red), and Basement (magenta). Insert (C) showing downlap, offlap and truncation relationships between restricted and regionally extensive reflectors.*

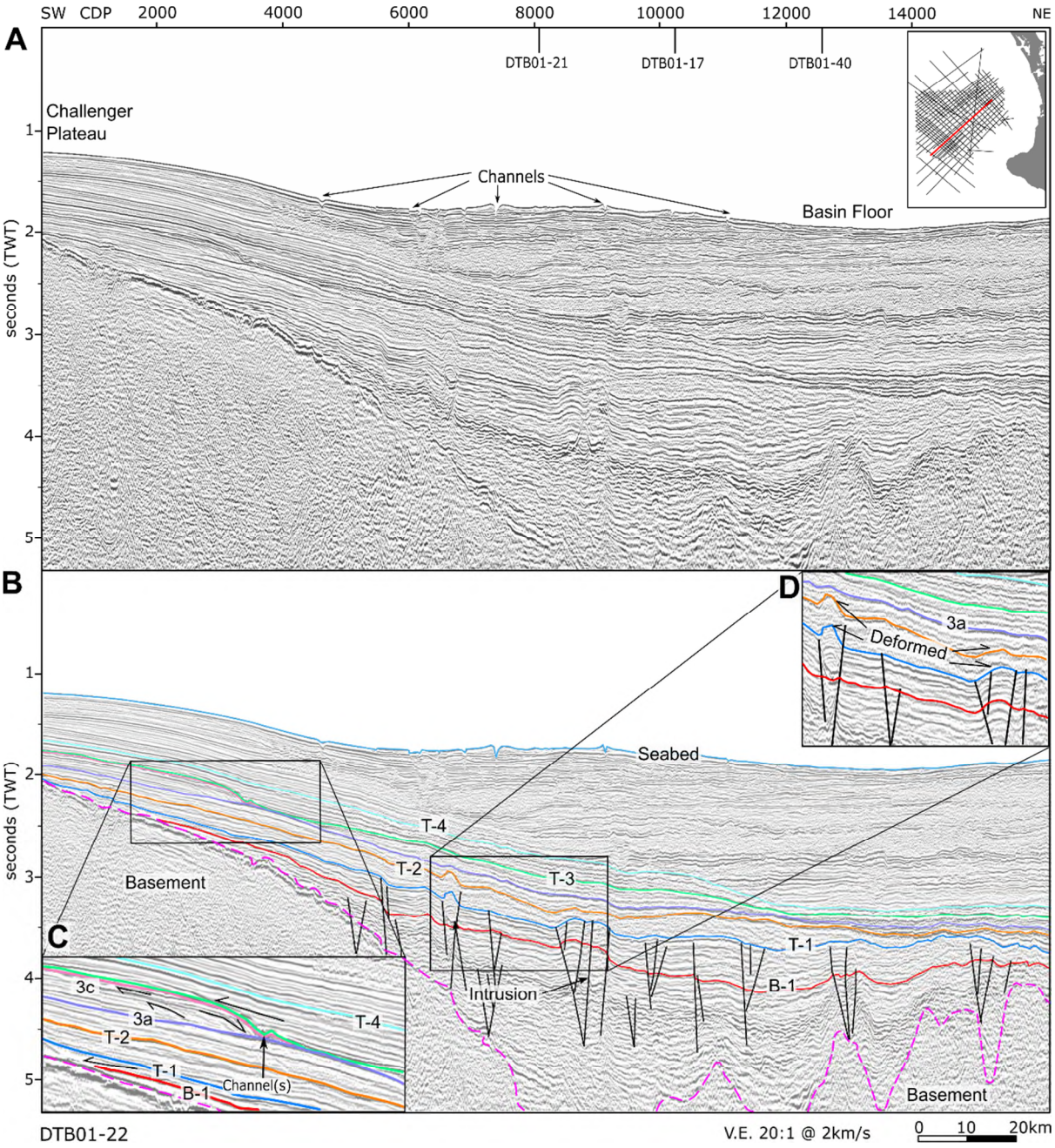

Figure 8 *Uninterpreted (A) and interpreted (B) seismic profile DTB01-22: a dip line into Aotea Basin. Reflectors: seabed (blue), T-AOT-4 (cyan), T-AOT-3 (light green), T-AOT-3c (pastel pink), T-AOT-3a (purple), T-AOT-2 (orange), T-AOT-1 (blue), B-AOT-1 (red), and Basement (magenta). Insert (C) shows: the onlap of U-AOT-4 strata and channel(s) incision(s) at the termination of reflector T-AOT-3c, toplap and downlap terminations of unit U-AOT-3c internal reflectors, and the onlap of reflector B-AOT-1 to basement. Insert (D) shows: deformation of reflectors below T-AOT-3a.*

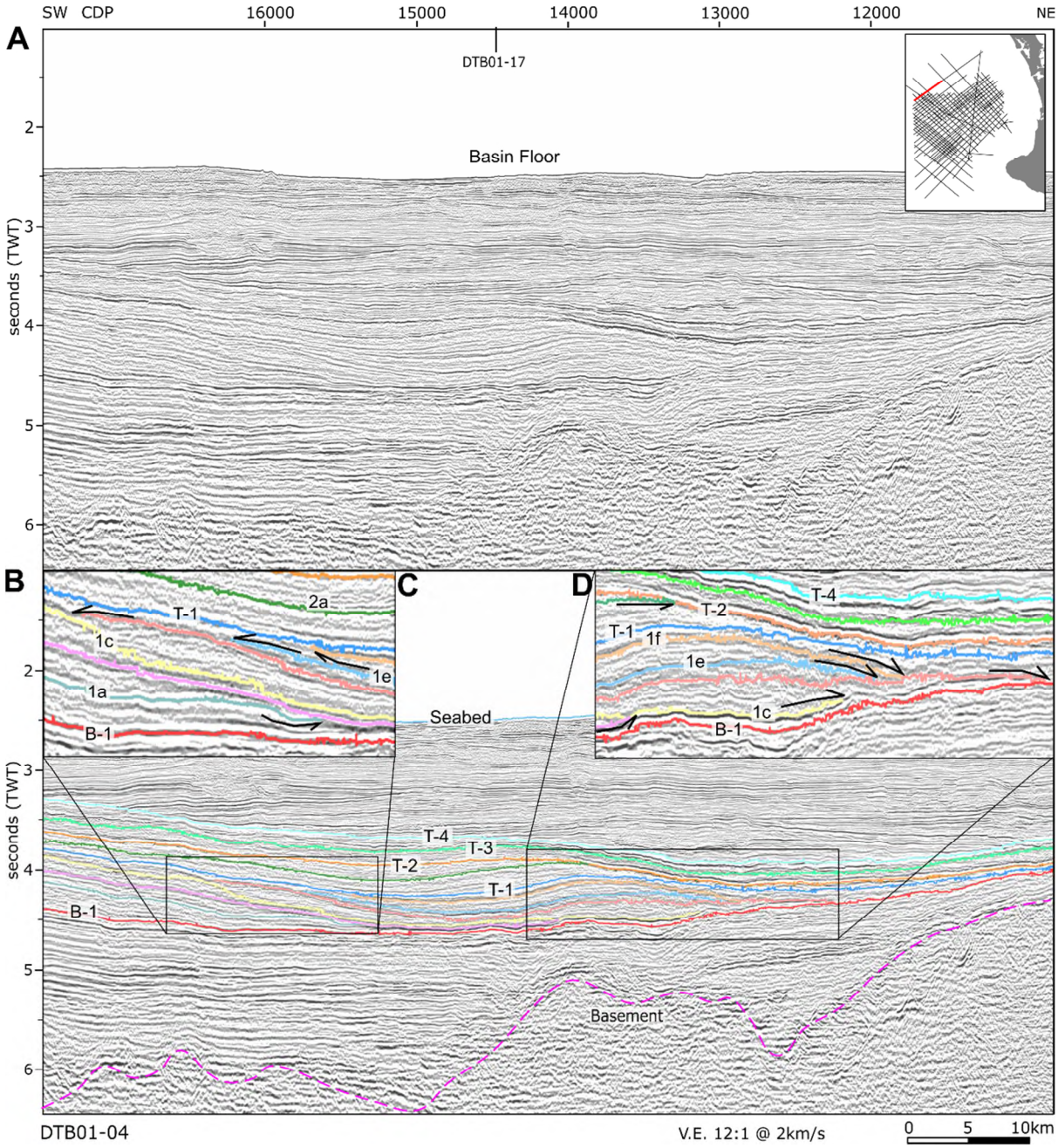

Figure 9 *Uninterpreted (A) and interpreted (B) seismic profile DTB01-04: a dip line in the north west of Aotea Basin. Reflectors: seabed (blue), T-AOT-4 (cyan), T-AOT-3 (light green), T-AOT-2 (orange), T-AOT-2a (dark green), T-AOT-1 (blue), T-AOT-1f (light orange), T-AOT-1e (light blue), T-AOT-1d (coral), T-AOT-1c (yellow), T-AOT-1b (pink), T-AOT-1a (turquoise), B-AOT-1 (red), and Basement (magenta). Inserts (C) and (D) showing toplap, offlap, truncation, and downlap relationship of reflector terminations.*

T-AOT-1a (turquoise horizon in Figure 10) is mapped as a moderate-amplitude positive polarity reflector, that ranges in depth from 3,500 to 4,550 ms TWT, and is restricted to the northwest of the study area in Aotea Basin (Figure 11F). Along the flank of Challenger Plateau, T-AOT-1a toplaps T-AOT-1b (Figure 10). T-AOT-1a downlaps B-AOT-1 to the north east (Figure 10), is truncated by T-AOT-1b at times (Figure 9) and is conformable in the northwest of the study area.

T-AOT-1b (pink horizon in Figure 7) is mapped as a moderate- to high-amplitude negative polarity reflector, that ranges in depth from 3,230 to 4,610 ms TWT, and is restricted to the axis of Aotea Basin (Figure 11E). Along the flank of Challenger Plateau, T-AOT-1b toplaps T-AOT-1 (Figure 12). In the axis of Aotea Basin, T-AOT-1b downlaps B-AOT-1 (Figure 9). Beneath the present-day slope, T-AOT-1b onlaps B-AOT-1 (Figure 7). T-AOT-1b is downlapped by overlying strata e.g. line DTB01-17 between CDP ~14,500 to ~17,300 (Figure 7).

T-AOT-1c (yellow horizon in Figure 7) is mapped as a moderate-amplitude negative polarity reflector, that ranges in depth from 3,310 to 4,560 ms TWT, and is restricted to the northwest of the study area in Aotea Basin (Figure 11D). Along the flank of Challenger Plateau, T-AOT-1c offlaps T-AOT-1b (Figure 10), to the south T-AOT-1c is truncated by T-AOT-1 (Figure 7), and T-AOT-1c downlaps T-AOT-1b and B-AOT-1 to the north and east, respectively (Figures 7 & 9). In the northwest of the study area in Aotea Basin T-AOT-1c is downlapped by overlying strata e.g. line DTB01-17 between CDP ~13,500 to ~16,500 (Figure 7). Along the flank of Challenger Plateau T-AOT-1c is onlapped by overlying strata (Figure 10)

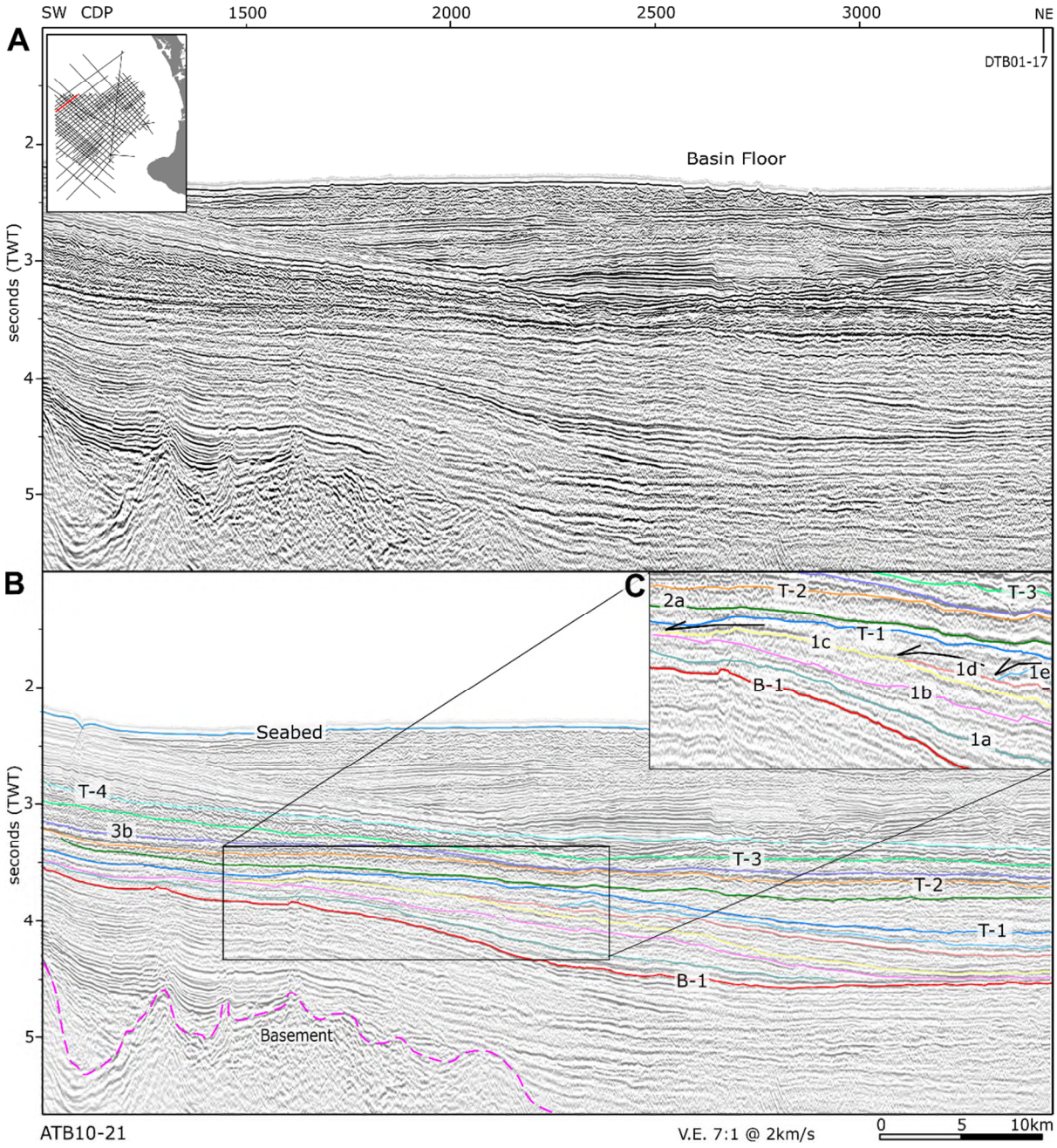

Figure 10 *Uninterpreted (A) and interpreted (B) seismic profile ATB10-21: a dip line in the north west of Aotea Basin. Reflectors: seabed (blue), T-AOT-4 (cyan), T-AOT-3 (light green), T-AOT-3a (purple), T-AOT-2 (orange), T-AOT-2a (dark green), T-AOT-1 (blue), T-AOT-1e (light blue), T-AOT-1d (coral), T-AOT-1c (yellow), T-AOT-1b (pink), T-AOT-1a (turquoise), B-AOT-1 (red), and Basement (magenta). Insert (C) showing the onlap, offlap and truncation relationships of reflectors.*

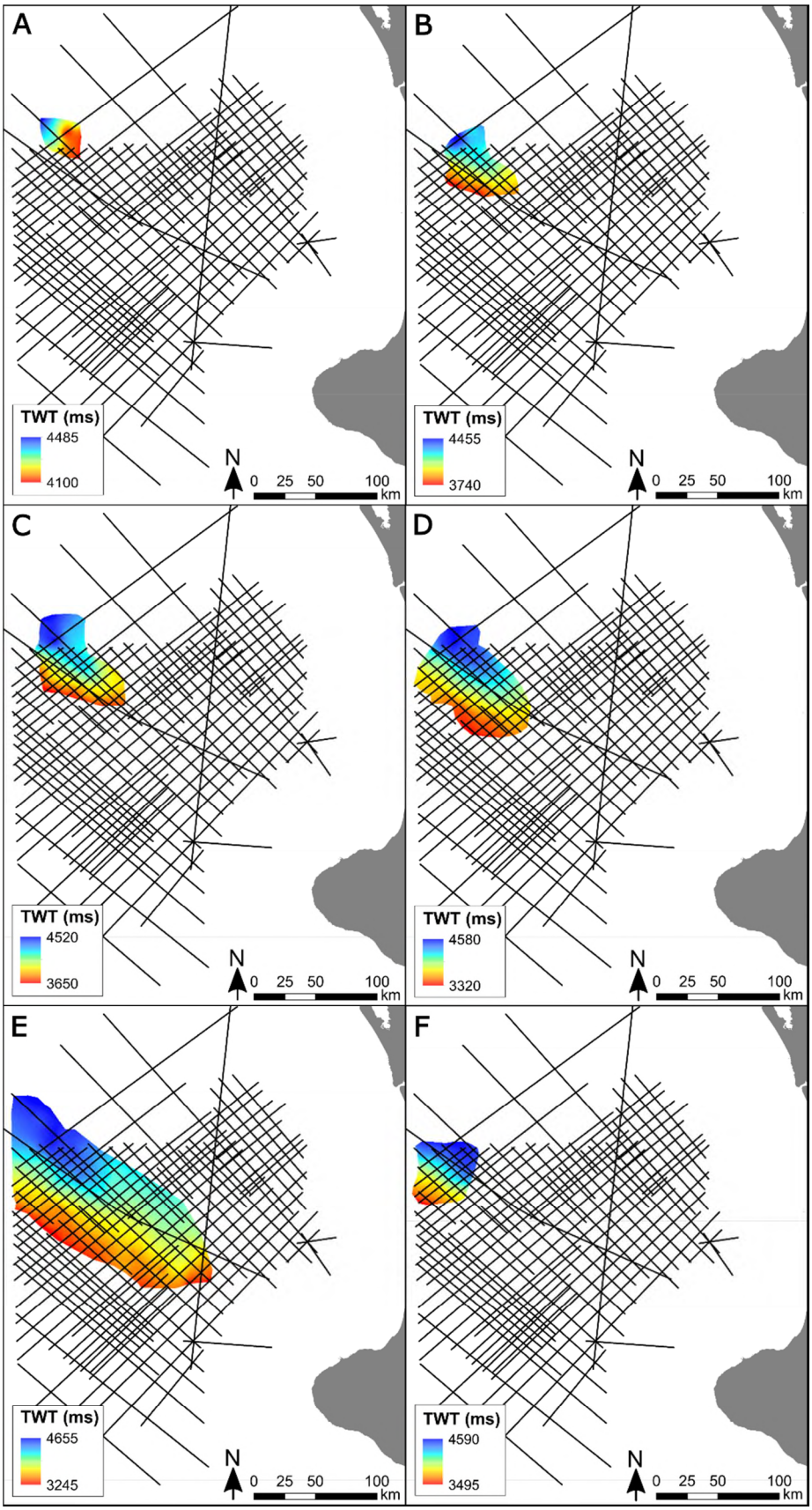

Figure 11 *Distribution of seismic reflectors (A) T-AOT-1f, (B) T-AOT-1e, (C) T-AOT-1d, (D) T-AOT-1c, (E) T-AOT-1b, and (F) T-AOT-1a shown as gridded surfaces in two-way time (TWT) milli seconds (ms).*

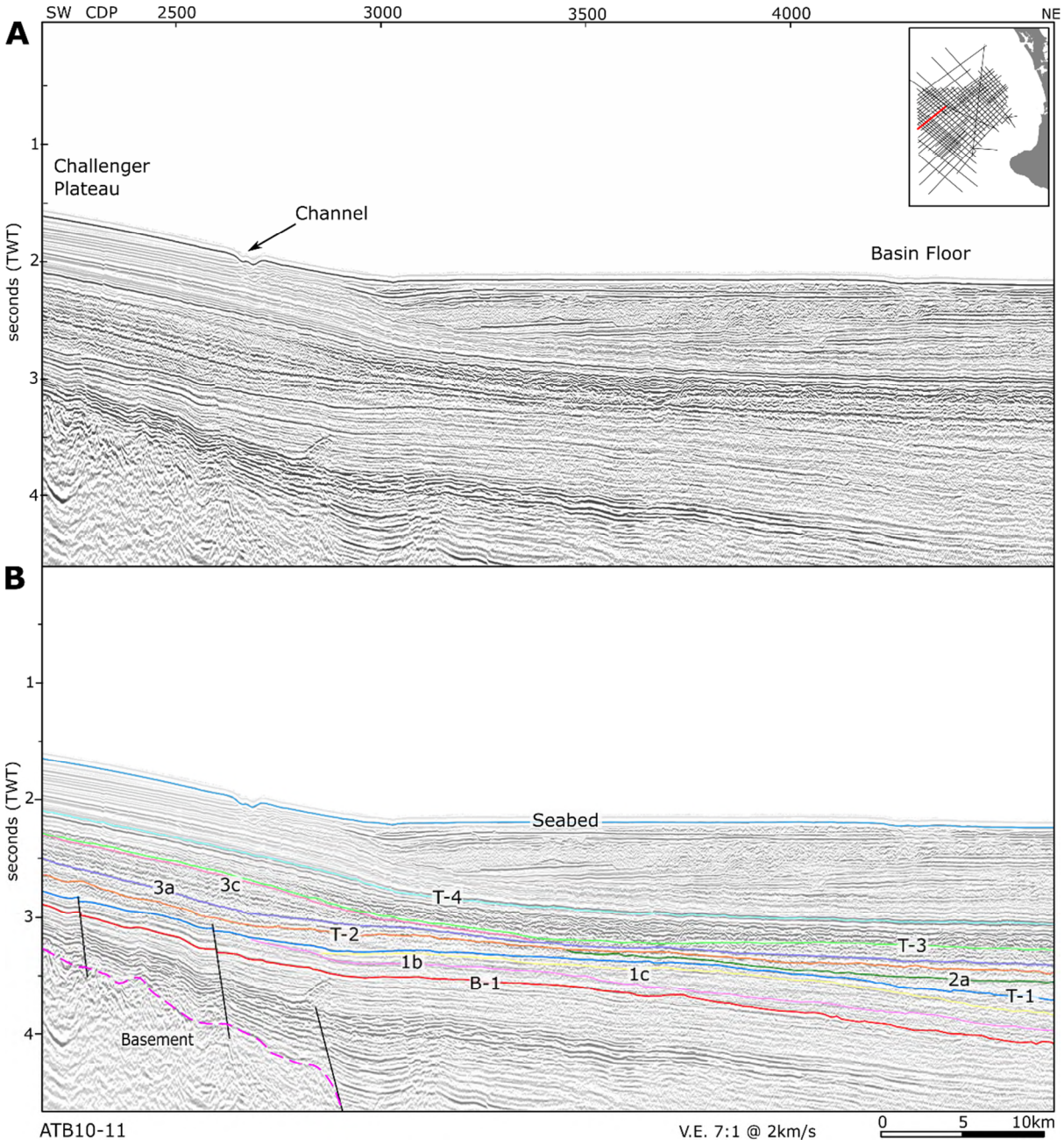

Figure 12 *Uninterpreted (A) and interpreted (B) seismic profile ATB10-11: a dip line in the north west of Aotea Basin. Reflectors: seabed (blue), T-AOT-4 (cyan), T-AOT-3 (light green), T-AOT-3c (pastel pink), T-AOT-3a (purple), T-AOT-2 (orange), T-AOT-2a (dark green), T-AOT-1 (blue), T-AOT-1c (yellow), T-AOT-1b (pink), B-AOT-1 (red), and Basement (magenta).*

T-AOT-1d (coral horizon in Figure 7) is mapped as a moderate-high-amplitude negative polarity reflector, that ranges in depth from 3,750 to 4,500 ms TWT, and is restricted to the northwest of the study area in Aotea Basin (Figure 11C). T-AOT-1d offlaps T-AOT-1c in the south and west (Figures 7 & 10), and downlaps T-AOT-1b and B-AOT-1 to the north and east, respectively (Figures 7 & 9). In the northwest of the study area in Aotea Basin T-AOT-1d is downlapped by overlying strata e.g. line DTB01-17 between CDP ~15,000 to ~17,000 (Figure 7)

T-AOT-1e (light blue horizon in Figure 7) is mapped as a moderate- to high-amplitude negative polarity reflector, that ranges in depth from 3,880 to 4,440 ms TWT, and is restricted to the northwest of the study area in Aotea Basin (Figure 11B). T-AOT-1e offlaps T-AOT-1d in the south and west (Figures 7 & 10), and downlaps T-AOT-1d to the north and east (Figures 7 & 9). T-AOT-1e is onlapped by overlying strata (Figures 7 & 9).

T-AOT-1f (light orange horizon in Figure 7) is mapped as a moderate-amplitude negative polarity reflector, that ranges in depth from 3,900 to 4,510 ms TWT, and is restricted to the northwest of the study area in Aotea Basin (Figure 11A). T-AOT-1f is truncated by T-AOT-1 to the south and west, and downlaps T-AOT-1d and T-AOT-1c, to the east and north, respectively (Figures 7 & 9). T-AOT-1f truncates underlying strata and is onlapped by overlying strata (Figure 7).

T-AOT-1 (dark blue horizon in Figure 7) is mapped as a high-amplitude continuous positive polarity reflector, that ranges in depth from 1,950 ms TWT in the Challenger Plateau region, to 2,840 ms TWT in the shelf region, to 4,540 ms TWT in the northwest of Aotea Basin (Figure 1 & 6C). Along the flank of Challenger Plateau, T-AOT-1 onlaps basement and is

sub-parallel to T-AOT-2, and T-AOT-1 is onlapped by overlying strata and truncates underlying strata (Figure 8). In the present-day shelf region, T-AOT-1 is onlapped by overlying strata and is sub-parallel to T-AOT-2 (Figures 3 & 13). Proximal to Waka Nui-1, T-AOT-1 is onlapped by overlying strata and onlaps basement highs (Figure 3). In the axis of Aotea Basin, T-AOT-1 is conformable with overlying strata and truncates underlying strata (Figure 7). T-AOT-1 is onlapped by overlying strata on the flanks of the Romney structure (Figure 14). In the northwest of the study area, T-AOT-1 is conformable with overlying and underlying strata (Figure 7).

3.2.4 U-AOT-1

Sequence U-AOT-1 is predominantly composed of moderate- to high-amplitude continuous parallel reflectors, and is bound by B-AOT-1 and T-AOT-1 (Figures 5, 7 & 8). U-AOT-1 ranges in thickness from 0 to 545 ms; and is thickest in a northwest-trending trough in the centre of study area (Figure 15A). In the northeast of the study area, proximal to Waka Nui-1, U-AOT-1 is restricted to basement lows (Figures 3 & 15A).

In the central trough area, U-AOT-1 is split into 7 sub units (Figures 7 & 9).

U-AOT-1a is a transgressive unit based on predominantly parallel high-amplitude continuous internal reflectors that terminate as onlaps onto B-AOT-1 and Basement in places under the shelf, Waka Nui sub-basin and on Challenger Plateau (Figures 3, 7 & 8).

U-AOT-1b and U-AOT1c are high-stand regressive units based on their wedge geometry, the downlapping of reflectors onto B-AOT-1, and clinoform geometry of T-AOT-1b and T-AOT-1c (Figure 10C).

U-AOT-1d and U-AOT-1e are interpreted as a low-stand forced regressive units based on the offlap of T-AOT-1d and T-AOT-1e onto T-AOT-1c and T-AOT-1d; respectively, and the downlapping of reflectors onto T-AOT-1c, T-AOT-1b and B-AOT-1 (Figures 7, 9C & 10C).

U-AOT-1f is interpreted as a transgressive unit based on moderate- to high-amplitude continuous parallel internal reflectors that onlap T-AOT-1e (Figures 7 & 9).

U-AOT-1g is interpreted as a transgressive unit based on moderate- to high-amplitude continuous parallel internal reflectors that onlap T-AOT-1f (Figures 7 & 9).

U-AOT-1 is interpreted as a second order transgressive sequence based on the onlapping of reflectors onto B-AOT-1 and Basement. The sub units are interpreted as third order transgressive and regressive sequences.

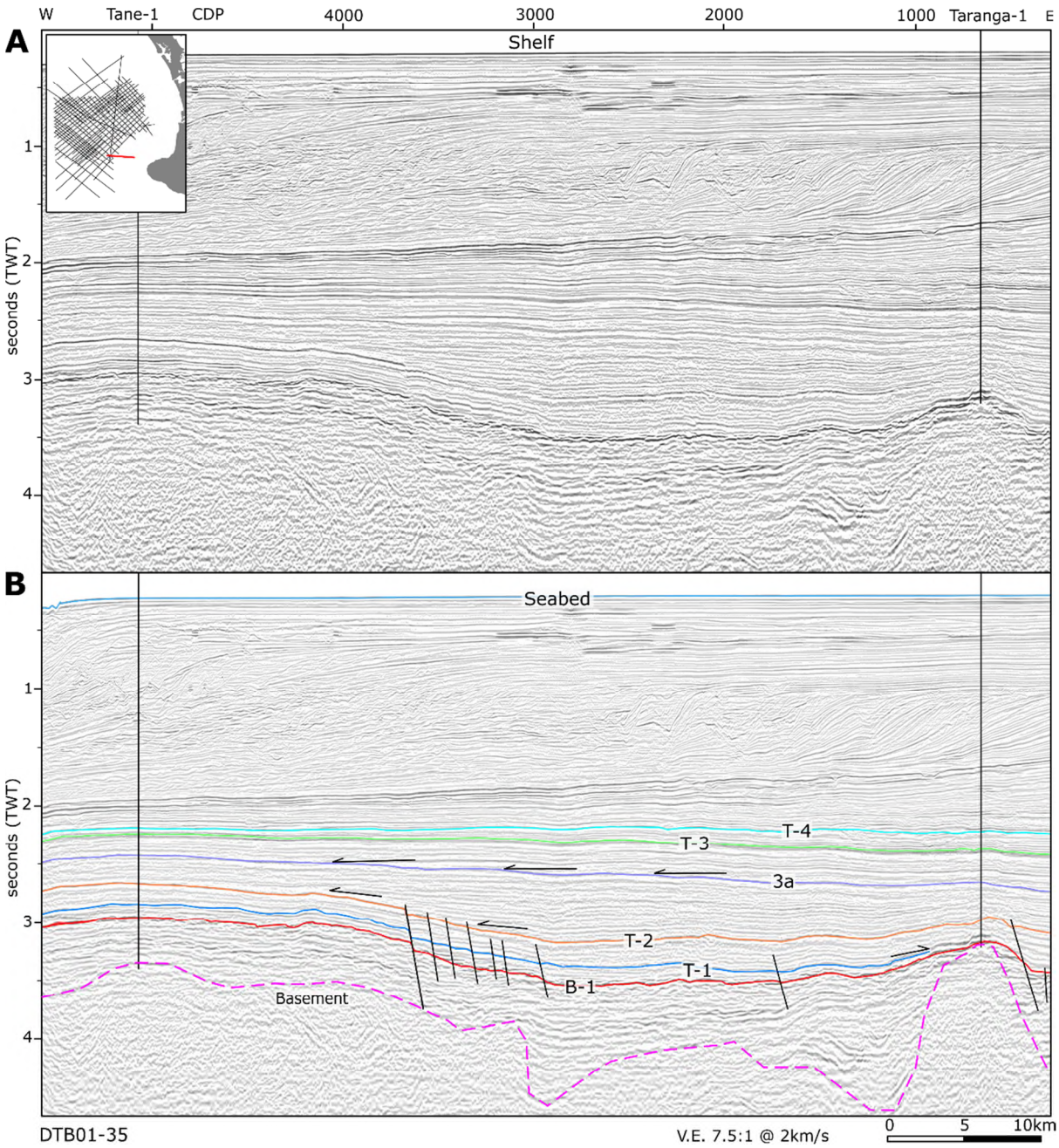

Figure 13 *Uninterpreted (A) and interpreted (B) seismic profile DTB01-35: a dip line into Taranaki Basin. Reflectors: seabed (blue), T-AOT-4 (cyan), T-AOT-3 (light green), T-AOT-3a (purple), T-AOT-2 (orange), T-AOT-1 (blue), B-AOT-1 (red), and Basement (magenta).*

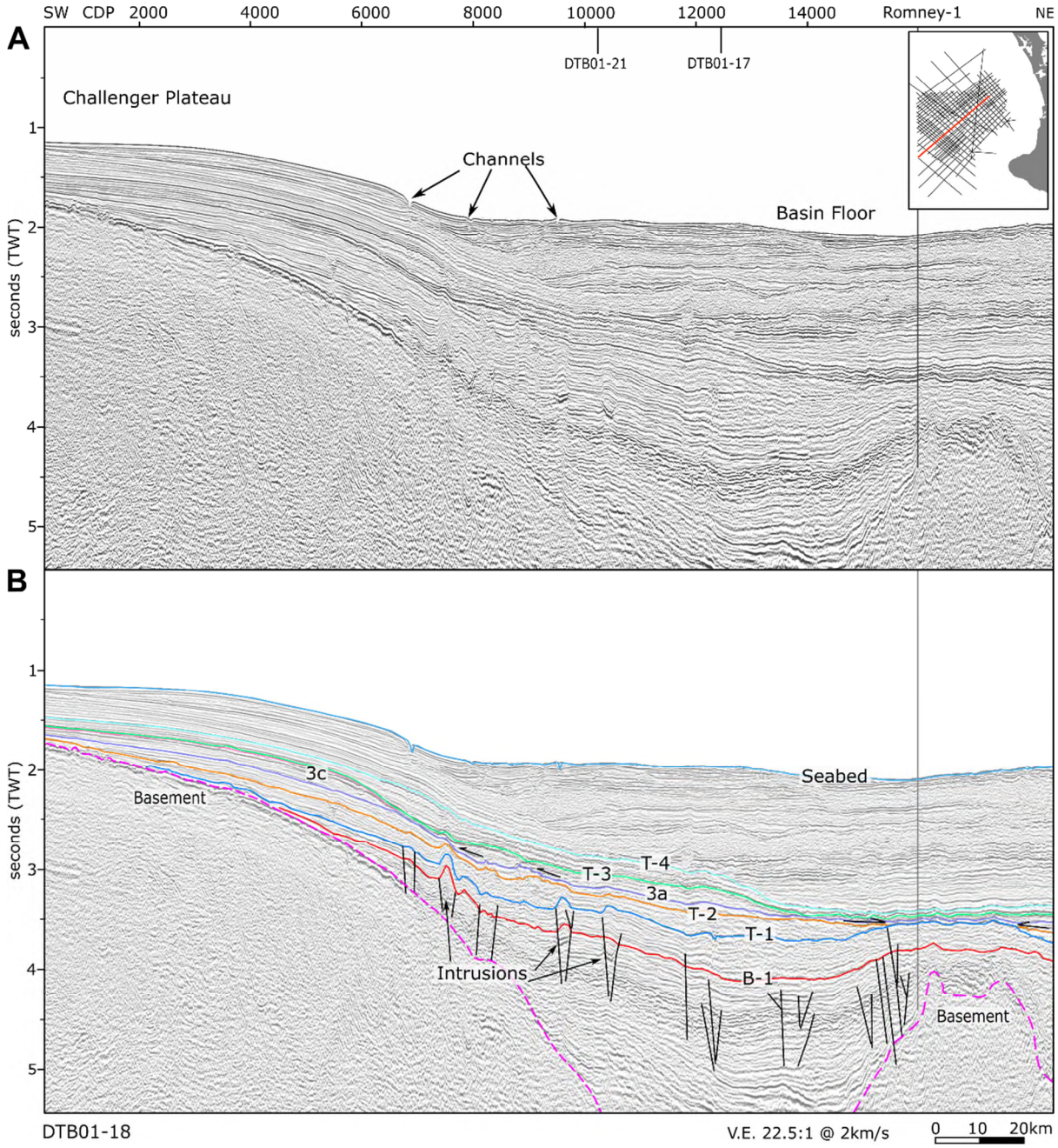

Figure 14 *Uninterpreted (A) and interpreted (B) seismic profile DTB01-18: a dip line across Aotea Basin. Reflectors: seabed (blue), T-AOT-4 (cyan), T-AOT-3 (light green), T-AOT-3c (pastel pink), T-AOT-3a (purple), T-AOT-2 (orange), T-AOT-1 (blue), B-AOT-1 (red), and Basement (magenta).*

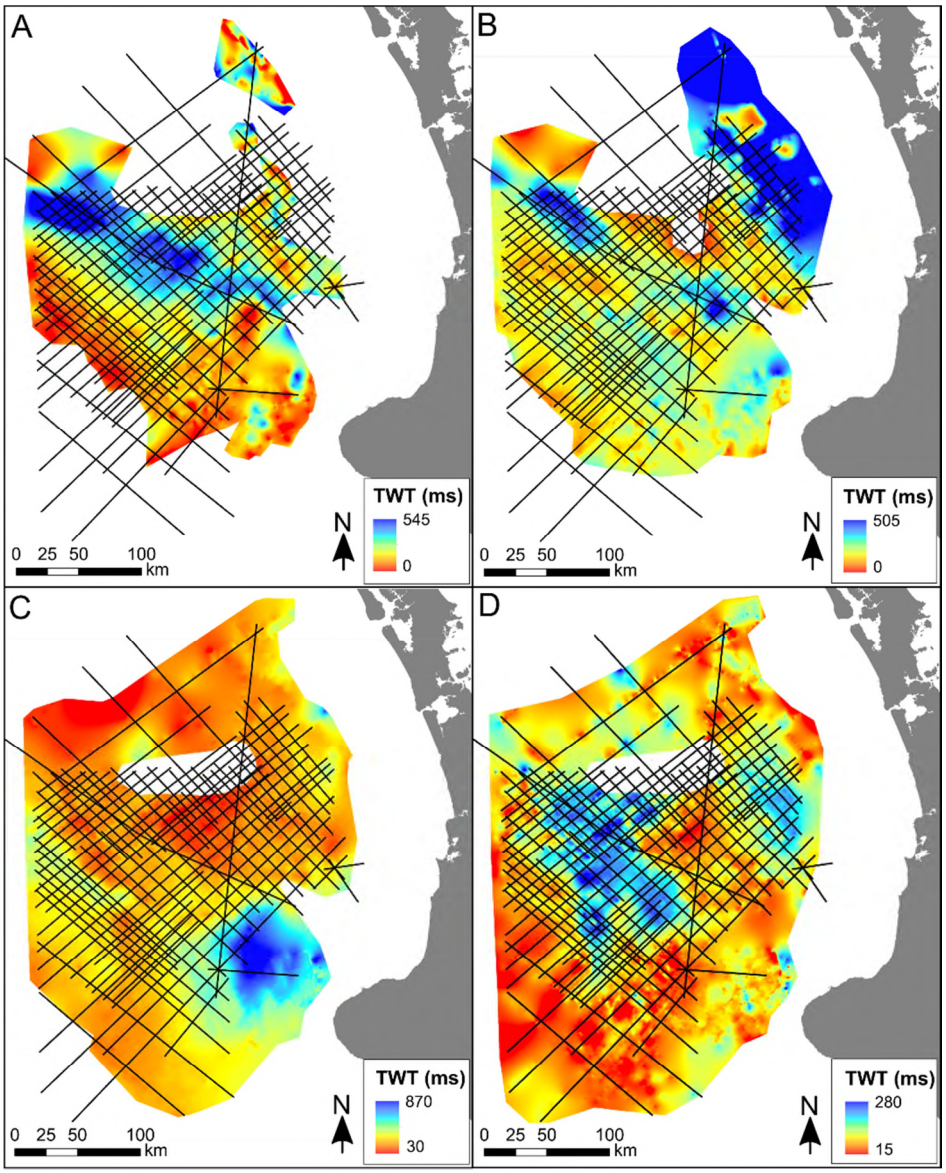

Figure 15 *Isopach maps calculated from gridded two-way-time (TWT) milli seconds (ms) reflectors. (A) U-AOT-1, (B) U-AOT-2, (C) U-AOT-3, and (D) U-AOT-4.*

3.2.5 U-AOT-2 reflectors

T-AOT-2a (dark green horizon in Figure 7) is mapped as a moderate to high-amplitude positive polarity reflector, that ranges in depth from 3,300 to 4,490 ms TWT, and is restricted to the northwest and northeast regions of the study area (Figure 16C). T-AOT-2a toplaps T-AOT-2 along the flank of Challenger Plateau, and in the southeast and northeast of Aotea Basin (Figures 7 & 10), is conformable with T-AOT-2 and T-AOT-1 in the northwest of Aotea Basin axis (Figure 7), and is downlapped by overly strata (Figs. 5 & 8). Proximal to the toplap of T-AOT-2, T-AOT-2a is onlapped by overlying strata (Figure 7). Proximal to Waka Nui-1, T-AOT-2a toplaps T-AOT-2 to the south and east, conformable with T-AOT-2 to the north, and is downlapped by over lying strata. (Figure 3).

T-AOT-2 (orange horizon in Figure 7) is mapped as a continuous moderate- to high-amplitude positive polarity reflector, that ranges in depth from 1,660 ms TWT in the Challenger Plateau region, to 2,760 ms TWT in the shelf region, to 4,480 ms TWT in the northwest of Aotea Basin (Figure 1 & 6D). Beneath the present-day shelf, T-AOT-2 is onlapped by overlying strata (Figure 7 & 13). Along the flank of Challenger Plateau, T-AOT-2 is onlapped by overlying strata and converges with T-AOT-3a, is conformable with T-AOT-1 below, and onlaps basement (Figure 14). In the southeast of Aotea Basin, T-AOT-2 is conformable with the overlying and underlying strata. In the northwest of Aotea Basin, T-AOT-2 is downlapped by overlying strata but converges and becomes parallel to T-AOT-3, e.g. DTB01-17; CDP 16,000 – 19,500 (Figure 7). On the flanks of the Romney structure, T-AOT-2 onlaps T-AOT-1 (Figure 14).

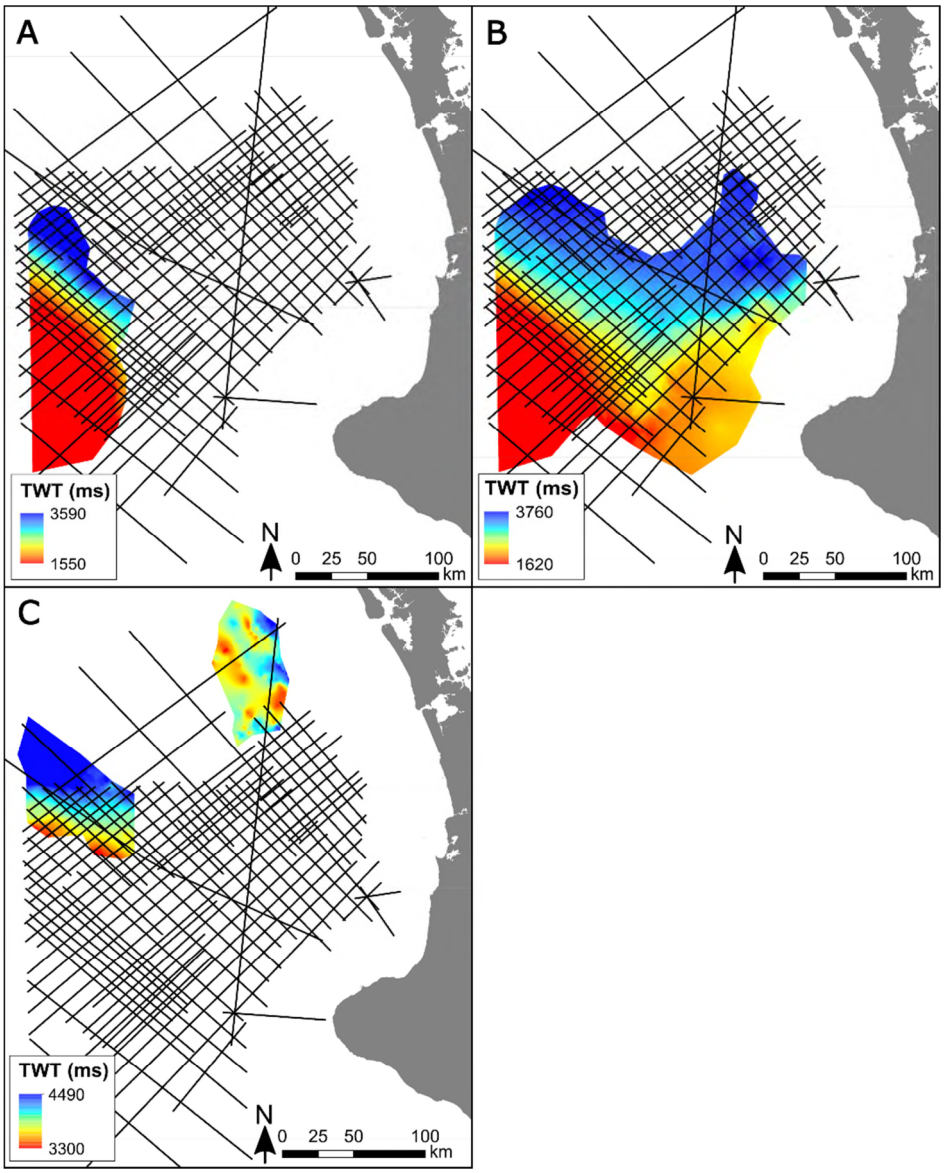

Figure 16 *Distribution of seismic reflectors (A) T-AOT-3c, (B) T-AOT-3a, and (C) T-AOT-2a shown as gridded surfaces in two-way-time (TWT) milli seconds (ms).*

3.2.6 U-AOT-2

Sequence U-AOT-2 is composed of moderate-amplitude continuous parallel reflectors under the present-day shelf and Challenger Plateau. In the axis of Aotea Basin and proximal to Waka Nui-1, U-AOT-2 is composed of moderate-amplitude reflectors that broaden and become less continuous. U-AOT-2 is bound by T-AOT-1 and T-AOT-2 (Figures 3, 5, 7 & 8). U-AOT-2 ranges in thickness from 0 to 505 ms; and is thickest the north east of the study area proximal to Waka Nui-1 (Figures 3 & 15B). In the axis of Aotea Basin, U-AOT-2 is also thicker in the same north-west trending trough as U-AOT-1 (Figure 15).

U-AOT-2 is split into 2 sub units (Figures 3 & 7).

U-AOT-2a is a transgressive unit based on the onlapping of reflectors onto underlying reflectors T-AOT-1 (Figures 7 & 14).

U-AOT-2b is a low-stand regressive unit based on its overall wedge geometry, reflectors becoming discontinuous or mounded, and reflectors downlapping T-AOT-2a (Figures 7 & 10).

U-AOT-2 is interpreted as a first order transgressive sequence based on the onlapping of reflectors onto T-AOT-1 and Basement, with the sub units representing second order sequences (Figures 3 & 8).

3.2.7 U-AOT-3 reflectors

T-AOT-3a (light purple horizon in Figure 3) is mapped as a continuous high-amplitude positive polarity reflector, that ranges in depth from 1620 to 3760 ms TWT, and is restricted to the present-day shelf, Challenger Plateau and central region of Aotea Basin, (Figure 16B). Beneath the crest of Challenger Plateau, T-AOT-3a is conformable with overlying strata, is

downlapped along the flank, and is onlapped by overlying strata towards the axis of Aotea Basin (Figures 8 & 14). In the present-day shelf slope region, T-AOT-3a is onlapped by overlying reflectors near Tane-1 and is parallel or sub-parallel with T-AOT-3 (Figures 7 & 13). In the axis of Aotea Basin, T-AOT-3a becomes conformable with T-AOT-2 and is onlapped by overlying strata (Figures 3 & 7).

T-AOT-3c (pastel pink horizon in Figure 8) is mapped as a continuous, moderate- to high-amplitude, positive polarity reflector, that ranges in depth from 1550 to 3590 ms TWT, and is restricted to Challenger Plateau (Figure 1 & 16A). Along the crest of Challenger Plateau, the T-AOT-3c reflector is parallel to both T-AOT-3 above and T-AOT-3a below. Along the flank of Challenger Plateau, T-AOT-3c downlaps T-AOT-3a, This downlapping is the last in a sequence of prograding clinoform reflectors (Figures 8C & 14). On line DTB01-22, T-AOT-3c is incised by a channel(s) at its northeast termination against T-AOT-3a (Figure 8C).

T-AOT-3 (light green horizon in Figure 7) is mapped as a continuous high-amplitude negative polarity reflector, that ranges in depth from 1,540 ms TWT in the Challenger Plateau region, to 2,200 ms TWT in the shelf region, to 4,400 ms TWT in the northwest of Aotea Basin (Figure 1 & 6E). In the shelf region, T-AOT-3 is conformable with overlying moderate-amplitude strata and underlying moderate-amplitude strata (Figures 3 & 13). Along the flank of Challenger Plateau T-AOT-3 is onlapped by overlying strata from the northeast at ~ 2° angle, and onlap terminations increase in obliquity to the southwest until overlying strata become conformable (Figure 8C). On the flanks and axis of Aotea Basin, T-AOT-3 truncates underlying strata (Figures 3, 8 & 14).

3.2.8 U-AOT-3

Sequence U-AOT-3 is predominantly composed of moderate-amplitude continuous parallel reflectors (Figures 3, 7, 8 & 13). In the axis of Aotea Basin, U-AOT-3 is composed of discontinuous high-amplitude reflectors (Figures 5, 8 & 12). U-AOT-3 is bound by T-AOT-2 and T-AOT-3 (Figures 5, 7 & 8). U-AOT-3 ranges in thickness from 30 to 870 ms; and is thickest under the present-day shelf (Figures 13 & 15C).

U-AOT-3 is split into 3 sub units (Figures 7 & 8).

U-AOT-3a is represents deepening of the basin based on the onlapping of reflectors onto T-AOT-2 (Figures 7, 13 & 14).

In the axis of Aotea Basin and flanks of Challenger Plateau, U-AOT-3b represents a deepening of the basin based on the onlapping of overlying reflectors (Figures 7 & 14).

U-AOT-3c is a prograding regressive unit based on the oblique clinoform reflectors that toplap T-AOT-3c and downlap T-AOT-3a (Figure 8C).

U-AOT-3 is a complex unit, it shows both a deepening of central Aotea Basin and under the present-day shelf and shallowing on Challenger Plateau. This would imply local tectonic effects on base level and sediment supply as opposed to regional tectonics or eustatic sea level changes.

3.2.9 U-AOT-4 reflectors

T-AOT-4 (cyan horizon in Figure 7) is mapped as a continuous and conformable high-amplitude positive polarity reflector in Challenger Plateau and shelf regions (Figure 8). Along the flanks of Aotea Basin, T-AOT-4 has low to moderate continuity and is mapped as an onlap surface (Figures 5 & 8). In the axis of Aotea Basin, T-AOT-4 is mapped as a

continuous high-amplitude positive polarity reflector that is onlapped at a low angle (<1°) by overlying strata (Figures 7 & 8). T-AOT-4 ranges in depth from 1,500 ms TWT in the Challenger Plateau region, to 2,000 ms TWT in the shelf region, to 4,250 ms TWT in Aotea Basin (Figures 1 & 6F). From the slope base to central basin floor, T-AOT-4 is downlapped by overlying strata, e.g. DTB01-17; CDP 3,000 – 10,000 (Figure 7).

3.2.10 U-AOT-4

Sequence U-AOT-4 is composed of moderate- to high-amplitude predominately continuous parallel reflectors (Figures 7, 8 & 13). In the axis of Aotea Basin, U-AOT-4 is composed of discontinuous high-amplitude reflectors (Figures 9, 10 & 12). U-AOT-4 is bound by T-AOT-3 and T-AOT-4 (Figures 5, 7 & 8). U-AOT-4 ranges in thickness from 20 to 370 ms; and is thickest in the axis of Aotea Basin (Figures 8 & 15D).

U-AOT-4 is interpreted to represent drowning of Challenger Plateau and a starvation of sediment to Aotea Basin (Figure 15D). Drowning of Challenger Plateau is based on the onlapping of reflectors onto T-AOT-3, and the starvation of sediment to Aotea Basin is based on T-AOT-3 truncating (eroding) underlying strata along the axis of Aotea Basin (Figures 5, 8 & 14).

4 Wells

4.1 Introduction

All well data were sourced from the Ministry of Business, Innovation and Employment's 'Online Exploration Database' and the '2018 Block Offer Data Pack' (www.nzpam.govt.nz). These data were loaded into the seismic interpretation package Seisware™ 10.0, and hence, seismic reflectors and intervening seismic units were integrated with age and paleoenvironmental data from wells.

Five petroleum wells were selected based on their location and that they contain lithological, check shot, biostratigraphic, and geophysical wireline log data. All five wells are vertical, allowing for direct thickness and depth below seabed comparisons to be made. Figure 17 is a transect through these five wells showing how they relate to each other with regards to thickness, lithology and chronostratigraphy. Figure 17 was hung off the base of the late Tongaporutuan (Tt) to remove the influence of Late Miocene to recent progradation at shelfal wells. Unless otherwise stated all depths are metres along hole below drill floor (m AHBDF).

Paleobathymetric interpretations used are modified from (Van Morkhoven et al., 1986):

- Non-marine taken as above mean sea level (amsl) = >0 m amsl
- Marginal marine = 0 – 10 m below mean sea level (bmsl)
- Inner shelf = 0 – 50 m bmsl
- Mid shelf = 50 – 100 m bmsl
- Outer shelf = 100 – 200 m bmsl
- Upper bathyal = 200 – 600 m bmsl
- Mid bathyal = 600 – 1000 m bmsl
- Lower bathyal = 1000 – 2000 m bmsl

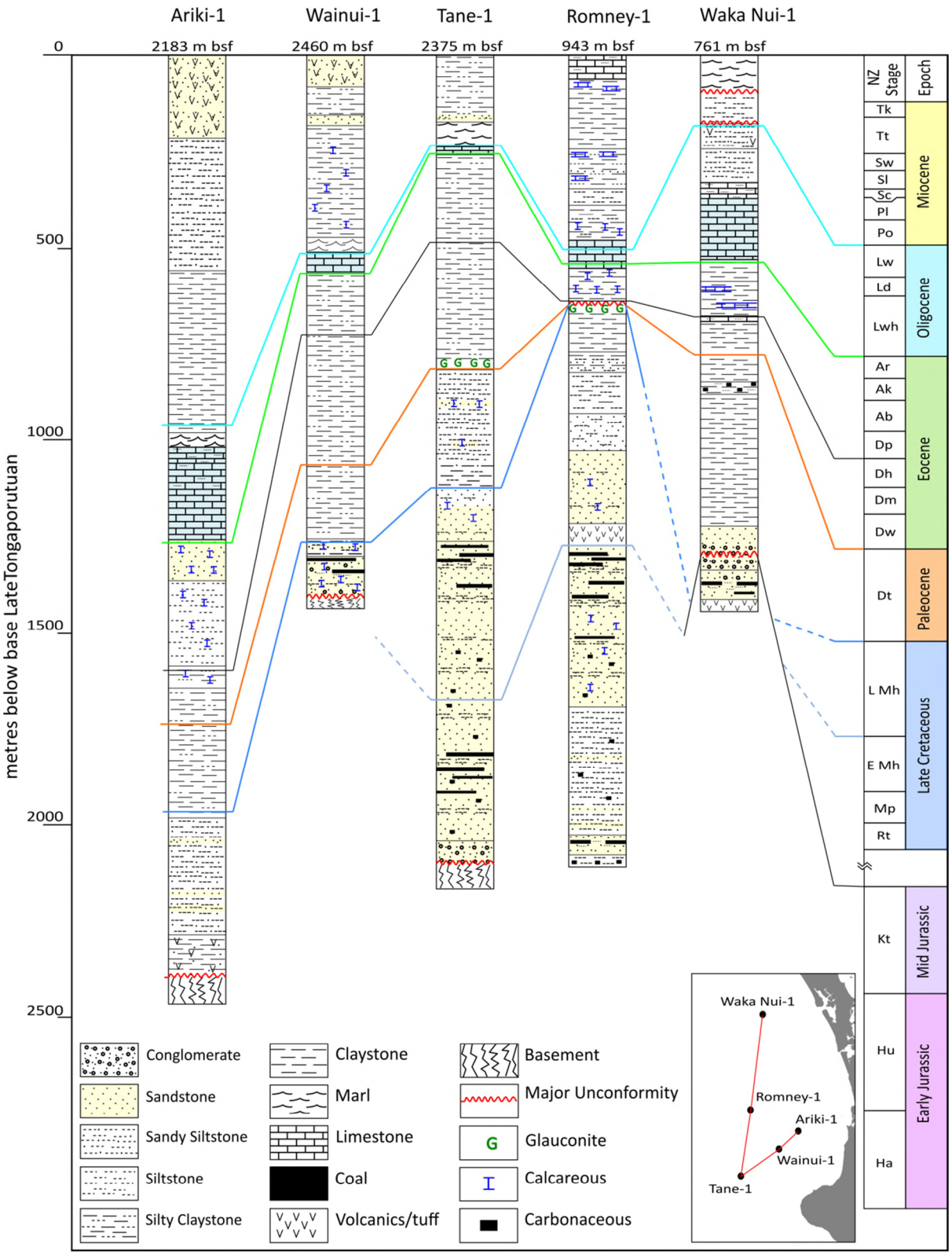

Figure 17 *Well correlation diagram of wells in the study area. See inset map for their location and Figure 1 for relation to seismic sections. All wells are hung off the base of Late Tongaporutuan (Tt) to remove the influence of the late Miocene to recent progradation from the present-day shelf wells.*

4.2 Ariki-1

4.2.1 Summary

Ariki-1 was drilled by Shell BP Todd Oil Services Ltd (SBPT) in 1984, approximately 100 km north northwest of New Plymouth, in 152 m of water, and was drilled to a total depth of 4,822 m. Ariki-1 intersected 4,610 m of Cenozoic and Late Cretaceous sediments, and terminated in the Early Cretaceous Brook Street Volcanics basement terrain (SBPT, 1984).

4.2.2 Time Depth Relationship

Due to hole problems that led to geophone wire becoming key-seated, a full check shot survey was not able to be conducted, and only a total depth measurement was made below the Te Kuiti Group (SBPT, 1984). A total of 5 recordings were made and are plotted in Figure 18 to show the time verse depth relationship. Check-shot number 2 has been plotted but removed from the polynomial calculation, as it has an anomalously fast interval velocity of ~7,500 m/s.

4.2.3 Lithology

Lithology is taken from SBPT (1984).

172.4 (seabed) – 474 m

Riserless drilling/ no returns.

474 – 2,174 m

Massive interbedded, light-greenish-grey to moderate-grey, siltstones and silty claystones. Microfossils and macrofossils range from rare to common, and the later form debris beds.

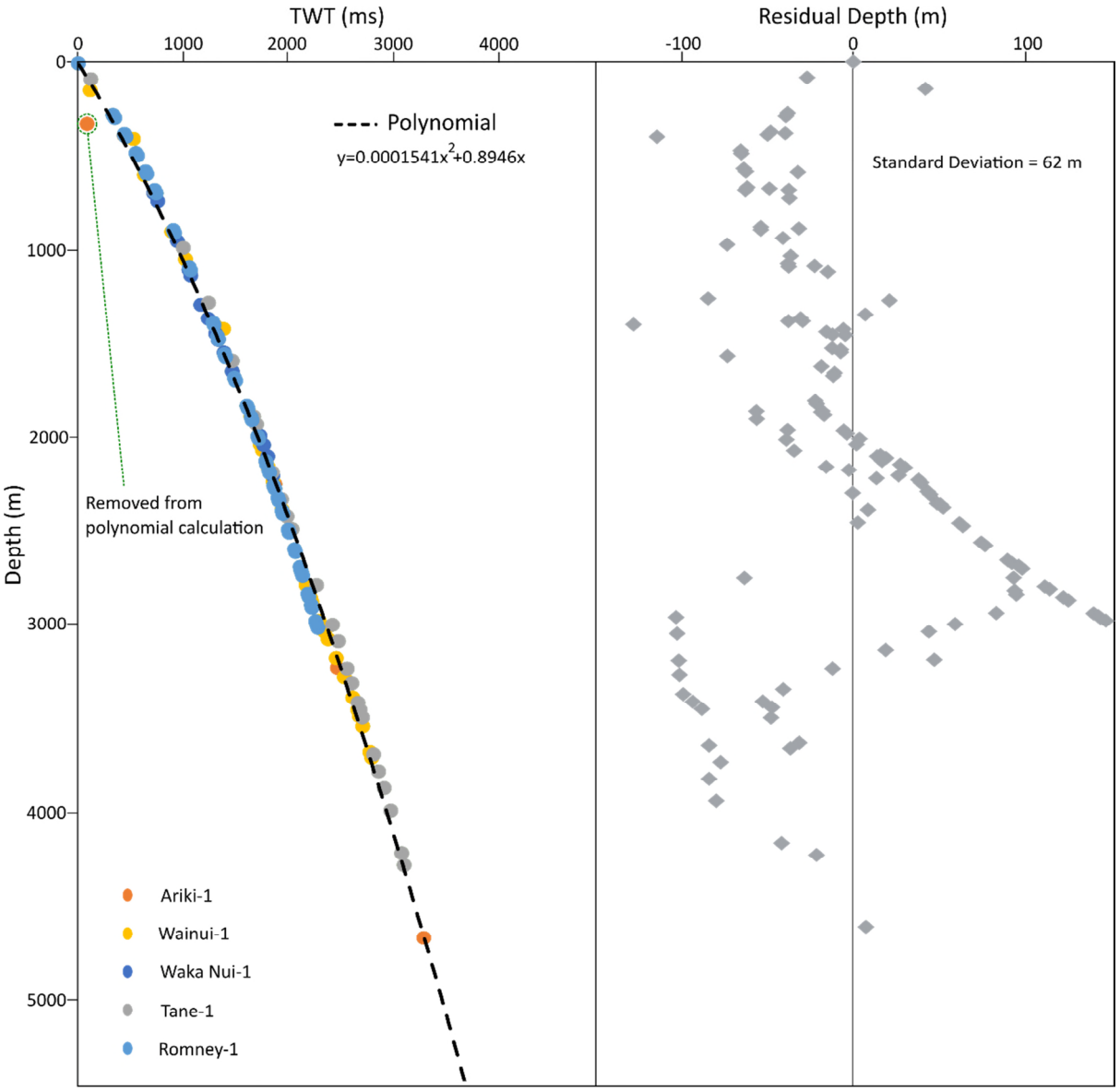

Figure 18 *Left: compilation of all check shot survey data for the wells in the study area to allow for a polynomial to be generated, y = depth in metres (m) below seabed and x = two-way time in milli seconds (ms). Right: residual of all check shot survey data from the polynomial. Note a check shot survey was not carried out at Waka Nui-1, the Stagpoole (2011) two-way time (TWT) to depth relationship has been used in its place. Also note that check shot number 2 for Ariki-1 has been plotted but not used in the polynomial calculation as it is anomalously fast.*

2,174 – 2,256 m

Light-to-moderate-greenish-grey argillaceous planktonic-foraminiferal marl.

2,256 – 2,565 m

Moderate-grey claystones with tuffaceous matrix including biotite, chlorite and pyrite. Grade downhole to light-to-moderate-grey sandy tuffs, which contain abundant angular to sub-angular, fine to medium, poorly-sorted volcaniclasts; biotite, garnet, olivine, hornblende, and aphanitic material.

2,565 – 2,916 m

Predominately light-to-moderate-grey argillaceous siltstones that are very poorly sorted, and angular to round grained. Interbedded with moderate-grey sandstone streaks and lenses that are poorly-sorted, angular to sub-rounded, and predominately fine to medium grained.

2,916 – 3,340 m

White to greenish-grey claystone. Calcareous content increases and silt disappears downhole.

3,340 – 3,364 m

Greenish-grey, soft, planktonic-foraminiferal marl.

3,364 – 3,611 m

Light-grey to white, hard, pure lime-wackstone to occasional lime-packstone.

3,611 – 3,724 m

Buff to grey, angular to sub-angular, fine to coarse grained, poorly to moderately-well sorted, arkosic sandstone. This sandstone interval is separated into two main bodies by an 8 m light-grey lime-wackstone (3,622 – 3,630 m).

3,724 – 3,938 m

Predominately light-greenish-grey to brown, moderately hard, calcareous claystone with common foraminifera. Interbedded with buff to grey, fine to medium grained, tight calcareous cemented, thin sandstone stringers and lenses.

3,938 – 3,996 m

Brick-red to brown, calcareous, silty claystone. Foraminifera are abundant but are poorly preserved with tests being replaced by the red sediment.

3,996 – 4,282 m

Monotonous moderate-to-dark-grey, hard to very hard, fissile, silty and non-calcareous claystone.

4,282 – 4,319 m

Moderate-to-dark-grey, hard, blocky, predominately argillaceous siltstone with rare carbonaceous streaks.

4,319 – 4,638 m

Light-grey to dark-greenish-brown, hard, argillaceous and well cemented siltstones. Finely interbedded with white to moderate-grey, very-fine to fine grained, sub-angular to round, poorly-sorted, well cemented, and tight sandstones.

4,638 – 4,762 m

Light-to-moderate-grey and occasionally greyish-brown, very hard, fissile, non-calcareous claystone. Sand content varies from trace to common, except at the base of the section where sand-grade volcaniclastics are recognised; biotite, garnet, and pyrite.

4,762 – 4,822 m (basement)

Metamorphosed basic igneous rocks.

4.2.4 Biostratigraphy

Paleobathymetry estimates from foraminiferal (benthic) analysis by Hayward (1986) on cuttings from Ariki-1 reveal a history of transgression, maximum flooding, and regression (Figure 19). The site initially experienced marginal marine to shelfal environments during the Haumurian to early Teurian, with rapid deepening to lower bathyal depths in late Teurian that persisted until Waitakian, when the site further subsided in Otaian (maximum flooding). The site began a slow regression during Southland to Taranaki series with rapid shallowing to outer shelf depths during Wanganui series (Hayward, 1986).

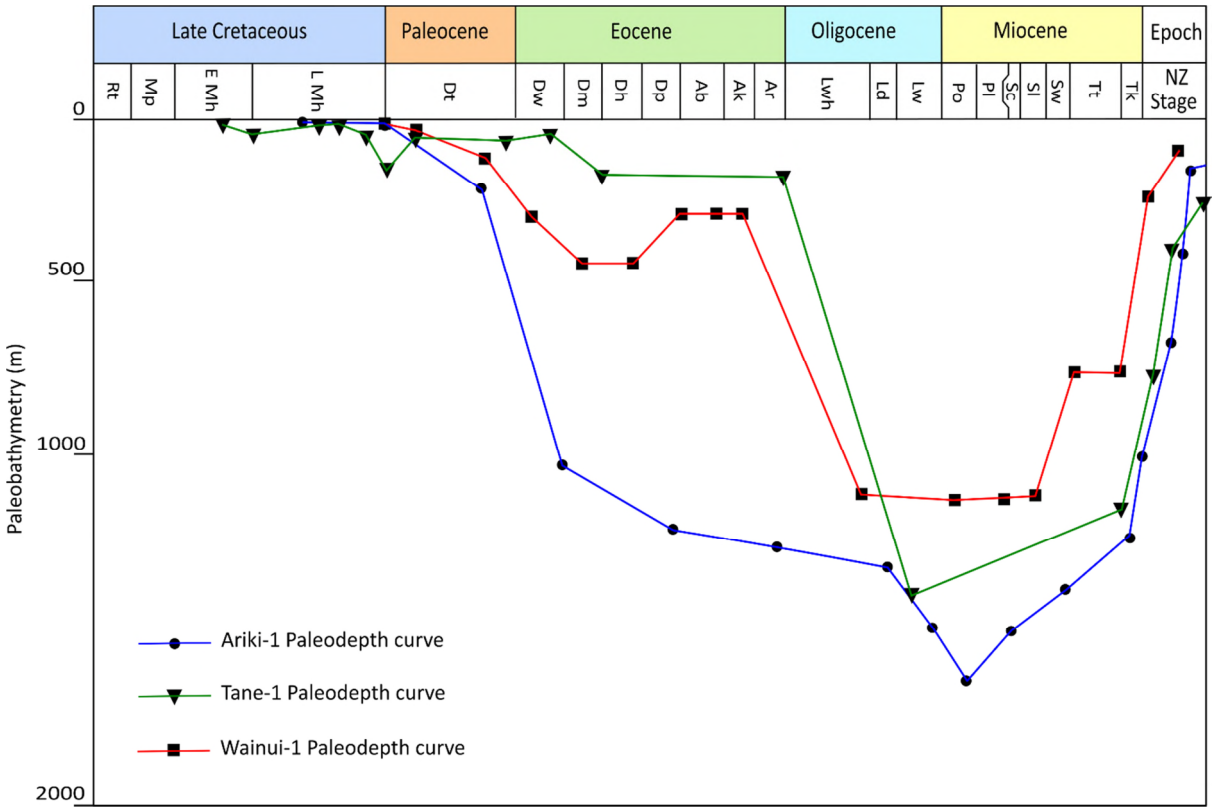

Figure 19 *Paleobathymetry curve with respect to geologic time for Ariki-1 and Wainui-1 derived from foraminifera (Hayward (1986), Hayward (1984), Hayward (1985)).*

Palynological analysis by SBPT (1984) allows for interpretation to be made on second or possibly third order sequences during Haumurian to late Teurian and possibly as young as Runangan to be super imposed on the first order mega-sequence. Diagnostic species of exact paleoenvironment are not present, however, ratios of pollen and spores to dinoflagellates allows for estimates of base level change i.e. change in water depth, sediment supply or combination of both (Catuneanu et al., 2011, Allen and Allen, 2013). The ratios in Ariki-1 over the depth interval 3699 – 4760 m indicate a marine environment that fluctuated from marginal marine/estuarine to outer shelf, i.e. regression and transgression cycles. Figure 20 shows the site experienced regression from 4749 to 4734 m (Haumurian), transgression 4620 to 4508 m (Haumurian), regression 4508 to 4379 m (Haumurian), transgression 4379 to 3939 m (Dannevirke series), and regression from 3939 to 3699 m (Arnold series).

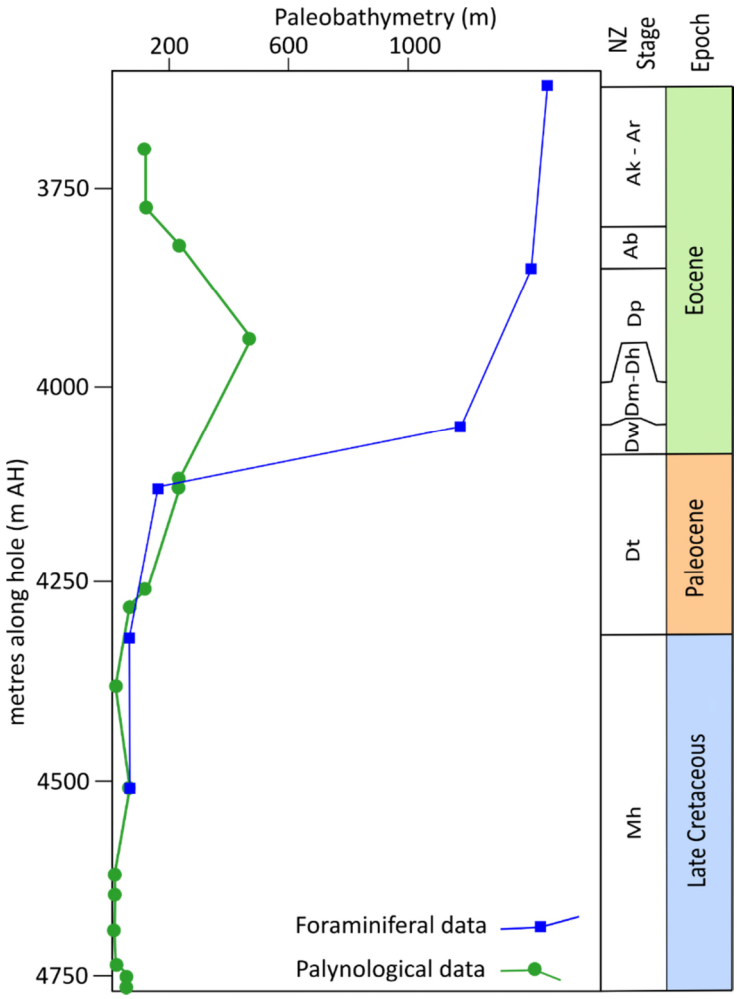

Figure 20 *Paleodepth curve of Ariki-1 over the Eocene to Late Cretaceous sediments. Foraminiferal depths are derived from benthic species (Hayward, 1986). Palynological depths are determined on the abundance of dinoflagellates and their ratio to terrestrial pollen and spore (SBPT, 1984).*

Eocene samples show a large discrepancy between foraminiferal and palynological interpretations (Figure 20). Foraminiferal data are considered more reliable for paleobathymetry estimates, due to foraminifera being environmentally diagnostic and it is not possible to transport deep water sediments into shallow water, but it is possible to transport shallow water sediments downslope. Hence, it is interpreted that the site was experiencing lower bathyal environment, and the palynology shows that the basin was experiencing base level fluctuations. Late Eocene regression indicated by the palynology is further evidenced by the deep water fan facies of the Tangaroa Formation (3611 to 3724 m AH) in Ariki-1 (SBPT, 1984). Deep water fans are regularly associated with progradational or forced

regression systems as a result of either increased sediment supply or falling base level, respectively (Catuneanu et al., 2009, Catuneanu et al., 2011, Allen and Allen, 2013, Neal and Abreu, 2009, Mitchum Jr and Vail, 1977, Mitchum Jr et al., 1977). These deepwater fan systems introduce proximal shelf sediments and their associated paleobathymetry markers i.e. pollen, spores, dinoflagellates, and foraminifera into bathyal environments.

4.2.5 Geophysical logging

A comprehensive suite of wireline geophysical logs were run during the drilling of Ariki-1 (SBPT, 1984). However, hole conditions over the 8.5" section from 3760 m to total depth is considered poor with an extremely rugose borehole, see caliper log (Figure 21). Despite the poor hole conditions impacting the quality of data collected, the gamma ray log displays 3 coarsening up motifs between 4740 and 4280 m (Haumurian to early Teurian) that broadly agree with the palynological data discussed in section 4.2.4 (Figures 20 & 21).

4.2.6 Additional observations

"Unit 3" in the Turi Formation (formally Kaiata Formation) 3938 – 3996 m is described as a brick red to brown, calcareous, silty shales. This very distinctive unit was also intersected in Tangaroa-1 (SBPT, 1984). Foraminifera are abundant but are poorly preserved as the tests have been dissolved and replaced by red sediment. The unit is dated to the Porangan and Heretaungan boundary(SBPT, 1984).

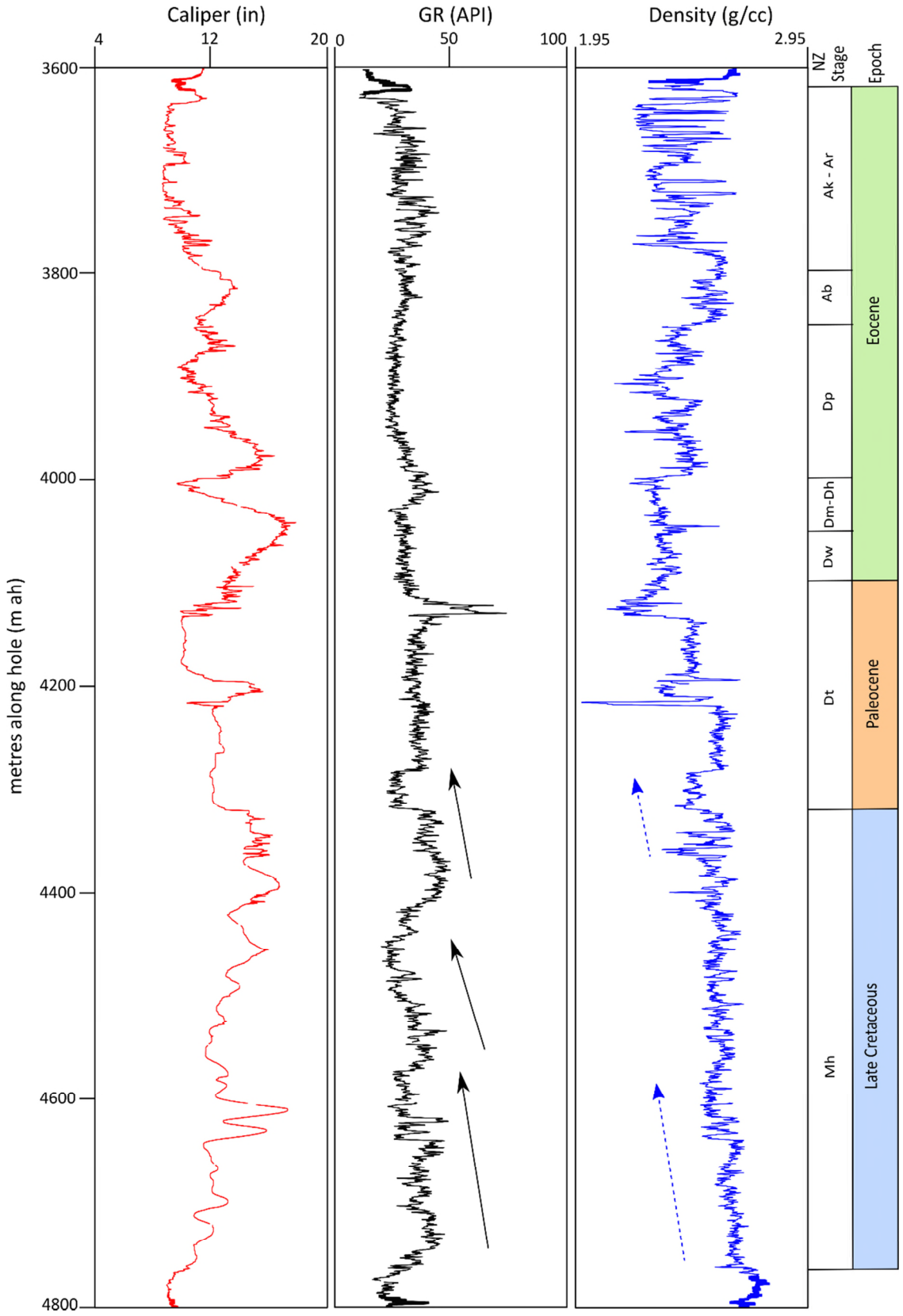

Figure 21 *Plot of the caliper log (red) and two geophysical wireline traces for Ariki-1 over the 8 ½" open hole section, gamma ray (GR, black), and density (blue). Black solid arrows highlight 3 coarsening upwards motifs seen on the gamma ray trace, this is interpreted to indicate 3 regressive cycles. The upper and lower motifs can also be seen in the density trace, blue dashed arrows.*

4.3 Wainui-1

4.3.1 Summary

Wainui-1 was drilled by Shell BP Todd Oil Services Ltd (SBPT) in 1981, approximately 96 km northwest of New Plymouth, in 153.7 m of water, and was drilled to a total depth of 3,894 m. Wainui-1 intersected 3,724.6 m of Cenozoic and Late Cretaceous sediments, and terminated in what is thought to be Palaeozoic aged schist (SBPT, 1982).

Due to severe wind gusts blowing the drilling vessel off location during the drilling of the 12 ¼" hole, an emergency disconnect was performed by shearing the drill string and dropping 1,427 m of pipe to the bottom of the hole (3,500 m). The sheared drill string could not be fished, so the decision was made to cement plug back to 1,580 m and Wainui-1 was successfully side-tracked with a kick-off at 1,630 m (SBPT, 1982).

4.3.2 Time Depth Relationship

A check shot survey was undertaken with recordings made at 28 levels in Wainui-1 (SBPT, 1982). Good downhole breaks were obtained over the interval 1,671 m – 3,881 m ah (SBPT, 1982). The results of these recordings are displayed on Figure 18 and were incorporated in the polynomial calculation.

4.3.3 Lithology

Lithology is taken from SBPT (1982)

165.4 (seabed) – 464 m

Riserless drilling/ no returns.

464 – 1,664 m

Unconsolidated to poorly consolidated, moderate-grey, predominately silty claystone. Interbedded with coarse, poorly sorted, shelly sandstones and siltstones.

1,664 – 2,215 m

Moderate-grey silty claystones, occasional carbonaceous streaks, increasingly calcareous downhole.

2,215 – 2,307 m

Dark green-grey, soft, marl, rich in foraminifera.

2,307 – 2,612 m

Moderate-grey, moderately consolidated to poorly consolidated, tuffaceous sandstone. Contains biotite, hornblende, and aphanitic clasts. Downhole grades to a silty claystone and tuffaceous material decreases.

2,612 – 2,931 m

Predominately light-to-moderate-blue-grey claystone, common foraminifera and carbonate content increasing downhole, glauconite and pyrite are observed regularly. Interbeds of moderate-grey, angular, medium grained quartz sandstone beds and stringers.

2,931- 2,968 m

Moderate-grey foraminiferal marl.

2,968 – 3,022 m

Light-grey to white, wackestone to packstone, foraminiferal limestone.

3,022 – 3,650 m

Monotonous sequence of light-grey and dark-grey, occasionally calcareous, sub-fissile, slightly silty claystones and claystones. This sequence is under compacted and results in typical conchoidal fractured cuttings.

3,650 – 3,718 m

Brownish-grey, fissile, silty claystone. Normal compaction.

3,718 – 37,62 m

Dark-to-moderate-grey, slightly calcareous, silty claystone. Interbedded with light grey sandstone stringers.

3,762 – 3,890 m

Typical coal measure sequence of sandstone, siltstone, carbonaceous claystone and coal seams. Sandstones are predominately composed of quartz with variable amounts of plagioclase and feldspar, regularly carbonate cemented, local glauconite and calcite. Siltstones and claystones range from light-greyish-brown to almost black depending on carbon content. Coals are hard, dark-brown to black, laminated and vitreous grading to dull lustre where grading to carbonaceous claystone.

3,890 – 3,894 m (basement)

Schist – assumed to have similar composition to that which outcrop in northwest Nelson.

4.3.4 Biostratigraphy

Paleobathymetry estimates from foraminiferal (benthic) analysis by Hayward (1984) on cuttings from Wainui-1 reveal a history of transgression, maximum flooding, and regression (Figure 19). This analysis also suggests either a major regression or transient tectonic uplift event in the Arnold Series (Figure 19). Original biostratigraphy carried out by SBPT (1982) also describes this first order mega-sequence; transgression, maximum flooding, and regression. However, SBPT (1982) do not interpret the major regression or transient tectonic uplift event in the Arnold Series but rather "a clear deepening uphole through Palaeocene to late Eocene times. Although this was a gradual process it was not continuous but a series of transgressive cycles". These transgressive cycles are only inferred based on benthic to planktonic ratios, there is no other biostratigraphic, lithologic, or wireline geophysical evidence to demonstrate them. Figure 22 shows the difference in interpretation between SBPT (1982) and Hayward (1984).

4.3.5 Geophysical logging

A comprehensive suite of wireline geophysical logs were run during the drilling of Wainui-1: gamma ray, resistivity (shallow and deep), sonic velocity, spontaneous potential, neutron porosity and density.

In the original hole open hole logs were run to 3,380 m, the hole was lost before the lower 120 m could be logged (SBPT, 1982). The logs are reasonably good quality, with hole gauge being within tolerance.

The 12 ¼" side-track was not open hole logged due to poor hole conditions. However, the gamma ray, density and neutron porosity tools were used to log through casing (1,630 –

3,550 m), in order to confirm that the lithologies in the side-track were similar in nature to those in the vertical hole (SBPT, 1982).

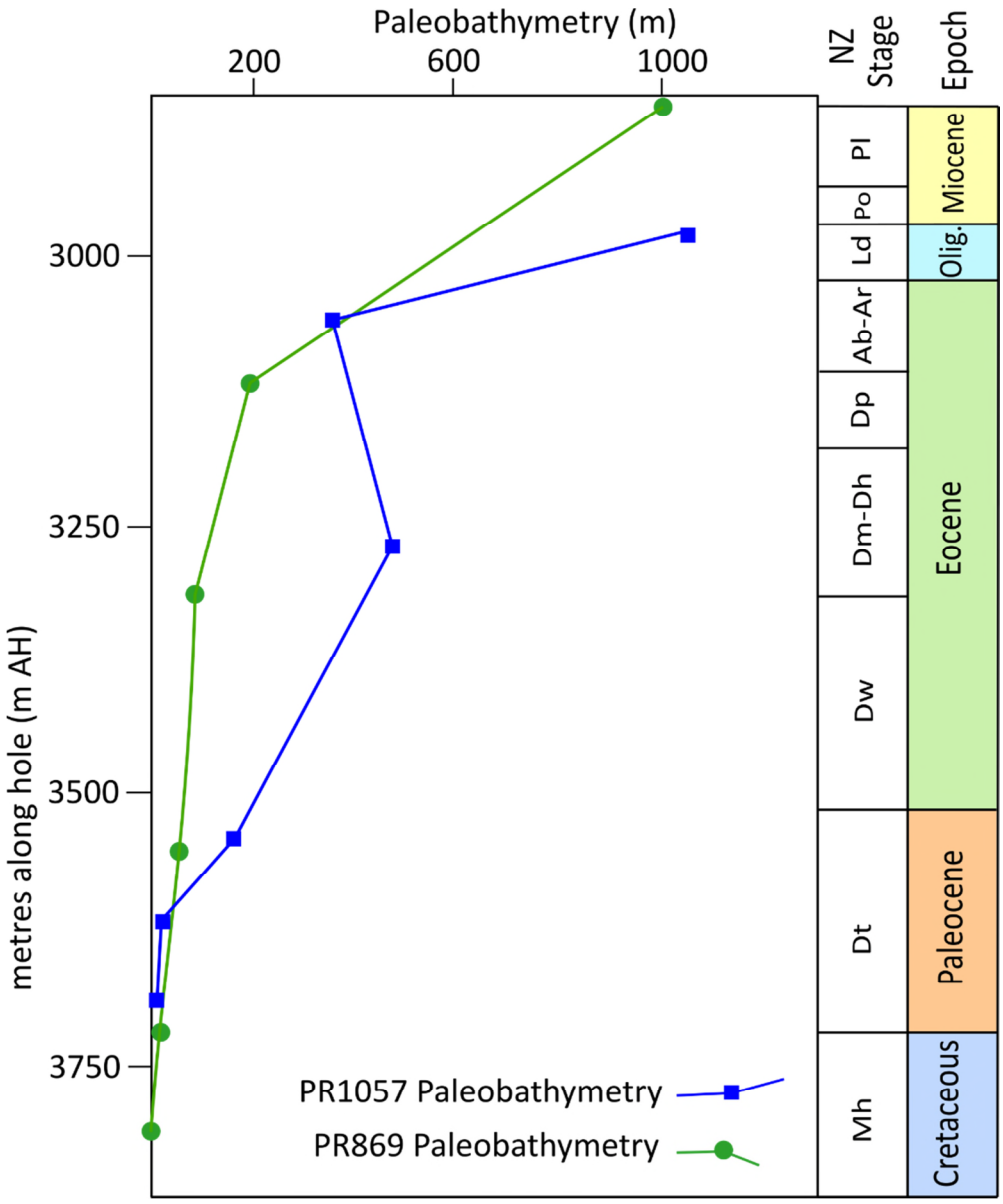

Figure 22 *Paleodepth curve of Wainui-1 over the Late Cretaceous to Eocene sediments. PR869 paleobathymetry is from SBPT (1982) and PR1057 paleobathymetry derived from foraminifera by Hayward (1984).*

Based on the rate of penetration it was predicted that the over pressured Eocene shales section had been completely drilled through at 3,470 m in the 12 ¼" hole and was behind casing(SBPT, 1982). Due to this belief the mud weight was reduced for the drilling of the 8

½” hole. This proved to be incorrect and caused severe washouts (up to 20”) to occur from the casing shoe/3,550 m to 3663 m, at which depth the formation pressures returned to normal (SBPT, 1982). The severely out of gauge top portion of the hole and rugose nature of the lower section, resulted in poor quality logs that do not allow for any valuable insights to be gained.

4.4 Tane-1

4.4.1 Summary

Tane-1 was drilled by Shell BP Todd Oil Services Ltd (SBPT) in 1976, approximately 130 km west of New Plymouth, in 153.6 m of water, and was drilled to a total depth of 4,539 m. Tane-1 intersected 4,290.2 m of Cenozoic and Late Cretaceous sediments, and terminated in Separation Point Granite (SBPT, 1977).

4.4.2 Time Depth Relationship

Three well velocity surveys were carried out giving 26 reliable check shots (SBPT, 1977). The results of these recordings are displayed on Figure 18 and were incorporated in the polynomial calculation.

4.4.3 Lithology

Lithology is taken from SBPT (1977).

185 (seabed) – 485 m

Riserless drilling/ no returns.

485 – 2,140 m

Interbedded massive, unconsolidated, light-grey silty claystones, siltstones, and arenaceous siltstones. At times calcareous and micaceous.

2,140 – 2,210 m

Interbedded grey to white foraminiferal limestones and calcareous claystones with minor fine-grained sandstone stringers.

2,210 – 2,547 m

Massive, light-grey, highly calcareous claystone interbedded with blocky silty fine-grained sandstones up to 7 m thick.

2,547 – 2,610 m

Massive, grey-brown grading to light-brown, argillaceous foraminiferal marl.

2,610 – 2,633 m

White foraminiferal lime wackstone grading into a packstone.

2,633 – 3,194 m

Massive, grey-brown to dark-grey, slightly glauconitic, pyritic, calcareous to non-calcareous claystone.

3,194 – 3,195 m

Dark green highly glauconitic sandstone containing varying amounts clay matrix.

3,195 – 3,455 m

Light-grey to grey-brown, micaceous, calcareous arenaceous siltstones. Interbedded with well to poorly sorted, slightly glauconitic, silty fine-grained sandstone.

3,455 – 3,492 m

Massive, grey-brown to dark-grey, slightly glauconitic, pyritic, calcareous to non-calcareous claystone.

3,492 – 3,638 m

Predominately a white to light-grey, calcareous, well to poorly sorted, fine to medium grained quartzose sandstones containing varying amounts of claystone matrix.

3,638 – 3,725 m

Dark-brown, non-calcareous, micaceous, carbonaceous, silty claystones and thin bituminous coals.

3,725 – 4,000 m

Predominately white, medium to coarse, moderately sorted, argillaceous quartzose sandstones. Interbedded with dark brown, silty, micaceous, carbonaceous claystones and coal streaks.

4,000 – 4,025 m

Dark-brown, non-calcareous, micaceous, carbonaceous, silty claystones and thin bituminous coals.

4,025 – 4,405 m

Predominately white, medium to coarse, moderately sorted, argillaceous quartzose sandstones. Interbedded with dark brown, silty, micaceous, carbonaceous claystones and coal streaks.

4,405 – 4,425 m

Dark-brown, non-calcareous, micaceous, carbonaceous, silty claystones and thin bituminous coals.

4,425 – 4,475 m

Conglomerate consisting of granitic material.

4,475 – 4,539 m (basement)

Separation Point Granite.

4.4.4 Biostratigraphy

Hayward (1985) described the paleobathymetry of Tane-1 derived from foraminiferal analysis as first order mega-sequence; transgression, maximum flooding, and regression (Figure 19). The site initially experienced a slow transgression in Haumurian from non-marine to inner shelf in the early Teurian and progressing to outer shelf by the late Arnold. The site experienced rapid deepening to lower bathyal depths in Landon times that persisted until Pareora to early Southland Series (maximum flooding). The site began a rapid regression in late Southland progressing through mid-bathyal depths during Taranaki and upper bathyal depths during Wanganui Series reaching outer shelf depths in the mid Nukumaruan Stage (Hayward, 1985). Later work by Strong and Wilson (2002), and Raine

and Schiøler (2012) agree with this initial interpretation of a first order mega sequence and add detail with possibly second or third order events recognised in late Haumurian and early Teurian (Figure 23). These second order sequences are recognised as lithologic changes: shallowing of water depths between ~3,640 and ~3,720 m is represented by coal beds and carbonaceous siltstones implying a coastal plain environment (Figure 23).

4.4.5 Geophysical logging

A comprehensive suite of wireline geophysical logs were run during the drilling of Tane-1: gamma ray, density, resistivity (shallow and deep), neutron porosity, sonic velocity and spontaneous potential (SBPT, 1977).

The logs are good quality as the borehole is relatively smooth with significant washouts only occurring between 2,715 m and 2,770 m in uncompacted late Eocene claystone, and at the 9 5/8" casing shoe 3,085 – 3,180 m, see caliper log in Figure 23.

The density and sonic velocity log traces show several important changes in lithology (Figure 23). At the base of Oligocene limestone (2,633 m) there is a sharp downhole decrease in both density and sonic velocity in late Eocene claystone (SBPT, 1977). At the Eocene-Paleocene boundary (3,195 m), there is a downhole increase in both density and sonic velocity as the lithology changes from claystone to siltstone, but this shift is slightly obscured by the washout caused by the casing shoe above. At the Paleocene-Cretaceous boundary (3,492 m), there is a subtle increase downhole in sonic velocity. Below the Paleocene-Cretaceous boundary, log traces display a spiky motif of thin low gamma ray, density and velocity intervals that indicate coal beds, and thin low gamma ray, high density and high velocity intervals which indicate limestone stringers or carbonate cemented sandstones.

The density and sonic velocity log traces show a trend of steady increase with depth below the base of the Oligocene limestone (2,633 m) (Figure 23).

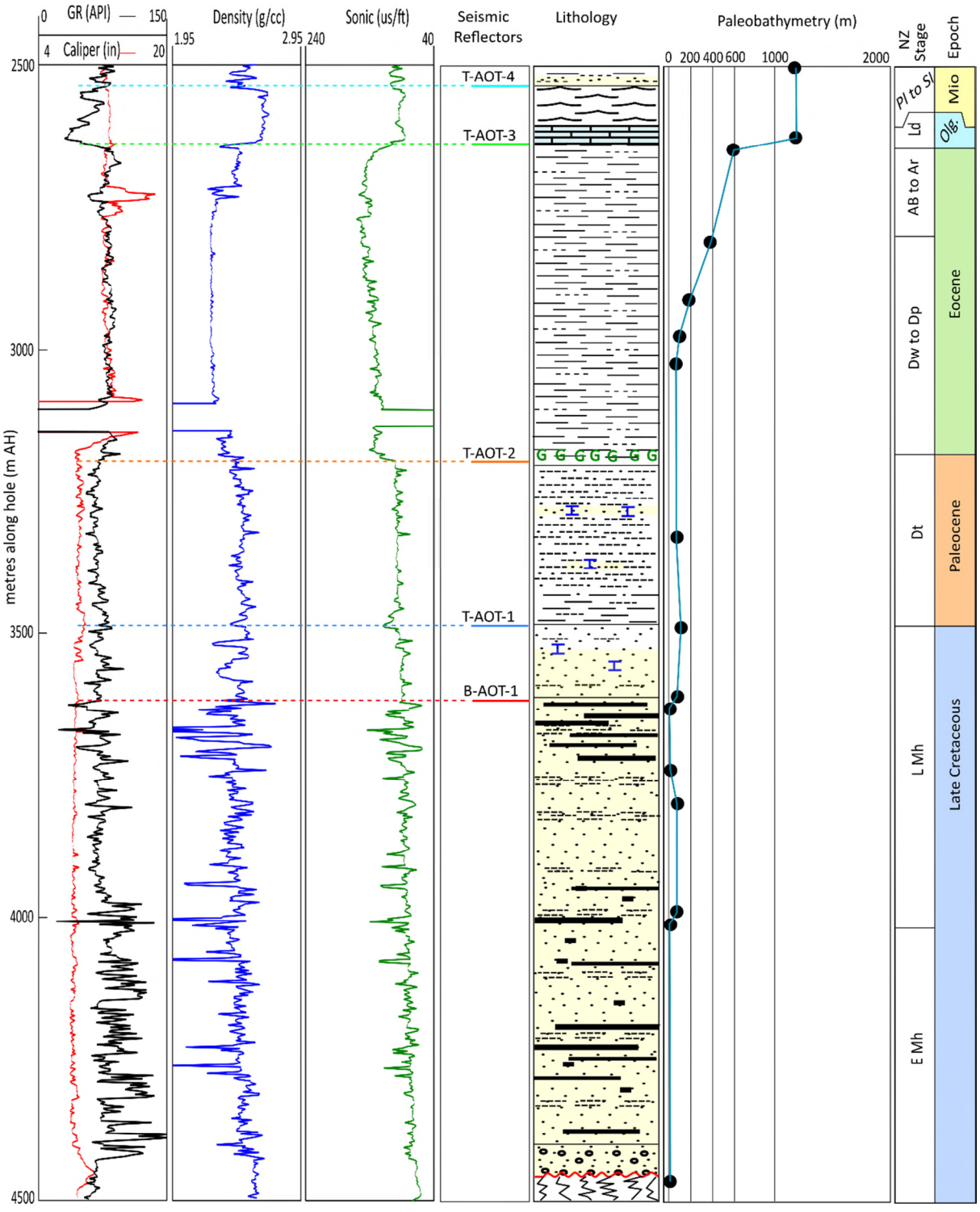

Figure 23 *Composite log of Tane-1 showing the relationship between wireline geophysical logs, seismic reflectors, chronostratigraphy and paleobathymetry in relation to lithology. There is good agreement between the lithofacies described in the mud log (SBPT, 1977) and the paleoenvironment interpretations by Strong and Wilson (2002), and Raine and Schiøler (2012) e.g. the shallowing of water depths between ~3,640 and ~3,720 m is represented by coal beds and carbonaceous siltstones implying a coastal environment. Note the strong correlation of seismic reflectors to changes in wireline geophysical logs and lithology. See Figure 17 for lithology key.*

4.5 Romney-1

4.5.1 Summary

Romney-1 was drilled by Anadarko New Zealand Taranaki Company (Anadarko) in 2015, approximately 175 km northwest of New Plymouth, in 1,546.6 m of water, and was drilled to a total depth of 4,619 m. Romney-1 intersected 3,074.4 m of Cenozoic and Late Cretaceous sediments, and terminated in Teratan aged carbonaceous siltstone (Rad, 2015).

4.5.2 Time Depth Relationship

A check shot survey was undertaken after total depth was reached at Romney-1. A total of 28 shots were recorded with a two shuttle (15.12 m spacing) downhole tool giving a total of 56 recordings (Rad, 2015). Data quality below 2,048 m (477.14 m below seabed) is considered very good, above this depth casing noise significantly affects quality (Rad, 2015).

The results of these recordings are displayed on Figure 18 and were incorporated in the polynomial calculation.

4.5.3 Lithology

Lithology is taken from (Rad, 2015).

1571 (seabed) – 2,369 m

Riserless drilling/ no returns.

2,369 – 2,506 m

Calcareous claystone with trace very fine sand, grading to silty claystone downhole. Limestone stringers were encountered throughout.

2,506 – 2,576 m

Predominantly limestone interbedded with argillaceous limestone, calcareous claystone and siltstone. Grades to calcareous claystone over lowermost 10 m.

2,576 – 2,993 m

Predominantly calcareous claystone, grading to interbeds of siltstone and argillaceous limestones in places. Rare thin sandstone and limestone stringers.

2,993 – 3,067 m

Predominantly clean limestone with rare calcareous claystone stringers. Lowermost 6.5 m grades into calcareous claystone.

3,067 – 3,161 m

Calcareous claystone interbedded with minor thin limestone beds and stringers.

3,161 – 3,286 m

Claystone interbedded with minor calcareous claystone and generally rare glauconite beds. Samples at top of section (e.g. 3,178 m) had up to 50% dark greenish to black fine rounded, well sorted glauconite grains in a clay matrix.

3,286 – 3,439 m

Claystone interbedded with siltstone and minor sandstone.

3,439 – 3,733 m

Predominantly sandstone grading to interbeds of argillaceous sandstone, arenaceous siltstone, and siltstone in places. Rare volcaniclastics appearing below 3,680 m.

3,733 – 3,784 m

Predominately volcanics – variably weathered and degraded volcaniclastics, basalt, and tuff. Interbedded with siltstone in places.

3,784 – 4,204.5 m

Graded beds/interbeds of sandstone and siltstone with coal seams up to 3 m thick but mostly 0.5 – 1 m thick.

4204.5 – 4528 m

Stacked broadly coarsening uphole cycles of siltstone becoming medium grained sandstone.

4,528 – 4,537 m

Thin graded interbeds of sandstone, siltstone and coal seams (0.5 – 1 m thick).

4,537 – 4,586 m

Interbeds of sandstone and siltstone with minor claystone.

4,586 – 4,619 m (total depth)

Carbonaceous silt dominated with very minor sandstone and siltstone in places.

4.5.4 Biostratigraphy

Schiøler et al. (2014) reviewed samples from Romney-1 for foraminifera and nannofossil (51 cuttings samples), and palynomorphs (76 cuttings and 3 sidewall core samples). Their work shows that the paleoenvironment at the site of Romney-1 can be divided into two; marginal marine to shelfal during the Late Cretaceous to late Waipawan, and lower bathyal from Heretaungan to present (Figure 24).

During the Late Cretaceous (4,619 – 3,169 m), the site experienced a first-order transgressive sequence with second-order and possibly third-order regressive/transgressive sequences super imposed, e.g. from 4,550 to 4,450 m the site experienced a transgression followed by a regression from 4,410 – 4,270 m (see paleobathymetry in Figure 24).

From Heretaungan to present (seabed is 1,546.6 m bmsl), the site has experienced lower bathyal environment (Figure 24), the Tongaporutuan shallowing event to mid bathyal depths is interpreted to be the result of reworked sediment being deposited on the basin floor via mass wasting of the prograding shelf edge.

The significant transition from marginal and shelfal marine environments of the Late Cretaceous to late Waipawan, to lower bathyal environment of the Heretaungan to present, is complicated by a hiatus followed by a condensed Eocene section (Figure 24 & 25). This is highlighted by the findings of Schiøler et al. (2014), which is summarised below.

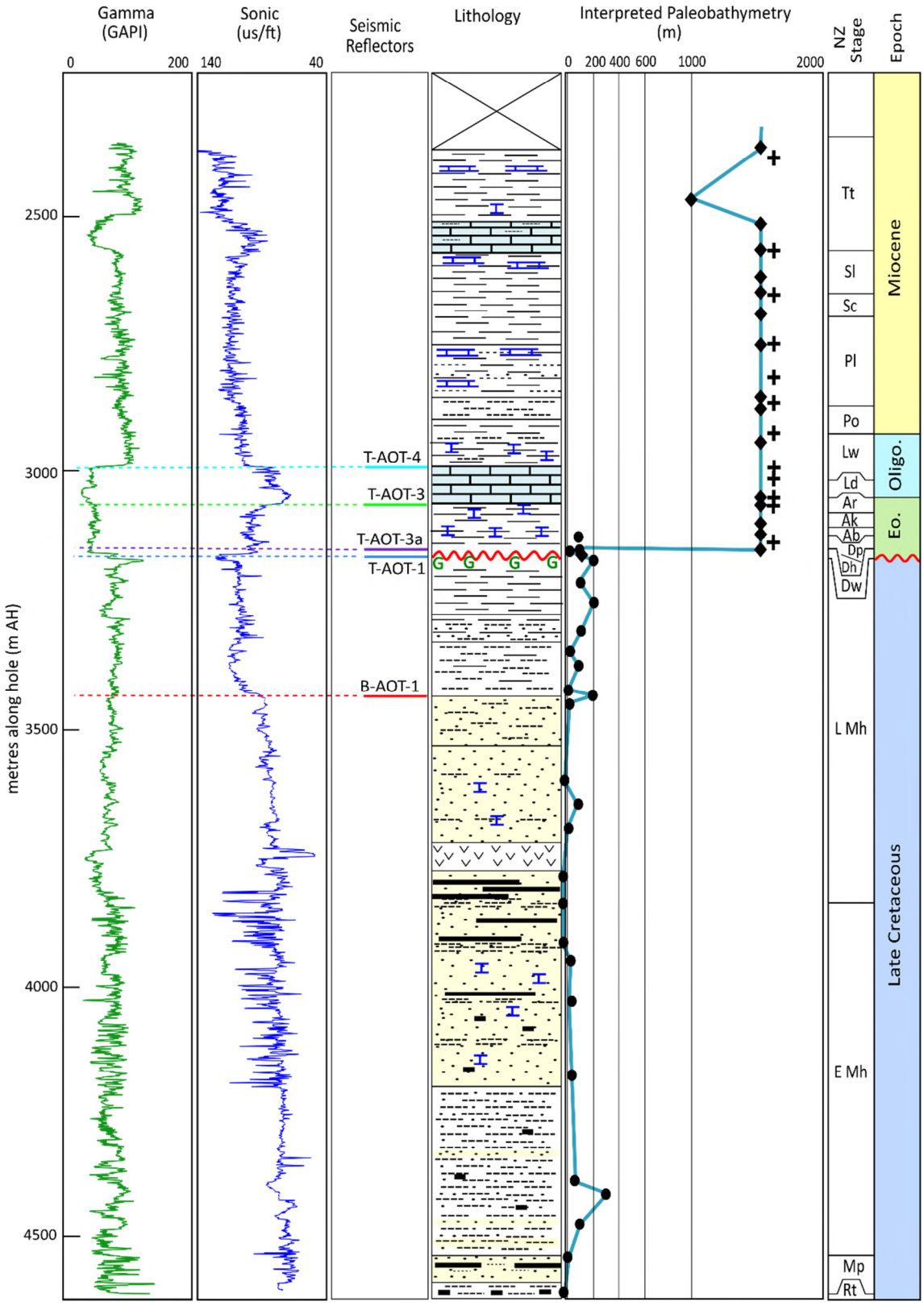

Figure 24 *Composite log of Romney-1 showing the relationship between wireline geophysical logs, seismic reflectors, chronostratigraphy and paleobathymetry (diamond = foraminifera, cross = nannofossil, circle = palynology) (Schiøler et al., 2014) in relation to lithology. The chronostratigraphy shows a significant hiatus and condensed section at the base of the Eocene top of the Late Cretaceous, this boundary is represented by a significant change in paleobathymetry and glauconite rich bed. Note the strong correlation of seismic reflectors to changes in wireline geophysical logs and lithology. See Figure 17 for lithology key.*

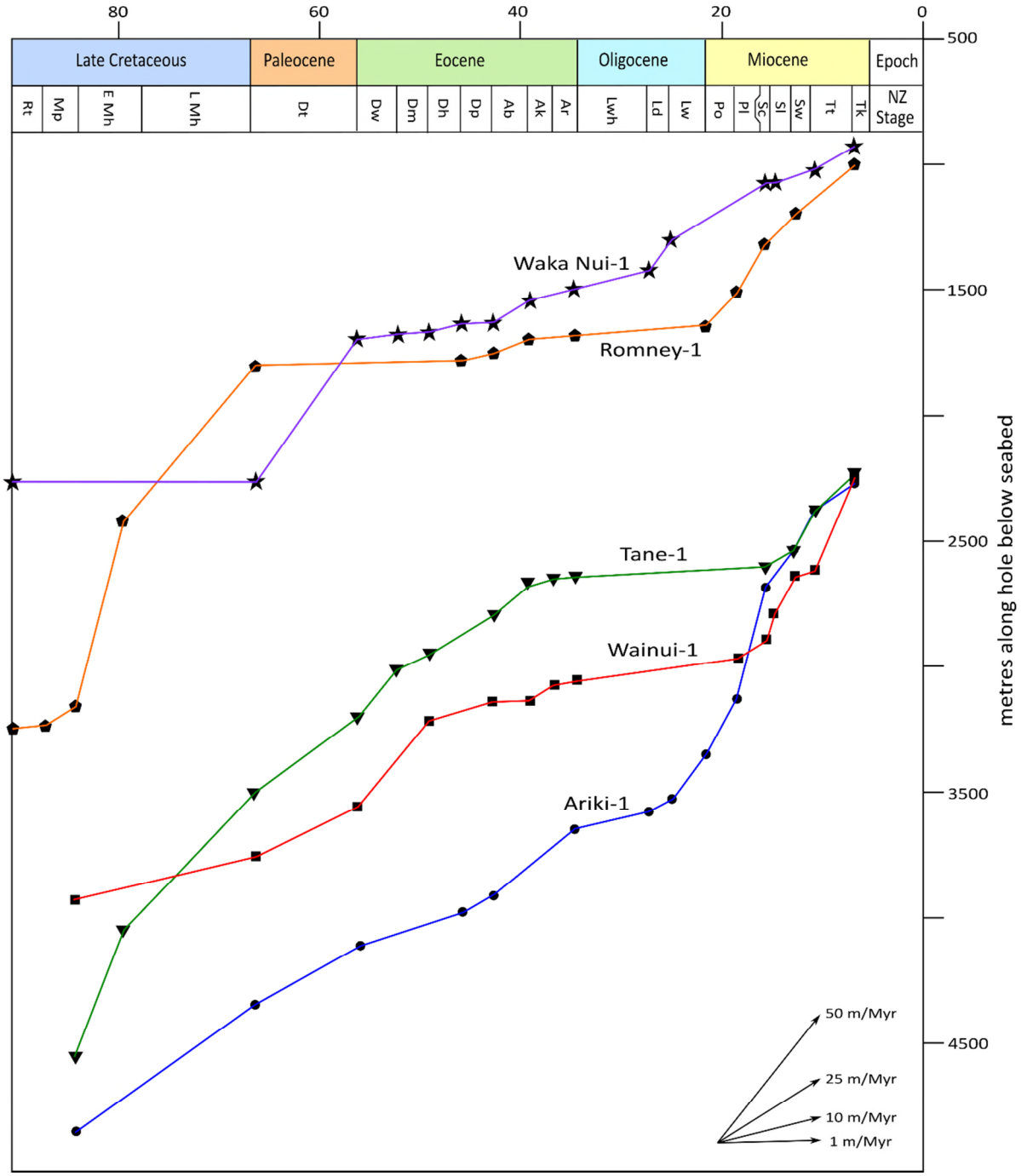

Figure 25 *Sediment accumulation verse geologic time curve for all wells in the study area. Note the Early to Middle Jurassic for Waka Nui-1 has not been included.*

Foraminifera

Cuttings from 3,126 – 3,151 m are interpreted to be deposited in open oceanic conditions at lower bathyal depths during Porangan. Cuttings from 3,151 – 3,160 m are interpreted to be deposited in open oceanic conditions at lower bathyal depths during Heretaungan. Cuttings from 3,169 – 3,196 m are interpreted to deposited in restricted marine environment, possibly bathyal, during the latest Haumurian to potentially Teurian. Cuttings from 3,509 – 4,550 m are indeterminate for age but indicate mid shelf to estuarine environment.

Nannofossils

Cuttings from 3,142 – 3,151 m yield a moderate volume and high diversity of nannofossils, and are assigned to the Zone CP13b (Porangan). Cuttings from 3,151 – 3,160 m yield a moderate volume and diversity of nannofossils, and are assigned to Zone CP13a – CP12b (Porangan to possibly Heretaungan).

Palynology

Cuttings from 3,126 – 3,135 m are interpreted to be deposited in an outer shelfal environment during the PM3B-MH1 miospore Zone and are assigned to the *Wilsonidium echosuturatum* dinoflagellate Zone (Porangan). Cuttings from 3,151 – 3,160 m are interpreted to be deposited in a shelfal marine environment during the PM3B-MH1 miospore Zone and are assigned the *Wetzeliella spinulosa* dinoflagellate Zone (Waipawan). However, cuttings from 3,151 – 3,160 m do contain rare Teurian and late Haumurian taxa, these older taxa are thought to be reworked from underlying or proximal strata (Schiøler et al., 2014). Cuttings from 3,160 – 3,241 m were deposited in nearshore to shelfal and possibly offshore marine (i.e. deeper water downhole) during the PM2 miospore Zone and are assigned to the *Manumiella druggii* dinoflagellate Zone (Haumurian).

4.5.5 Geophysical logging

Romney-1 was comprehensively geophysically logged both via logging while drilling (LWD) and open hole wireline geophysical logs (Rad, 2015).

LWD data acquisition of gamma ray and resistivity information was acquired over the entire borehole length, and sonic velocity was acquired from 2,369 m to 4,619 m (total depth) (Rad, 2015).

A total of 6 open hole wireline logging runs were made after total depth was reached (3,410 - 4,619 m).

Figure 24 plots the spliced gamma ray and sonic velocity traces from both the LWD and open hole geophysical wireline logging suites. These two traces were chosen as they demonstrate several significant events that correlate strongly with the lithology intersected:

- At 2,508 m, there is a sharp increase in the sonic velocity trace and a sharp decrease in the gamma ray trace that corresponds to the top of the early Tongaporutuan limestone. At the base of this unit (2,574 m), there is a sharp decrease in the sonic velocity trace and increase in the gamma ray trace.
- From 2,574 – 2,993 m, the sonic velocity and gamma ray traces are relatively smooth with the occasional spike and are on an increasing trend with downhole.
- At 2,993 m, there is a sharp increase in the sonic velocity trace and a sharp decrease in the gamma ray trace that corresponds to the top of the Oligocene Limestone. At the base of this unit (3,067 m), there is a steep gradational decrease in the sonic velocity trace downhole but relatively little change in the gamma ray. This indicates that the underlying unit is still carbonate rich but not as compact.
- At 3,161 m, there is a sharp decrease in the sonic velocity trace and a sharp increase in the gamma ray trace that corresponds to a change from calcareous claystone to claystone. This sharp change is seen as a spike followed by a shift in the traces to

follow a new consistent trend downhole. The spike is associated with high concentrations of glauconite; up to 50% of sample, (see 4.5.3 Lithology), due to glauconite being rich in potassium (McRae, 1972). Biostratigraphy shows that a major unconformity occurs at this level, with the Palaeocene and possibly earliest Eocene missing (see biostratigraphy above and Figures 24 & 25).

- From 3,400 to 3,440 m, there is a gradational increase in the sonic velocity trace to a new normal trend. This change is associated with a change to a more arenaceous sequence. There is very little change in the gamma ray trace at this depth, indicating there is still a high claystone content; consistent with cutting descriptions (Rad, 2015).
- At 3,733 m, there is a sharp increase in the sonic velocity trace and decrease in the gamma ray trace. This change is associated with the mid Late Haumurian volcanics. At the base of this volcanic sequence (3,784 m) the sonic velocity decreases and gamma ray trace increases to follow the previous trend.
- From 3,784 to 4,205 m, the sonic velocity and gamma ray traces follow the same trend as above the mid Late Haumurian volcanics but become spiky as a result of the interbedded sandstones, siltstones and coals.
- From 4,205 to 4,528 m, the sonic velocity trace is relatively smooth and follows the same trend as above. The gamma ray trace also follows the same trend as above, but is more blocky as a result of the interbedded siltstones and clean sandstones.
- From 4,528 to 4,619 m, the sonic velocity and gamma ray trace continue on the same trend, but become slightly spiky as a result of the interbedded nature of the unit, which includes thin coals and carbonaceous claystone.

The sharp shifts in the sonic velocity log have implications for seismic reflection data. A decrease in sonic velocity transit travel time results in an increase in amplitude impedance and this is displayed as a positive amplitude seismic reflection data due to its polarity being

set to SEG-Normal and vice versa in n the case of an increase in sonic velocity transit travel time. Figure 24 shows the relationship between interpreted significant seismic reflectors, the lithology and wireline data for Romney-1.

4.6 Waka Nui-1

4.6.1 Summary

Waka Nui-1 was drilled by Conoco Northland Ltd (Conoco) in 1999, approximately 100 km west of the Kaipara Harbour, in 1454.9 m of water, and was drilled to a total depth of 3,681 m. Waka Nui-1 intersected 2065.6 m of Cenozoic sediments and terminated in Early Jurassic volcanogenic metasediments (Milne and Quick, 1999).

4.6.2 Time Depth Relationship

During the drilling of Waka Nui-1 neither sonic velocity wireline logs nor check shot data were acquired, making correlation with seismic data uncertain (Milne and Quick, 1999, Stagpoole, 2011). Stagpoole (2011) developed a two-way time (TWT) to depth relationship by analysis of stacking velocities of nearby seismic data and logging-while-drilling (LWD) density data (Figure 18).

4.6.3 Lithology

Lithology is taken from Milne and Quick (1999).

1,479 (seabed) – 2,152 m

Riserless drilling/ no returns.

2,152 – 2,347 m

Light-green-grey marl, minor very fine to granular volcaniclastic interbeds.

2,347 – 2,525 m

Interbedded calcareous siltstones, very fine to fine, slightly calcareous sandstones, and very fine to granular volcaniclastics.

2,525 – 2,579 m

Interbedded calcareous (increasing downhole) siltstone, and very fine to granular volcaniclastics.

2,579 – 2,610 m

Marl grading to argillaceous limestone.

2,610 – 2,764 m

Limestone (wackestone) becoming cleaner downhole.

2,764 – 2,823 m

Marl grading to calcareous claystone downhole.

2,823 – 2,920 m

Moderately-calcareous claystone, with limestone stringers.

2,920 – 2,951 m

Argillaceous marl to limestone (wackestone).

2,951 – 3,092 m

Calcareous claystone grading to siltstone in places, and occasional limestone stringers.

3,092 – 3,118 m

Slightly carbonaceous, non-calcareous claystone grading to siltstone in places.

3,118 – 3,455.5 m

Slightly to non-calcareous claystone grading to siltstone in part, and occasional limestone stringers.

3,455.5 – 3474 m

Predominately moderately-sorted fine grained sandstone, ranges from very fine to coarse. Slightly calcareous, contains lithics, quartz and volcanics, and is slightly argillaceous.

3,474 – 3544.5 m

Predominately poorly-sorted coarse conglomerate of volcanogenic lithics. Interbedded with poorly-sorted fine to coarse sandstone and non-calcareous claystone.

3,544.5 – 3,576 m

Non-calcareous claystone grading to siltstone/very fine sandstone, possibly Laterite.

3,576 – 3,651 m

Interbedded siltstones, sandstones, and coal with a diabase sill.

3,651 – 3681 m (total depth)

Interbedded tuff and fine to medium grained volcanogenic sandstone, common argillaceous matrix and siliceous cement.

4.6.4 Biostratigraphy

The work of Strong et al. (1999) shows that at the site of Waka Nui-1 experienced a non-marine environment during the Early to Mid-Jurassic, a marginal to shelfal marine environment during the earliest Teurian, transitioning to mid bathyal depths from early Teurian, and to a lower bathyal environment by the early Eocene (Figure 26).

The predominately agglutinated Teurian fauna constitutes a flysch-type agglutinated assemblage which can occur in a wide depth range and are not diagnostic of a precise water depth, they are considered most likely to represent mid bathyal to lower bathyal environments (Strong et al., 1999). The agglutinated assemblage indicates restricted bottom-water circulation and poor oxygenation. From Early Eocene to present the site experienced open oceanic conditions with good bottom water circulation (Strong et al., 1999).

Strong et al. (1999) note that the late Dannevirke Series (Waipawan to Porangan) rocks form a relatively condensed sequence from 2,910 – 2,970 m. At approximately 2,950 m the mud log describes a unique moderate reddish-brown marl, firm to occasional hard, calcareous matrix, in places grading to calcareous claystone (Milne and Quick, 1999), and is assigned to the Mangaorapan – Heretaungan stages by Strong et al. (1999).

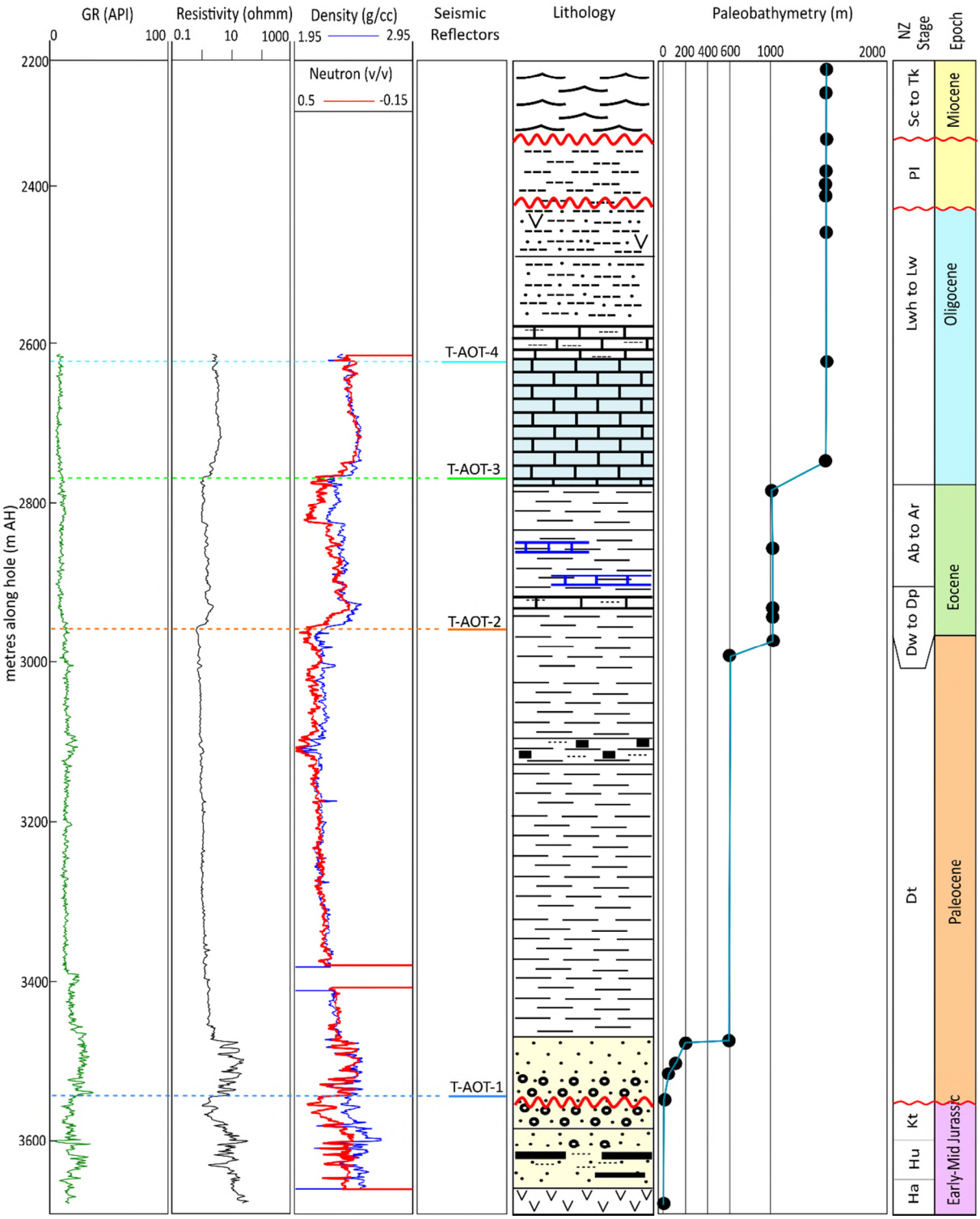

Figure 26 *Composite log of Waka Nui-1 showing the relationship between wireline geophysical logs, seismic reflectors, chronostratigraphy and paleobathymetry of Strong et al. (1999), in relation to lithology. The chronostratigraphy shows a significant hiatus at the base of the Paleocene top of the Middle Jurassic, and a condensed late Dannevirke Series. Note the strong correlation of seismic reflectors to changes in geophysical logs and lithology. See Figure 17 for the lithology key.*

4.6.5 Geophysical logging

LWD gamma ray, resistivity, neutron porosity and density logs were acquired from 2,610 – 3681 m (TD). A wireline gamma ray log was acquired from TD to 2,120 m to confirm drillers depths and correlate LWD logs. No additional wireline logs were run as the well had not encountered any significant hydrocarbon shows and the LWD logs provided enough geologic control (Milne and Quick, 1999).

The gamma ray log response is supressed from 2,120 – 3,393 m, as it is run through casing and cement, and only two informative observations can be made in this interval:

- There is a downhole increase approximately 2,950 m, indicating a reduction in the carbonate content; consistent with cutting descriptions (Milne and Quick, 1999) (Figure 26).
- From 3,090 – 3,120 m the trace shows a double peak increase which co-insides with a carbonaceous claystone described in lithology above and in cuttings description (Milne and Quick, 1999) (Figure 26).

Below 3,393 m the gamma ray log shows more character and responds to lithological changes as expected (see below and Figure 26).

The resistivity, neutron porosity and density logs respond in sync (Figure 26), corresponding to lithological changes notes in cutting descriptions (Milne and Quick, 1999):

- From 2,610 (top of log traces) to 2,775 m all log traces show a gradual increase downhole, indicating that the limestone carbonate content is increasing and more compact downhole.
- At 2,775 m, there is a sharp decrease in all log traces that is associated with a lithological change from limestone to claystone.

- At 2,823 m, there is a sharp increase in all log traces, associated with cuttings becoming 100% claystone downhole. From 2,823 – 2,920 m, all traces gradually increase with depth indicating increasing compaction and/or cementation.
- At 2,920 m, there is an initial sharp increase in all traces which then deceases with downhole to 2,951 m. This sharp increase is associated with a lithological change from calcareous claystone to argillaceous limestone. The deceasing trend indicates that the limestone becomes more argillaceous downhole.
- At 2,951 m, there is a sharp decrease in all traces that co-insides with a change from argillaceous limestone to claystone. From 2,951 – 3,464 m all log traces show a gradual increase indicating increased compaction downhole. There is a deviation from this trend in the neutron porosity and density log traces from 3,090 – 3,120 m; a sharp spiky decrease. This is associated with a lithological change from slightly calcareous claystone to non-calcareous slightly carbonaceous claystone.
- At 3,464 m, there is a sharp increase in all geophysical wireline log traces (including gamma ray), that is associated with a lithological change from claystone to sandstone. From 3,464 – 3,544 m all geophysical wireline log traces become spiky and reflect the interbedded nature of the sandstone and conglomerates.
- At 3,544 m, there is a sharp decrease in the resistivity, neutron porosity, and gamma ray log traces. This decrease is associated with a change in lithology to weathered coal measures and an approximately 100 Ma hiatus.
- From 3,544 – 3,681 m (total depth), the resistivity, neutron porosity and density all show an increasing trend downhole and are spiky due to the interbedded nature of coal measures. The gamma ray is spiky in nature but similar average value downhole.

5 Basin Analysis

5.1 Introduction

The continent of Zealandia rifted from Gondwana in the mid Cretaceous (c. 105 – 83 Ma) (Mortimer et al., 2014, Mortimer et al., 2017). Fragmentation of Gondwana resulted in extension within Zealandia and produced northwest-trending half-grabens of varying magnitudes (Strogen et al., 2017, King and Thrasher, 1996). Aotea Basin is a 200 - 300 km wide and 1,200 km long northwest-trending rift basin, revealed by mapping and gridding of the basement reflector (Collot et al., 2009, Sutherland et al., 2010, Arnot and Bland, 2016). Figure 27 shows the southern extent of Aotea Basin as a northwest tending basement low. Collot et al. (2009) suggest that the oldest sediments in Aotea Basin are Cenomanian in age, and that Aotea Basin has been filling with sediment since this time.

This study focused on mapping significant seismic reflectors of Late Cretaceous to earliest Miocene age, and tying these reflectors to petroleum wells drilled on the southeast edge of Aotea Basin, including the recently drilled Romney-1 (Figure 1). The age of the mapped reflectors at the intersection of each well is shown in Table 2. This allows for seismic reflectors to be interpreted in the context of paleoenvironmental and lithological changes recorded in the wells.

The use of cuttings for determining age and environment of deposition introduces uncertainties, due to assumptions about the depth of the cutting sample, and from contamination. This is particularly true over a condensed and complex zone (e.g. 3,126 – 3,169 m in Romney-1). The depth of a cutting interval is an estimate based on a theoretical lag time. The lag time, is the time it takes for a cutting to travel from the drill bit to the cutting screen and is calculated by dividing the theoretical borehole annular volume by the

theoretical drilling fluid flow rate. The calculated annulus volume assumes an open hole diameter of the bit being used to drill the section, but an open borehole's diameter, and hence volume, can increase due to caving or decrease due to swelling clays or mud rings. The calculated drilling fluid flow rate assumes an efficiency of 90 – 100%. Therefore, the lag time is always an estimate, and hence the depth assigned to a cutting sample is only an estimate.

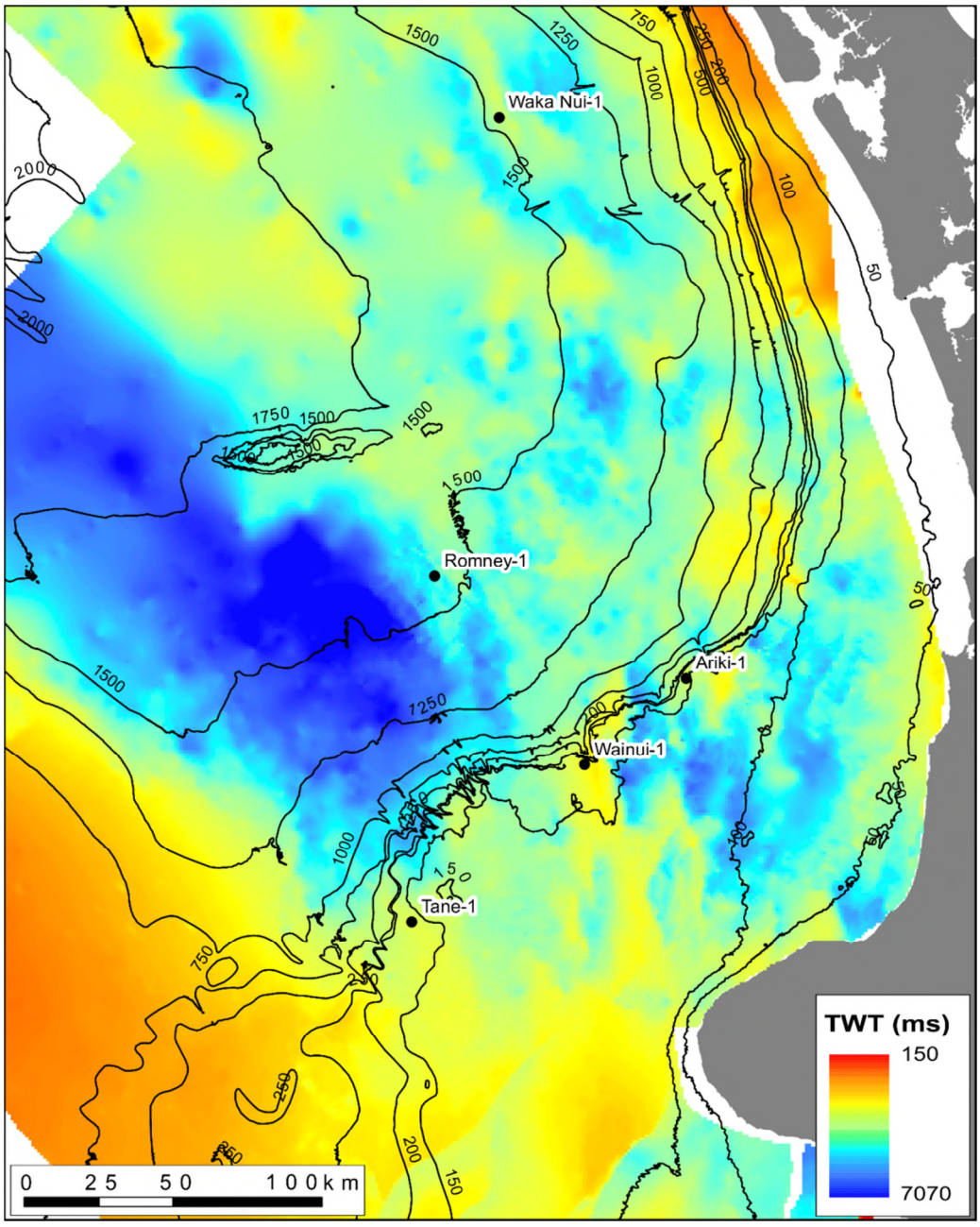

Figure 27 *Map showing the gridded basement surface in two-way time (TWT) milliseconds (ms)(Arnot and Bland, 2016), with bathymetry contours are overlain (Mitchell et al., 2012), and petroleum wells discussed in this study.*

Table 2 *Shows the relationship between mapped seismic reflectors and the age of the sediments in the wells they intersect.*

Horizon	Ariki-1	Wainui-1	Tane-1	Romney-1	Waka Nui-1
Seabed	Seabed	Seabed	Seabed	Seabed	Seabed
T-AOT-4	Ld - Lw	Po	Sc - Sl	Lw - Po	Ld
T-AOT-3	Ar	Ak	Ar	Ar	Ar
T-AOT-3c					
T-AOT-3a	Dh	Dh	Dh	Dh - Dp	
T-AOT-2	Dt	Dt	Dt	Hiatus	Dt
T-AOT-2a					Dt mid
T-AOT-1	Mh	Mh	Mh Late	Mh Late	Dt Early (base)
T-AOT-1f					
T-AOT-1e					
T-AOT-1d					
T-AOT-1c					
T-AOT-1b					
T-AOT-1a					
B-AOT-1	Mh mid Late		Mh mid Late	Mh mid Late	

Contamination is a problem when it comes to using cuttings and occurs in multiple ways: caving of the open borehole, turbulent fluid flow mixing cuttings from different depths in the annulus, settling of cuttings in the annulus when fluid flow is stopped (e.g. when making a drill string connection), and poor hygiene during sampling (i.e. not cleaning shaker screens or sieves properly). Contamination is also caused by the necessary use of stabilizers as part of the bottom hole assembly (BHA). A stabilizer is either a spiral or straight bladed section of drill pipe that has a diameter only slightly smaller than the drill bit e.g. 14.75” drill bit and 14.63” stabilizers were used in Romney-1 from 3,133 – 3,410 m. Stabilizers are used to maintain hole direction and gauge, reduce vibrations, and clear debris behind the drill bit. The action of clearing debris from behind the drill bit is where most contamination occurs, as stabilizers on the BHA are up to 60 m above the drill bit (personal experience on drilling rigs & Rad (2015)).

Seismic mapping and analysis of well data reveals the history of Aotea Basin: early Late Cretaceous inception and rapid infill, Late Cretaceous to Late Eocene transgression, Late Eocene to earliest Miocene flooding, and finally Early Miocene to present regression and prograding shelf (Figure 28) (Uruski, 2007, Collot et al., 2009, Sutherland et al., 2010, Uruski and Warburton, 2010, Baur et al., 2014). This study identifies diachroneity to tectonic subsidence and uplift events, and reveals a progression of events from north to south.

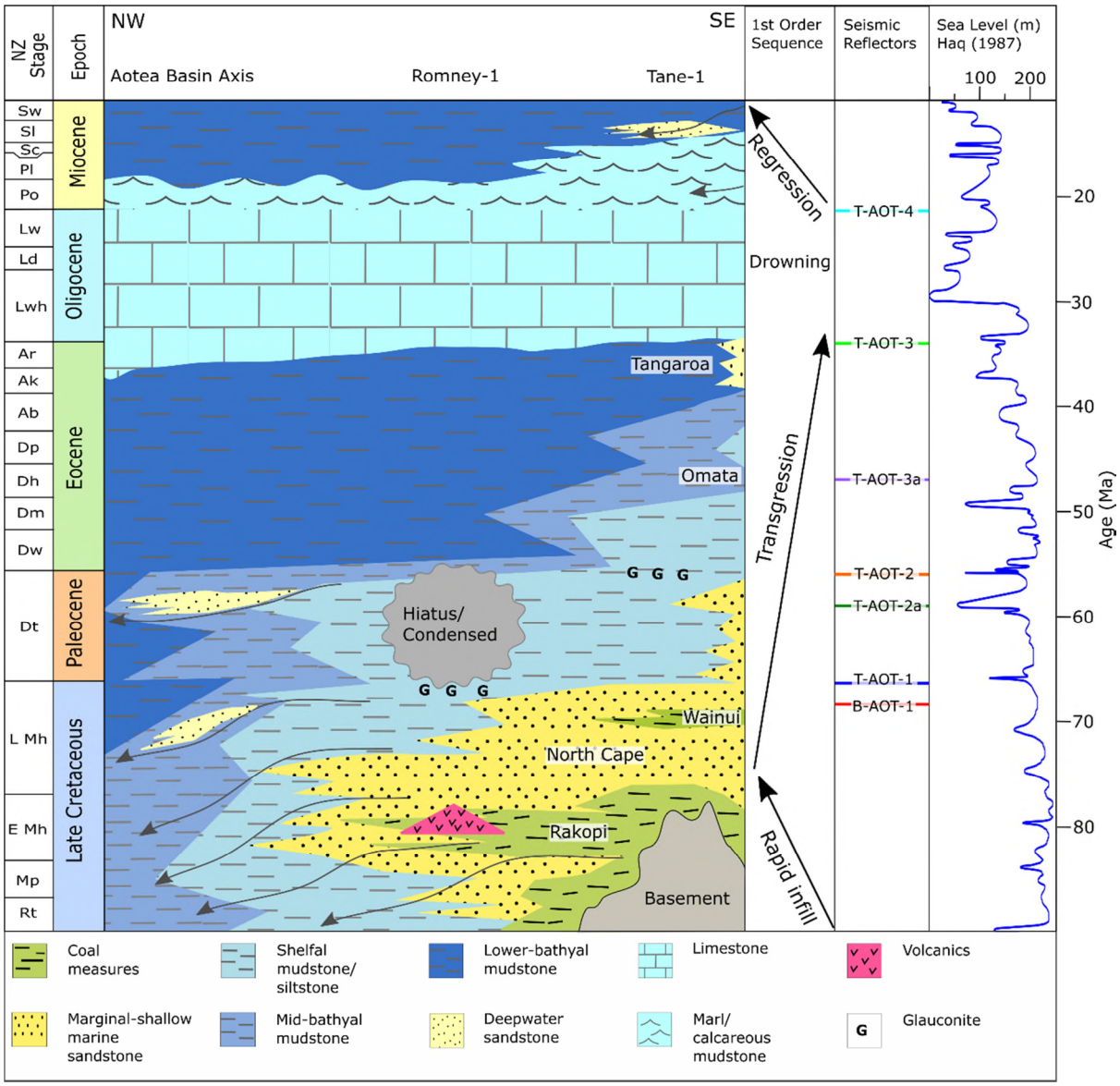

Figure 28 *Generalised stratigraphic chart of Aotea Basin. The chart shows facies distribution, age, discussed lithologic units, first order sequence stratigraphy, relationship of mapped seismic reflectors and Haq et al. (1987) eustatic sea level curve. Taranaki Basin stratigraphy based on King and Thrasher (1996) and incorporating results from Romney-1 (Rad, 2015).*

5.2 Late Cretaceous Rapid Infill (100 – 75 Ma)

Three wells penetrate Late Cretaceous sediment on the southeast edge of Aotea Basin within the study area: Romney-1, Tane-1, and Wainui-1 (Figures 1, 17 & 27). The oldest sediment intersected is Teratan (90.5 – 86.5 Ma) carbonaceous siltstone in Romney-1 (Rad, 2015, Schiøler et al., 2014). Seismic data show that a further 1.0 – 1.5 s TWT of sediment is mappable below the Teratan siltstone (Figures 3 & 8). Sutherland et al. (2010) suggest the seismic stacking pattern of these early sediments represent a prograding shelf slope break with an ascending trajectory, i.e. sediment supply was exceeding subsidence rates and outboard accommodation space was infilled (Allen and Allen, 2013, Catuneanu et al., 2011, Neal and Abreu, 2009). Romney-1 and Tane-1 show that sedimentation rates during the Late Cretaceous were rapid at 72 m/myr and 107 m/myr, respectively (Figure 25). This is consistent with the interpretation that infilling of Aotea Basin has occurred since at least the early Late Cretaceous at >100 m/myr.

Baur et al. (2014) show through seismic facies mapping of discontinuous high-amplitude reflectors inferred to be coaly facies that a significant regression resulted in deposition of terrestrial sediments in Aotea Basin at 75 Ma. These coal measures were intersected in both Tane-1 and Romney-1 (Figure 23 & 24), and were assigned by King and Thrasher (1996) and Rad (2015), respectively, to the Rakopi Formation.

5.3 Late Cretaceous to Late Eocene Transgression (75 – 35 Ma)

5.3.1 Haumurian (75 – 66 Ma)

The onset of basin-wide first-order transgression is marked by onlapping of seismic reflectors onto the Rakopi Formation (Baur et al., 2014, Uruski, 2007, Uruski and Warburton, 2010). These reflectors were intersected in both Tane-1 and Romney-1. Paleoenvironmental analysis of these wells shows that sediments were deposited in a marginal marine to shelfal environment (Figures 23 & 24), and were assigned by King and Thrasher (1996) and (Rad, 2015), to the North Cape Formation.

In the Late Haumurian, sedimentation rates at all wells in Aotea Basin decreased and transgression continued: Romney-1, Tane-1 and Wainui-1, record 46 m/myr, 43 m/myr, and 39 m/myr, respectively (Figure 25). Mapping of U-AOT-1 shows that a northwest-southeast trending depocentre existed in the axis of Aotea Basin (Figure 15A), and that despite decreasing sedimentation rate, the shelf continued to prograde into this depocentre during the Late Haumurian (Figure 7). U-AOT-1 is interpreted in seismic sections as a second order transgressive highstand sequence (see 3.2.4 U-AOT-1) that was deposited between 68 Ma and 66 Ma (Figure 29). The age was determined by mapping of B-AOT-1 into Tane-1 as an onlapping surface onto Wainui Member coal measures (stratigraphic assignment by King and Thrasher (1996)). Raine and Schiøler (2012) date the Wainui Member in Tane-1 at 67.5 – 68.5 Ma based on the dinoflagellate *P. granulatum* sub zone. T-AOT-1 is mapped into Romney-1, Tane-1, Wainui-1 and Ariki-1, and recognized as the top of the Late Cretaceous sequence in all wells i.e. 66 Ma (Table 2). From Romney-1 to Tane-1, U-AOT-1 is interpreted as a single transgressive sequence of shallow marine or shelfal mudstone and siltstone to sandstone (Figures 3 & 28).

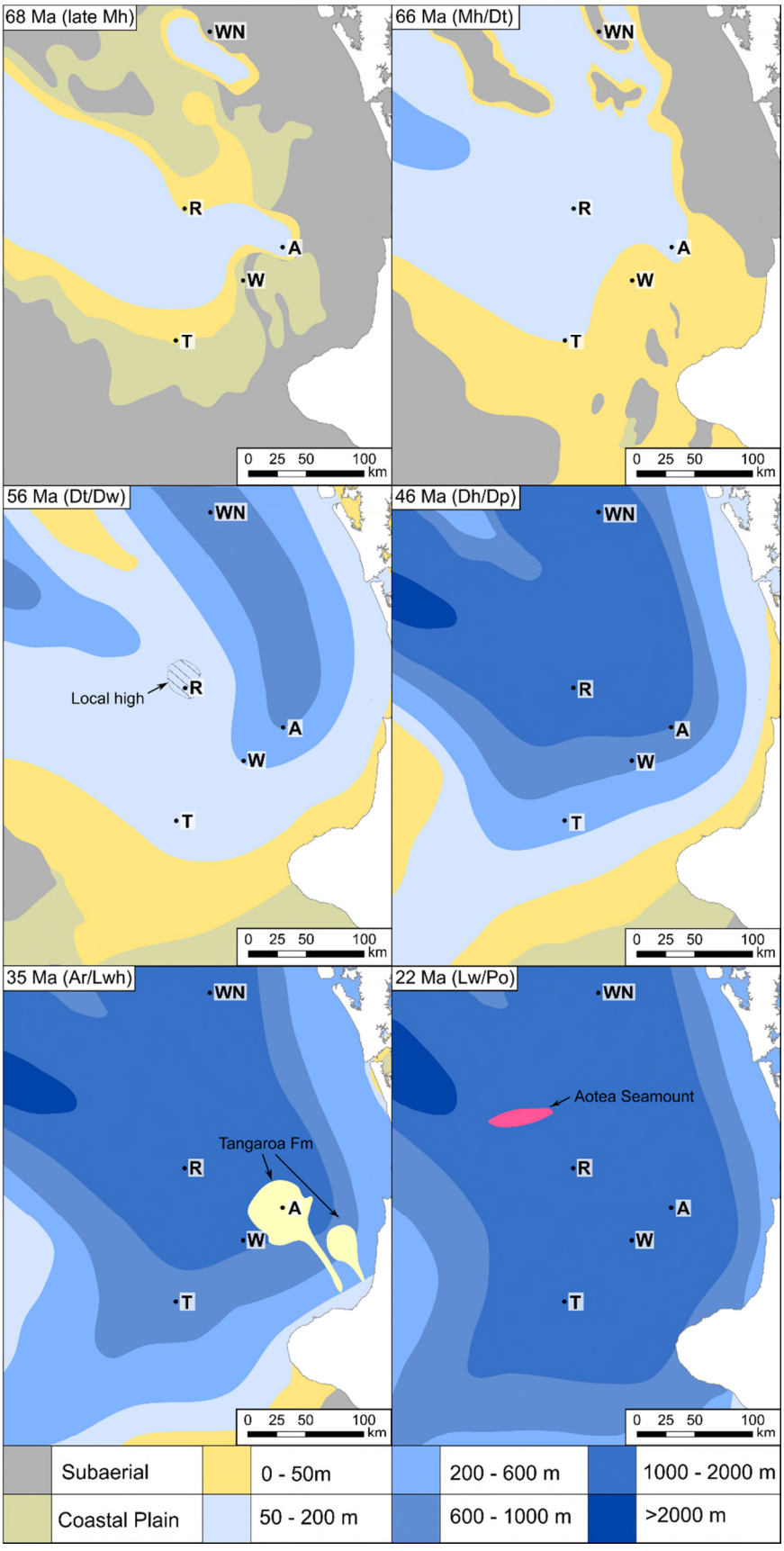

Figure 29 *Paleogeography of Aotea Basin, Taranaki Basin, and Northland Basin. Taranaki Basin and Northland Basin Paleogeography. Taranaki and Northland Basin Paleogeography based on Arnot and Bland (2016).*

In the axis of Aotea Basin, U-AOT-1 is split into 7 sub-units (Figures 7 & 9). These sub-units are interpreted to be deposited in bathyal slope environments, based on their wedge geometries (Allen and Allen, 2013, Catuneanu et al., 2011). These sub-units are not mapped into wells, as their bounding reflectors terminate in shelfal facies (Figure 7). U-AOT-1d and U-AOT-1e are interpreted as lowstand forced regressive units (see 3.2.4 U-AOT-1) that are correlated with eustatic sea-level falls seen in the Haq et al. (1987) curve (Figure 28), with peak regression at 66.9 Ma. This forced regression likely resulted in deposition of slope and basin floor sands near the axis of Aotea Basin. Paleoenvironmental analysis of Romney-1 over U-AOT-1 section reveals a regression at the top of the interval, which is also assigned to the 66.9 Ma eustatic sea-level fall of Haq et al. (1987). Paleoenvironmental analysis of Tane-1 and Wainui-1 over U-AOT-1 does not detect any change, possibly due to the shallow to marginal marine depositional environment resulting in non-deposition or poor preservation of benthic foraminifera.

In the Late Haumurian, Ariki-1 is separated from other Aotea Basin wells by a basement high (Figures 15A, 27 & 29). This separation due to basement high, leads to Ariki-1 being starved of sediment from the southeast and having a subdued sedimentation rate (Figure 25). Seismic interpretation shows that the Ariki basement high is onlapped by U-AOT-1, and paleoenvironmental analysis shows that Ariki-1 experienced marginal to shallow marine environments during this interval (Figure 20).

Late Haumurian sediments are absent in Waka Nui-1: an unconformity separates Mid Jurassic from Paleocene (Figure 26) (Milne and Quick, 1999). It is inferred Waka Nui-1 was a sub-aerial basement high during this period (Figure 29). U-AOT-1 is mapped in the adjacent Waka Nui sub-basin as a transgressive sequence (see 3.2.4 U-AOT-1 & Figure 3).

The divergence of internal reflectors of U-AOT-1, is interpreted as fan deposits from a local sediment source, which were drowned when fans were onlapped by Teurian marine sediment (Figure 3).

5.3.2 Teurian (66 – 56 Ma)

In the Teurian, transgression across Aotea Basin is mapped as U-AOT-2 (see 3.2.6 U-AOT-2 & Figure 28). T-AOT-2 is mapped into every well, except Romney-1, and is consistently dated as the top of the Teurian (Table 2). Paleoenvironmental analysis and lithology indicate that transgression progressed from north to south across the study area.

In Waka Nui-1, early Teurian conglomerates and shore face sands immediately overly weathered Jurassic coal measures (Milne and Quick, 1999). Paleobathymetry continued to deepen through the Teurian to upper and mid bathyal environments (Figure 26). Sedimentation rate was moderately high 57 m/myr (Figure 25), which is the reason for Waka Nui-1 experiencing a relatively stable paleoenvironment through the mid to late Teurian. Sediment supply approximately matched subsidence. Ariki-1 experienced shallow marine to shelfal environments through the early Teurian and deepened to bathyal environments from late Teurian to Waipawan (Figure 20). Wainui-1 experienced outer shelf to upper bathyal conditions during the Teurian (Figure 22). Tane-1 experienced shallow marine to mid shelf conditions (Figure 23). Sedimentation rates at Ariki-1, Wainui-1, and Tane-1 decreased during the Teurian, consistent with the transgression inferred from onlapping relationships at the base of U-AOT-2 (Figure 25).

U-AOT-2 is thickest in the sub-basin proximal to Waka Nui-1 and in the axis of Aotea Basin (Figure 15B). Reflector T-AOT-2a is mapped in both regions, and it intersects Waka Nui-1 at

the base of a 26 m thick slightly carbonaceous, non-calcareous claystone assigned to Waipawa Formation (Milne and Quick, 1999). Sykes (2008) demonstrated that the carbonaceous content of Waipawa Formation in Waka Nui-1 (vitrinite and inertinite) was dominated by terrestrial debris transported to and deposited in a marine slope environment. This, along with the inferred mid-bathyal depositional setting (Strong et al., 1999), leads to the interpretation that U-AOT-2b is a forced regressive sequence. U-AOT-2b is mapped in the axis of Aotea Basin and is interpreted as a regressive sequence on basis of reflector T-AOT-2a toplapping T-AOT-2 and the geometry of U-AOT-2b (see 3.2.5 U-AOT-2 reflectors). The Haq et al. (1987) eustatic sea level curve shows a major regression of ~150 m at ~58 Ma (Figure 28). The base of U-AOT-2b is assigned to this event.

There are no definitive Paleocene sediments intersected in Romney-1 (Figures 24). Seismic interpretation shows that the Romney structure was a local Paleocene high and its margins are onlapped during this interval (Figures 3, 15B & 28). The Late Cretaceous glauconitic siltstone at this hiatus is indicative of a sediment-starved shelfal or slope environment (Odin and Matter, 1981, McRae, 1972). Palynology analysis on the condensed Waipawan sequence indicates Romney-1 was at shelfal depths and proximal to land, based on “superabundant dinoflagellates and “abundant miospores” (Schiøler et al., 2014).

I interpret, based on biostratigraphic data, lithology, geophysical wireline logs (see well section), and seismic data (Figures 3 & 15B), that the Romney structure was a regional high and experienced condensed sedimentation or a hiatus during the Teurian. This was followed by deposition of a condensed section in the Early Eocene that coincides with an uphole change from a marginal marine or shelfal marine environment below 3,151 – 3,160 m AHBDF, to bathyal conditions above. Cuttings from 3,160 – 3,169 m AHBDF in Romney-1

are interpreted as marginal marine, based on the lack of planktonic foraminifera and nannofossils, rare (11%) dinoflagellates, and abundant (89 %) miospores. The Late Cretaceous age is based on palynology. Cuttings from 3,151 – 3,160 m AHBDF are assigned to the late Waipawan stage (*Wetzeliella spinulosa* dinoflagellate zone). The 60:40 ratio of dinoflagellates to miospores in the interval indicates a shelf environment proximal to land. Nannofossils and foraminifera indicate a Heretaungan stage and open ocean lower bathyal environment (86% planktonic foraminifera, and benthic foraminifera include *Nuttalides truempyi, Anomalinoides pseudogrosserugosus*, *Pleurostomella, Cyclammina spp.* and *Cibicides tholus*.). These apparently conflicting ages and environments are from a 9 m sample interval over a condensed stratigraphic interval. I propose that the palynology represents the lower portion of the sample interval, and foraminifera and nannofossils are from the upper part. Over this 9 m interval, an environmental change from shelf to lower bathyal is inferred.

5.3.3 Waipawan to Heretaungan (56 – 45.7 Ma)

During the Waipawan to Heretaungan, seismic mapping of U-AOT-3a and paleoenvironmental analysis of wells shows deepening from north to south (Figure 22). T-AOT-3a is the top of this sequence and is dated as Heretaungan at wells it intersects (Table 2).

In Waka Nui-1 and Ariki-1, paleoenvironmental analysis shows subsidence in the Waipawan to lower bathyal depths (Figures 26 & 20,respectively). Strong et al. (1999) note that in Waka Nui-1 “Waipawan to Porangan rocks form a relatively condensed sequence”. The sedimentation rate was low in Waka Nui-1, but at Ariki-1 sedimentation continued at a rate similar to the underlying Teurian rate (Figure 25). Ariki-1 is inferred to have remained

proximal to a sediment source, while Waka Nui-1 became isolated by changes in sediment transport pathways. There is an uphole change in lithology from non-calcareous to calcareous claystone in both wells (Figure 17).

In Romney-1, paleoenvironmental analysis shows rapid subsidence from shelfal in the late Waipawan to lower bathyal in the Heretaungan (see 4.5.4 Biostratigraphy and Figure 24). This change occurs over a condensed section in Romney-1 (thickness 9 m) and is associated with an uphole increase in calcareous content (Figure 24).

In Wainui-1, paleoenvironmental analysis shows subsidence in Waipawan time from upper bathyal to mid-bathyal depths (Figure 19). In the Heretaungan, sedimentation rate decreased and remained low throughout the rest of the Paleogene (Figure 25). Lithologically there are no major changes in the Eocene in Wainui-1 (Figure 17).

Tane-1 is the most southern well in the study area, paleoenvironmental analysis shows it subsided from shelfal to upper bathyal depths during the Waipawan to Heretaungan. A distinct dark green highly glauconitic sandstone is intersected between 3,19 – 3,195 m and is picked as the top of the Teurian interval (Figure 23). This is interpreted to represent a transgressive surface, as this type of facies is commonly associated with transgression (Hopcroft, 2009, Odin and Matter, 1981, McRae, 1972). Sedimentation rate remained steady at 30 m/myr, as sediment supply kept pace with accommodation space created at Tane-1 (Figure 25).

Under the present-day shelf, U-AOT-3 is significantly thicker than elsewhere in Aotea Basin (Figure 15C). The base of U-AOT-3a is offset by a series of down-to-the-east normal faults,

but with only minor offset (Figure 13). A local tensile stress regime is inferred for the Waipawan. Strong and Wilson (2002) interpret that Taranga-1 was at mid-bathyal depths in a restricted basin, based on agglutinated foraminifera species. A localised tectonic event apparently took place during the Waipawan to Heretaungan, based on the anomalous subsidence and minor faulting.

Along the flank of Challenger Plateau, several localised high amplitude seismic reflectors are interpreted as igneous intrusions (Figures 3, 8 & 14). These are interpreted to have been intruded during the Waipawan to Heretaungan, as T-AOT-2 (top Teurian) is the youngest reflector deformed so intrusion was after this reflector being deposited, and T-AOT-3a shows only minor deformation that is interpreted as compactional draping.

5.3.4 Heretaungan to Porangan (45.7 – 42.6 Ma)

During the latest Heretaungan to Porangan, onlap onto T-AOT-3a is interpreted to represent a deepening in axis of Aotea basin (see 3.2.8 U-AOT-3). T-AOT-3a was not mapped to Waka Nui-1, because it merges with T-AOT-3, but a "unique moderate reddish-brown marl" was described in the mud log (Milne and Quick, 1999) and was assigned a Mangaorapan to Heretaungan age by Strong et al. (1999). In Ariki-1, a distinctive brick red to brown, fossiliferous, calcareous silty shale of Heretaungan to Porangan age is described in the mud log, and SBPT (1984) note that this same unit is described in Tangaroa-1. The Omata Member of the Turi Formation in Taranaki Basin, is inferred by Higgs et al. (2012) to have formed during a Heretaungan to Porangan transgression. Based on the combined evidence, Aotea Basin and its Taranaki margin experienced deepening, transgression, and reduction in sediment supply during the Mangaorapan to earliest Porangan. Biostratigraphic data show this was diachronous, and progressed from north to south.

Wainui-1 and Tane-1 continued to subside during the Heretaungan to Porangan (Figures 22 & 24), but there is no lithological or paleoenvironmental evidence of transgression. The sedimentation rate curve in Figure 25, however, does show that both wells had lower sedimentation rates after the Heretaungan. Figure 13 shows T-AOT-3a is onlapped by overlying reflectors, indicating sediment infill of this local depocenter during the Porangan.

During the Porangan, Romney-1 records evidence of regression. Cuttings from 3,126 – 3,135 m AHBDF in Romney-1 are interpreted to be open ocean and lower bathyal, based on benthic foraminifera, 88% planktonic foraminifera, and high nannofossil diversity. However, a ratio of 42:58 dinoflagellates to miospores indicates proximity to land typical of shelfal environments (Schiøler et al., 2014). The calcareous nature of the claystone is consistent with the foraminifera interpretation of a lower bathyal environment. Mapping of U-AOT-3c shows clinoform reflectors of a prograding delta on the flank of Challenger Plateau during the Porangan to Runangan (Figure 8). The land adjacent to this prograding delta is inferred to be the source of the miospores in Romney-1.

5.3.5 Bortonian to Runangan (42.6 – 34.6 Ma)

During the Bortonian to Runangan, Tane-1 in the southeast of Aotea Basin subsided to lower bathyal depths (Figure 23). Romney-1 in central Aotea Basin, and Waka Nui-1 in the north of the study area, were in bathyal conditions far from sediment sources, and hence benthic foraminifera were insensitive to a minor sea-level changes (Figures 24 & 26). No palynology analysis was done on Romney-1 cutting samples above 3,126 m AHBDF (dated as Porangan).

Wainui-1 is anomalous, as paleoenvironmental analysis reveals an uphole change from mid bathyal to upper bathyal or outer shelf during the Bortonian to Runangan (Figure 19). In Ariki-1, a deep-water sandstone fan, the Tangaroa Formation, was deposited in the Kaiatan to Runangan (King and Thrasher, 1996, SBPT, 1984). In Wainui -1 there is no noted change in lithology (Figure 17), but I interpret the anomalous paleobathymetry to represent a distal deep-water fan system depositing thin stringers of sand or silt, originating from a shelfal environment, near the Wainui-1 site, i.e. Tangaroa Formation (Figure 28).

The clinoform sets (U-AOT-3c) of the Porangan to Runangan prograding delta on the flank of Challenger Plateau, show at least three changes in base-level occurred during this time (Figures 8 & 30). Bifurcating relationships of reflectors T-AOT-3a, T-AOT-3c and T-AOT-3 introduces ambiguity in mapping (Figure 30). In my preferred interpretation, reflector T-AOT-3a is downlapped by clinoform reflectors of U-AOT-3c at the junction and is conformable to the southwest, and reflector T-AOT-3 is mapped as the onlapped surface of U-AOT-3c (Figure 30B). In the alternative interpretation, reflector T-AOT-3a is truncated by reflector T-AOT-3 and reflector T-AOT-3 is downlapped by reflector T-AOT-3c (Figure 30C). The alternative interpretation of U-AOT-3c would place it in the Oligocene, and with no Whaingaroan or Duntroonian aged sediments intersected in Romney-1 (Schiøler et al., 2014), a minimum age of early Waitakian (25 Ma) would be assigned

A eustatic sea level fall during the Kaiatan to Runangan (Haq et al. (1987) curve in Figure 28) coincides with deposition of Tangaroa Formation (King and Thrasher, 1996). Mapping in this study did not find evidence of a lowstand or forced regressive sequence, as the shelf-break and upper slope where this would be evident are southeast of the study area (Figure 29) (Strogen et al., 2014, Arnot and Bland, 2016). It is inferred that the same uplifted and eroding

land mass that supplied sediment to U-AOT-3c, was also a source area for Tangaroa Formation.

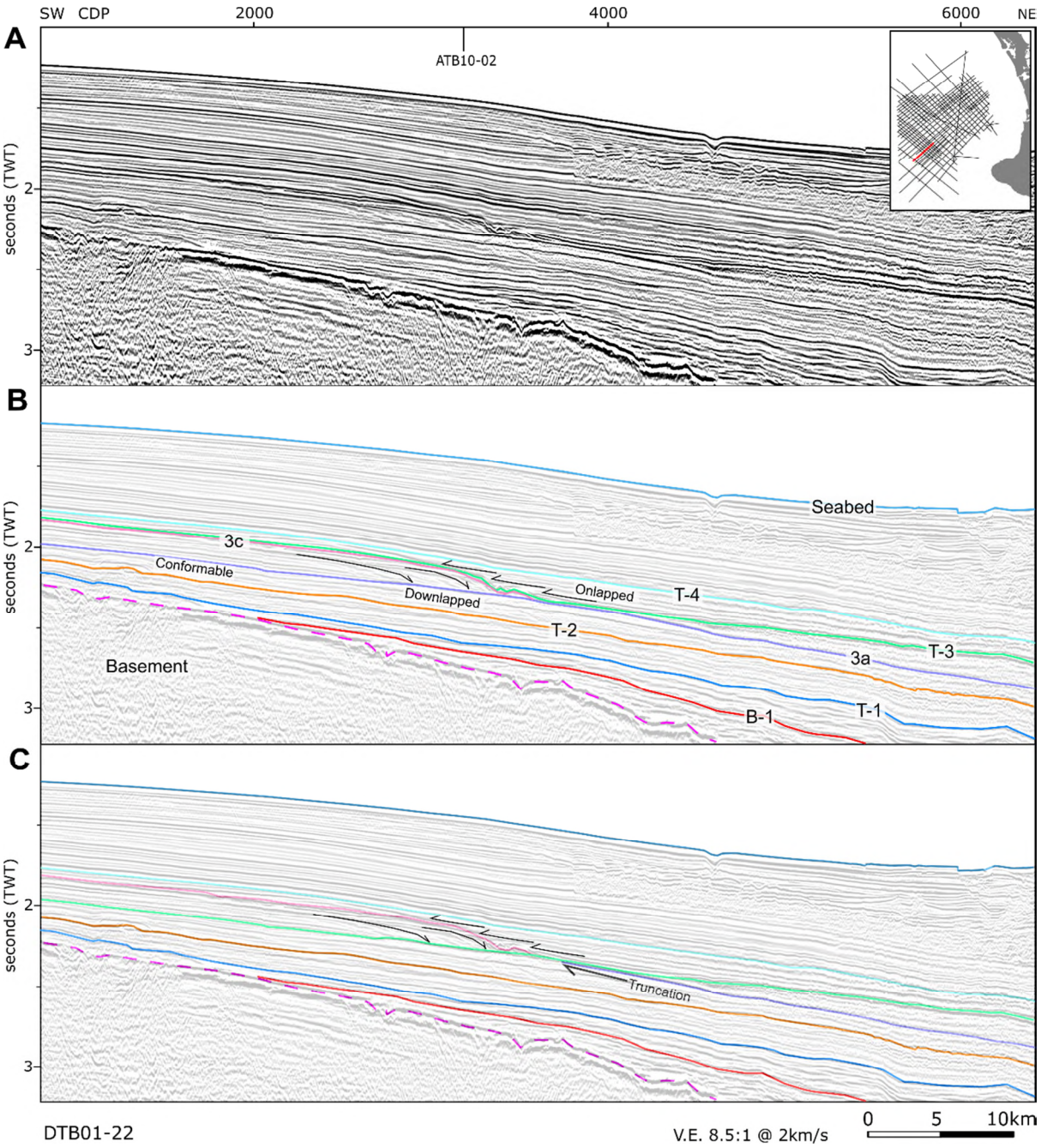

Figure 30 *(A) Uninterpreted southwest section of seismic profile DTB01-22: a dip line into Aotea Basin. In the preferred interpretation (B), T-AOT-3a is downlapped by clinoform reflectors before becoming conformable to the southwest and reflector T-AOT-3 is mapped as the onlapped surface. In the alternative interpretation (C), reflector T-AOT-3a is truncated by reflector T-AOT-3, and reflector T-AOT-3 is downlapped by clinoform reflectors of U-AOT-3c*

5.4 Late Eocene to earliest Miocene Drowning (35 – 21 Ma)

In the late Runangan to early Whaingaroan there is a change in lithology across the study area to limestone that is seen in all wells (Figures 17). Sedimentation rates across the region decrease (Figure 25) and biostratigraphy indicates a condensed Oligocene section with possible hiatus (Strong et al., 1999, Strong and Wilson, 2002, Schiøler et al., 2014). Paleoenvironmental analysis shows a deepening across the region at this boundary. This boundary is clearly seen on seismic sections and mapped as reflector T-AOT-3, which truncates underlying reflectors along the axis of Aotea Basin (Figures 3, 7 & 8). The truncation is interpreted as an erosional hiatus (Vail et al., 1977) caused by low sediment supply (Figure 25) and increased bottom currents due to Oligocene inception of the Antarctic Circumpolar Current (Kennett, 1977). In Romney-1, a hiatus from Runangan to Waitakian (34.6 – 25.2 Ma) indicates early Oligocene erosion or non-deposition (Schiøler et al., 2014)

On the flank of Challenger Plateau, T-AOT-3c is mapped as the top of a prograding delta that persisted until the late Runangan or Waitakian. It is estimated that maximum paleobathymetry at the break in slope of this delta was 200 m (+/- 50 m), based on present-day shelf edge morphology. At the intersection of seismic lines DTB01-22 and ATB10-02 (Figure 30B), the seabed is mapped at 1,455 ms and T-AOT-4a at 2,162 ms. The seabed is currently ~1,100 m bmsl. Using the seabed depth of 1,100 m bmsl and a polynomial ($y = 0.0001541x^2 + 0.8946x$) derived from well check shot data (Figure 18), T-AOT-3c is ~700 m bsf and ~1,800 m bmsl. T-AOT-3c is, therefore, estimated to have subsided approximately 1,600 m bmsl since the Runangan i.e. current depth minus paleodepth. Using the Crough (1983) equation for correction of sediment loading on basement, T-AOT-3c would have subsided to ~1,500 m bmsl without the Oligocene to recent overburden, and therefore, Challenger Plateau has tectonically subsided ~1,300 m (+/- 100 m) since the late Runangan,

i.e. back stripped depth minus paleodepth of 200 m bmsl (+/- 100 m for eustatic fluctuations during the late Eocene (Haq et al., 1987)).

The drowning of Challenger Plateau and Taranaki Basin (King and Thrasher, 1996, Strogen et al., 2014) in the Oligocene reduced supply of clastic sediment to Aotea Basin. This reduction in clastic sediment resulted in the Oligocene sequence being dominated by pelagic carbonate. The condensed sequence is mapped across the region as U-AOT-4 (Figure 15D).

Eruption of Aotea Seamount in the late Oligocene (Mortimer et al., 2018), provided volcanic-clastic sediment that was deposited in the axis of Aotea Basin and expanded U-AOT-4 locally (Figure 15D).

5.5 Early Miocene to Present Regression and Prograding Shelf (21 – 0 Ma)

Regional regression began in the latest Oligocene in the northeast (Waka Nui-1 and Ariki -1) of the study area and earliest Miocene in the southwest (Romney-1, Wainui-1 and Tane-1). The onset of this regression is seen in the lithology as an influx of uphole-coarsening clastic material gradationally changing limestone to marl and calcareous claystone (Figure 17). Paleoenvironmental analysis shows decreasing paleobathymetry began at Ariki-1, followed by Wainui-1 and finally Tane-1, and is continuing today (Figure 19). The seabed at Romney-1 and Waka Nui-1 is currently a lower bathyal environment so there is still no change in paleoenvironmental markers. The sedimentation rate curves in Figure 25, show that rates increased first in the north and east, and progressed south and west with time. The regressive signal is diachronous and progressed from north to south.

5.6 Discussion and Conclusions

The Hikurangi Plateau impacted the Gondwana subduction zone at 105 Ma, which resulted in a slowdown and ultimately cessation of subduction along the Gondwana margin by 100 Ma (Davy et al., 2008, Matthews et al., 2012, Laird, 1993). Rhyolite and tuffs dated as 101 – 97 Ma have been sampled across Zealandia and indicate a change to extension (Tulloch et al., 2009). Rifting continued until ~83 Ma, when Zealandia separated from Gondwana (Mortimer et al., 2017, Mortimer et al., 2014, Laird, 1993). Rifting resulted in formation of grabens and half-grabens that are now recognised as the Great South Basin (Cook et al., 1999), Taranaki Basin (King and Thrasher, 1996), Reinga Basin (Bache et al., 2012a), and Aotea Basin (Collot et al., 2009). Seismic reflection data and wells in Aotea Basin reveal rapid deposition of sediment during the rifting phase (100 – 83 Ma). The trajectory of the prograding shelf break to the northwest, suggests high sediment supply from land to the southeast.

Tasman seafloor spreading initiated at ~83 Ma and progressed northwards in a series of stages (Gaina et al., 1998, Sutherland, 1999). The onset of Tasman seafloor spreading led to cessation of rifting across much of Zealandia at 83 Ma, and is manifest as an 'uplift break-up unconformity' (Strogen et al., 2017) documented in West Coast (Nathan et al., 1986), Taranaki Basin (King and Thrasher, 1996), Great South Basin (Cook et al., 1999), and East Coast Basin (Crampton et al., 2019). The products of uplift and erosion in Taranaki and West Coast basins were deposited in Aotea Basin as the Taranaki Delta (Strogen et al., 2017). Transition from an active rift to passive thermal subsidence is manifest as a decrease in sedimentation rate and transition from fluvial to shallow marine or shelfal environments in Aotea Basin during the Haumurian and Teurian (83 – 56 Ma) (Figure 29). The recognition of eustatic sea level fluctuations during this period is made possible by the tectonic quiescence, slow subsidence, and moderate sediment supply.

During the late Waipawan to Porangan (53 – 43 Ma), the west Pacific experienced a major tectonic reorganisation and change in plate motions (Sutherland et al., 2017). Tasman seafloor spreading terminated at ~53 Ma (Gaina et al., 1998). The Izu-Bonin-Mariana subduction initiated at ~52 Ma (Arculus et al., 2015, Ishizuka et al., 2011). The Hawaii-Emperor bend initiated at ~50 Ma (O'Connor et al., 2013). The West Antarctic Rift System initiated at ~48 Ma (Müller et al., 2007). Acceleration in spreading rates between Australia and Antarctica initiated at ~45 – 43 Ma (Mutter et al., 1985, Cande and Stock, 2004).

In New Zealand, there is little recognised evidence of tectonic activity during the late Waipawan to early Porangan (53 – 45 Ma), but there are signs of renewed activity in Aotea Basin. Local tectonic subsidence is inferred from late Waipawan to Heretaungan (53 - 48 Ma) at Romney-1, based on the observed change from a shelfal to lower bathyal environment, i.e.~800 m of subsidence in ~4 Myr (Figures 24 & 29). Under the present-day shelf, U-AOT-3 is significantly thicker (~300 ms) than elsewhere in Aotea Basin (Figure 15C). In Taranga-1, paleoenvironmental analysis shows a change from shelfal to mid bathyal environment from Waipawan to Mangaorapan (56 – 49 Ma) (Strong and Wilson, 2002), i.e. ~400 m subsidence in 7 Myr. The base of U-AOT-3a is offset by a series of down-to-the-east normal faults, with small offset (Figure 13): a local tensile stress regime and subsidence is inferred for the Waipawan. Aotea Basin and its Taranaki margin experienced diachronous deepening and transgression from north to south during the Mangaorapan to earliest Porangan (52 – 45 Ma), as recognised in Waka Nui-1 and Ariki-1 as condensed sections, and as the Omata Member in Taranaki Basin. A pulse of volcanism during the Waipawan to Heretaungan (56 – 46 Ma) is observed as localised small-scale intrusions in Aotea Basin (Figures 3, 8 & 14). Rapid tectonic subsidence and diffuse volcanism is interpreted as the

first signs of initiation of the Australia-Pacific plate boundary. There is a hint that maybe the earliest signs of activity are older than 53 Ma, paleoenvironmental analysis at Waka Nui-1 shows rapid subsidence from early Teurian (Figure 26), and at Ariki-1 from latest Teurian (Figure 20).

Convergence and uplift in northern New Zealand, and rifting in southern New Zealand during the early Porangan to late Runangan (45 – 35 Ma) was associated with motion at the Australia-Pacific plate boundary. In Reinga Basin, contraction and uplift is documented, but timing is poorly constrained to after 53-48 Ma and before 36 – 34 Ma (Sutherland et al., 2017, Bache et al., 2012b). Recent drilling near Cape Reinga (IODP U1508) identifies onset of folding at 39 Ma (Sutherland, 2019). The Taranaki Fault System initiated as reverse fault along ~400 km of strike, west of Auckland to west of Wanganui, in the Bortonian (43 – 40 Ma), and is considered to be an antithetic fault to the initiating Tonga-Kermadec subduction zone (Stagpoole and Nicol, 2008). Rifting of Emerald Basin initiated at ~45 Ma south of New Zealand (Sutherland, 1995), and extension propagated north (King, 2000b), resulting in deposition of the Brunner Coal Measures in northwest South Island during the Bortonian (43 -39 Ma) (Leask, 1993). In Aotea Basin, shelfal prograding clinoform reflectors in U-AOT-3c suggest that uplift of Challenger Plateau occurred in the early Porangan (~46 Ma) (supported by miospores in Romney-1) (Figures 29 & 30). This regression is inferred to have persisted until the late Runangan (35 Ma) or Waitakian (25 Ma), and experienced at least three eustatic changes in base level (Figure 30). Beneath the present-day shelf, reflectors onlap T-AOT-3a (Figure 13), consistent with regression in Taranaki Basin associated with the deposition of Mangahewa Formation (Cooper et al., 2001, Higgs et al., 2012, King and Thrasher, 1996).

Regional subsidence is recorded in northwest New Zealand during the Whaingaroan to Otaian (34 – 18.7 Ma), and this subsidence progressed from north to south. In Reinga Basin, wave cut platforms on Reinga Ridge and West Norfolk Ridge have subsided > 1 km since the Runangan to Whaingaroan (36 – 30 Ma) (Bache et al., 2012a, Bache et al., 2012b, Sutherland et al., 2017). In Aotea Basin, shelfal prograding clinoform reflectors of U-AOT-3c on the flank of Challenger Plateau have tectonically subsided ~1,300 m since 35 – 25 Ma. Tectonic subsidence at wells suggesting the onset of regional subsidence progressed from north to south during the Whaingaroan to early Waitakian (34 – 24 Ma) (Baur et al., 2014). In Taranaki Basin, paleobathymetric curves show that rapid subsidence occurred in the latest Waitakian to early Otaian (22 – 18 Ma) (Stern and Holt, 1994). Activity on Taranaki Fault stopped from north to south (Port Waikato to Awakino) during this period, and the change is inferred to relate to clockwise rotation of the Hikurangi subduction thrust (Stagpoole and Nicol, 2008).

In the late Oligocene to early Miocene (23 – 21 Ma), dextral offset along the Alpine Fault and subduction beneath North Island began, i.e. a situation similar to the current Australian-Pacific plate boundary was established (King, 2000b). The Northland Allochthon was emplaced during the establishment of subduction (Isaac, 1994, Herzer, 1995). During the Neogene to present (21 – 0 Ma), deformation associated with convergence across the Australian-Pacific plate boundary created uplift and erosion, and hence a sediment supply for the regressive megasequence that is still being deposited (King, 2000b, King and Thrasher, 1996). Deformation and volcanism in north New Zealand migrated eastward and southward (King, 2000b). In Aotea Basin, an increase in sedimentation rate is associated with this regressive sequence (Figure 25), but no deformation or volcanism is observed.

6 Petroleum System Analysis

6.1 Introduction

The essential elements of a petroleum system are: source rock, reservoir rock, seal rock, a suitable structure or stratigraphic relationship to trap hydrocarbons, and overburden rock (Magoon and Dow, 1994, Allen and Allen, 2013). Seismic reflector mapping predict these elements exist in Aotea Basin (Uruski, 2007, Uruski and Warburton, 2010, Baur et al., 2014, Uruski and Wood, 1991), and the drilling of Romney-1 has confirmed them (Rad, 2015). However, no wells have discovered economic petroleum reserves.

In this section I asses the elements of the petroleum system, identify three play concepts, and determine the critical moment for Aotea Basin.

6.2 Source rock

The foundation of a petroleum system is a mature, hydrocarbon expelling source rock (Allen and Allen, 2013, Magoon and Dow, 1994). Drilling of Romeny-1 confirmed two packages of source rock are present in Aotea Basin. A third potential source rock has been intersected in borehole U1509 (Sutherland, 2019).

Romney-1 reached total depth in Teratan aged carbonaceous siltstone, (33 m of this unit was intersected). The total thickness of this unit is not known as drilling of the well was terminated prior to reaching its base. The unit was described as brown to brownish black carbonaceous siltstone to claystone. The description of the unit is promising, but no further analysis on this unit is available, i.e. total organic content or hydrogen index, so little can be said about the quality of this source rock.

Romney-1 intersected 657 m of Haumurian coal measures, assigned to the Rakopi Formation by Rad (2015). The Rakopi Formation is a prolific source rock in Taranaki Basin (King and Thrasher, 1996, Sykes, 2007, Uruski and Warburton, 2010). The Rakopi Formation has previously been mapped across 20,000 km^2 over the southern extent of the study area (Uruski and Warburton, 2010, Baur et al., 2014).

Modelling of marine influenced coaly source rocks by Sykes (2007) shows that oil generation begins at ~95 °C and predicts a burial depth of ~3,200 m below seabed is the top of the oil generation window. This is based on a thermal gradient of 3 °C/100 m, which was modelled by Stagpoole et al. (2007). The maximum bottom hole temperature in Romney-1 was determined to be 116 °C by wireline logging measurements, giving a thermal gradient of 3.5 °C /100 m (Rad, 2015). This gradient is higher than that predicted gradient by Stagpoole et al. (2007) and coaly sediments buried ~2,700 m below seabed are now calculated to be in the oil generation window. Vitrinite reflectance analysis on a sample from 2,950 m below seabed (4,500 m AHBDF), shows a %Ro value of 0.8 that confirms it is within the oil generation window (Rad, 2015).

Depth conversion by Uruski and Warburton (2010), shows that through the centre of the study area the top of the Rakopi Formation is within the oil generating window (Figure 31). Oil shows and oil stained sandstone were observed over multiple intervals in the Rakopi Formation, and methane to pentane was recorded in gas readings from ~3,150 – 4,619 m (TD) (Rad, 2015). These direct readings validate the model and proves that there is active thermogenic hydrocarbon generation.

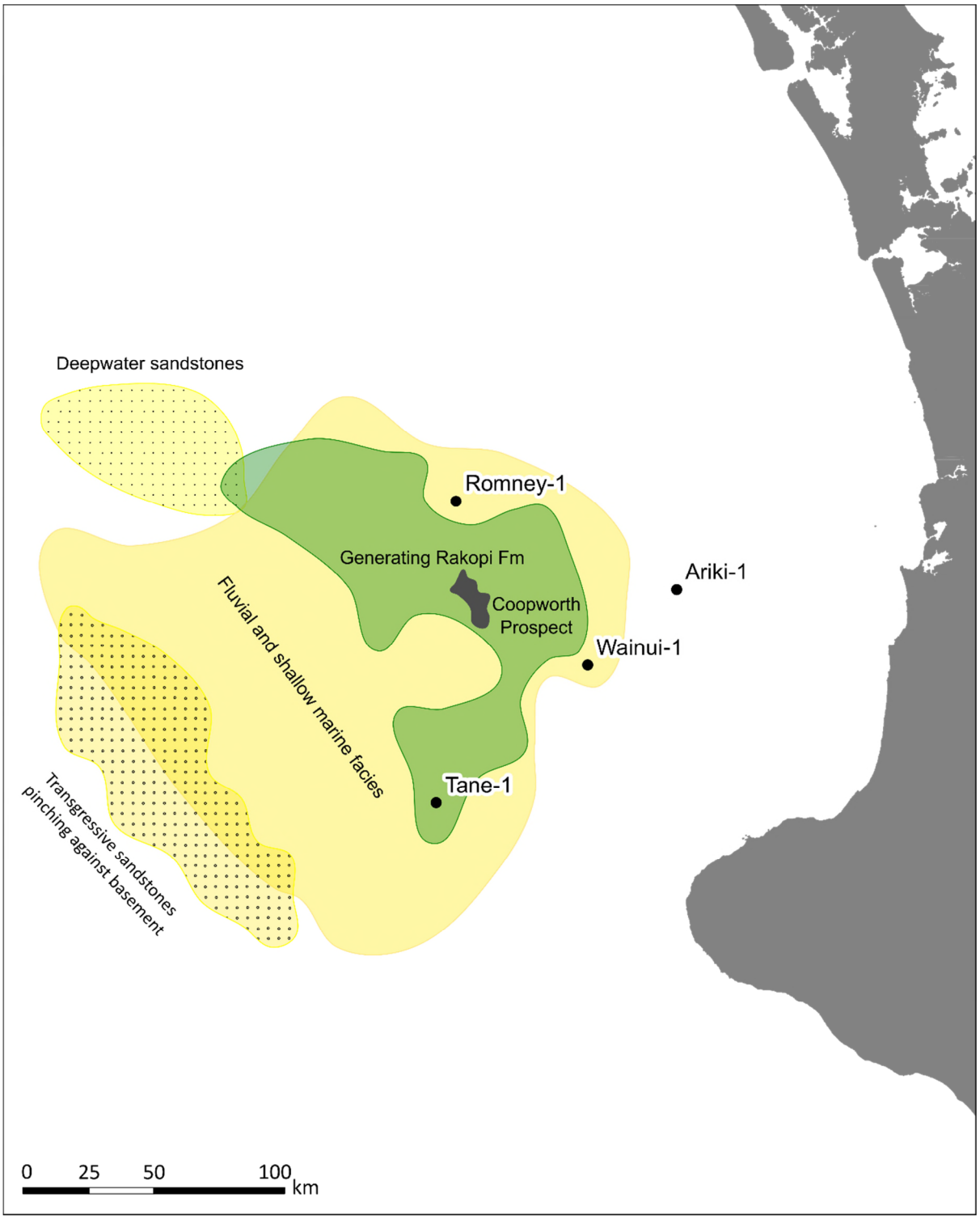

Figure 31 *Map showing extent of top Rakopi Formation that has entered the hydrocarbon generating window, the Coopworth prospect (Uruski and Warburton, 2010) and potential reservoir distributions of fluvial and shallow water facies, transgressive foreshore facies and deepwater sandstone facies.*

Site U1509, drilled during Expedition 371 of the International Ocean Discovery Program (IODP) intersected a Late Cretaceous brown claystone (Subunit IIb) with a 1% total organic content (Sutherland, 2019). Methane to propane were detected from 400 m bsf and the methane to ethane ratio did not drop below 100. This is evidence of thermogenic hydrocarbon generation. U1509 is located 640 km west of New Zealand, on the western edge of New Caledonia Trough at the base of the Lord Howe Rise slope (Sutherland, 2019). The site is outside the study area, but is within Aotea Basin, and it is conceivable that Subunit IIb is present within the outboard marine sequence in the northwest of the study area.

6.3 Reservoir

Aotea Basin contains three potential reservoir facies that are distributed across the study area:

- Late Cretaceous fluvial sandstones
- Late Cretaceous to Paleocene shoreface and shallow marine sandstones
- Late Cretaceous, Paleocene and Neogene deep water fans and channel systems

The Rakpoi Formation consists of fluvial, shoreface and shallow marine sandstones. Romney-1, intersected 236 m of shallow marine facies in the lower part and 421 m of terrestrial facies in the upper part of the Rakopi Formation (Rad, 2015, Schiøler et al., 2014). Petrological analysis conducted on sidewall cores of fluvial sandstones in the Rakopi Formation recorded porosity of up to 21.9 % and permeability up to 64.3 mD (milli Darcy). In Tane-1, the Rakopi Formation is 475 m thick and consists entirely of terrestrial facies (Uruski and Warburton, 2010, SBPT, 1977). In Tane-1, it is calculated to contain approximately 60% sandstone (Uruski and Warburton, 2010). There is no petrophysical analysis for Romney-1, but geophysical wireline logs and cutting descriptions suggest a similar conclusion (Figure 24).

The North Cape Formation is a Late Cretaceous transgressive sequence that is intersected in wells across the study area. In Romney-1, North Cape Formation consists of shelfal facies with a high proportion of friable, well sorted, fine sandstones that have up to 24.4 % porosity and 18.2 mD (Rad, 2015). In Tane-1, North Cape Formation consists of a lower 360 m sequence of terrestrial coal measures and an upper 146 m sequence of transgressive shoreface to shallow marine sandstones (Figure 23). The transgressive sequence has porosities of up to 25% and excellent permeabilities of close to ~1000 mD (SBPT, 1977). This is mapped as U-AOT-1a in the study area. Wainui-1 intersected 113 m of North Cape Formation: a 55 m lower sequence of coastal plain coal measures, and an upper 58 m sequence of shelfal marine facies (SBPT, 1982). The coal measures consisted of 24 m (or 44%) net sandstone and are considered a viable reservoir.

Mapping in this study shows that Late Cretaceous U-AOT-1 and Paleocene U-AOT-2, are transgressive sequences that onlap basement highs under the present-day shelf and Challenger Plateau. It is predicted that high quality transgressive sandstones, as intersected in Tane-1, will be present in these locations (Figures 8 & 31).

Seismic mapping in this study has identified a potential Late Cretaceous to late Paleocene deep-water sandstone sequences: U-AOT-1d, U-AOT-1e and U-AOT-2b (see 3.2.4 U-AOT-1 & 3.2.6 U-AOT-2 & Figures 7 & 31). To appraise these reservoirs, it is recommended that analysis of amplitude with offset is undertaken on existing 2D seismic data, to appraise the fluid and/or gas content of these potentially porous facies. It is also desirable that a tighter grid of 2D or a 3D seismic survey is acquired to better map the architecture of the sequences.

Deepwater channel and turbidite fan systems have been mapped and documented throughout the Neogene sequence by multiple workers (Uruski, 2007, Uruski and Wood, 1991, Grahame, 2015, King and Thrasher, 1996, Strogen et al., 2014, Baur et al., 2014). They have all described these features as mounded with high amplitude reflectors, suggesting that they are sand filled. Uruski and Warburton (2010), suggest that, due to their shallow burial, these Neogene channels and fans are likely to have high porosity and permeability.

6.4 Seal

The Eocene sequence consists of bathyal claystones and siltstones and are considered a good regional seal (Figure 17). In Romney-1, direct formation pressure measurements show that sandstones in the North Cape Formation are up to 280 psi above hydrostatic pressure, e.g. at 3478.63 m total vertical depth a formation pressure of 5232 psi was recorded (Rad, 2015), hydrostatic pressure for this depth is calculated at 4949 psi. This is direct evidence that the Eocene bathyal sequence forms an effective seal.

Oligocene carbonate facies are also highly likely to be regional seals. These marls and limestones have high density and sonic velocity measured in Tane-1, Romney-1 and Waka Nui-1, indicating low porosity (Figures 23, 24 & 26).

Neogene channels and turbidites were deposited at bathyal depths in a claystone dominant sequence (Figures 23, 24 & 26). This claystone is expected to form an effective seal, as it has proven to be one in Taranaki Basin, e.g. Ngatoro Oilfield (King and Thrasher, 1996).

6.5 Trap and Migration

Three trapping styles have been identified across Aotea Basin: 4-way dip structures, transgressive pinch-out forming 3-way dip structure with stratigraphic top-seal, and deep marine sandstone stratigraphic trap.

Figure 8D, shows reflectors of Late Cretaceous to Paleocene age are locally deformed to form 4-way dip structures. These structures formed in the late Paleocene to mid Eocene, based on T-AOT-2 being deformed and T-AOT-3a showing minimal deformation. Each of structure has a set of normal faults at its core, and the faults generally intersect underlying Rakopi Coal Measures, providing vertical migration pathways for hydrocarbons into the structures.

Along the flank of Challenger Plateau, mapping shows a Late Cretaceous transgressive sequence onlapping basement (Figures 8 & 14). It is predicted that these reflectors are the equivalent shoreface facies of the North Cape Formation intersected in Tane-1 and Romney-1, and are hence excellent reservoir targets (Figures 23 & 24). The topography of basement creates 3-way dip closure, and the fine-grained nature of the overlying Paleocene sequence forms a stratigraphic pinch-out top-seal (Figures 17 & 27). Migration of hydrocarbons is via the same shoreface facies acting as lateral carrier beds from the central kitchen area (Figure 31).

Mapping of units U-AOT-1d, U-AOT-1e, and U-AOT-2b has identified a stacked sequence of Late Cretaceous and late Paleocene low-stand regressive units (see 3.2.4 U-AOT-1 & 3.2.6 U-AOT-2 & Figures 7C & 31). This is the same facies as the Late Eocene Tangaroa

Formation intersected in Ariki-1. The mechanism for trapping in these reservoir targets is stratigraphic, both laterally and a top seal.

6.6 Overburden

In the Early to Middle Miocene, wells in Aotea Basin record a rapid increase in sedimentation rate (Figure 25). This influx of sediment is associated with inception of the present-day shelf and it is prograding towards the northwest (King and Thrasher, 1996, Uruski and Warburton, 2010, Uruski and Wood, 1991). This influx of sediment provided the required overburden to bury Rakopi Formation to ~2,700 m below seabed, i.e. the oil window. Modelling by Stagpoole et al. (2007) show that the Rakopi Formation first entered the oil window in the Late Miocene, and it remains in the oil window.

6.7 Summary

Romney-1 demonstrates that Aotea Basin contains all the required elements of a petroleum system. Mapping and well analysis in this study has identified three play types: 4-way dip structures containing Late Cretaceous fluvial and transgressive shoreface sandstones; stratigraphic pinch-out of Late Cretaceous to Paleocene transgressive shoreface sandstones with 3-way dip closure along the flank of Challenger Plateau; and stacked Late Cretaceous to Paleocene deep-water fan sequences. These plays are charged by Teratan siltstone, Rakopi formation and marine equivalents, and sealed by Paleogene claystones and carbonates.

The petroleum system event chart shows that all elements of each play were in place prior to the overburden being emplaced and Rakopi Formation entering the oil window, i.e. the critical moment (Figure 32).

The most prospective play in Aotea Basin is 4-way dip structures containing Late Cretaceous fluvial and transgressive shoreface sandstones that immediately overly mature Rakopi Formation and are sealed by Paleogene claystones and carbonates (Figures 8, 14 & 31). Delineation of leads and prospects is beyond the scope of this study, however, the Coopworth prospect identified by Uruski and Warburton (2010) is considered to meet these criteria (Figure 31).

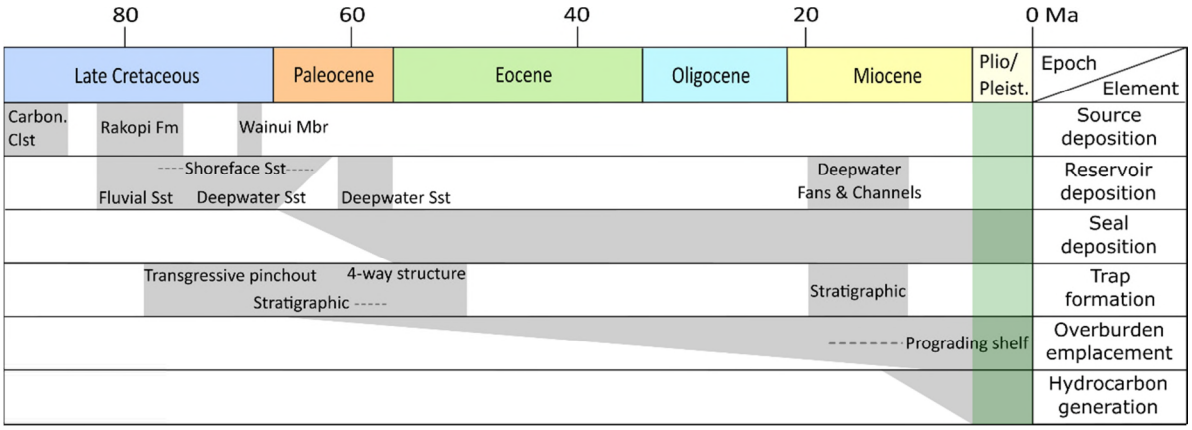

Figure 32 *Events chart for each element of Aotea Basin Petroleum System. The grey rectangles represent the time at which element was deposited or occurred. The green vertical rectangle is the critical moment when all elements need to be in place to preserve hydrocarbons.*

7 References

AITCHISON, J., CLARKE, G., MEFFRE, S. & CLUZEL, D. 1995. Eocene arc-continent collision in New Caledonia and implications for regional southwest Pacific tectonic evolution. *Geology,* 23**,** 161-164.

ALLEN, P. A. & ALLEN, J. R. 2013. *Basin analysis: Principles and application to petroleum play assessment*, John Wiley & Sons.

ARCULUS, R. J., ISHIZUKA, O., BOGUS, K. A., GURNIS, M., HICKEY-VARGAS, R., ALJAHDALI, M. H., BANDINI-MAEDER, A. N., BARTH, A. P., BRANDL, P. A. & DRAB, L. 2015. A record of spontaneous subduction initiation in the Izu–Bonin–Mariana arc. *Nature Geoscience,* 8**,** 728.

ARNOT, M. J. & BLAND, K. J. 2016. Atlas of Petroleum Prospectivity, Northwest Province: ArcGIS geodatabase and technical report. GNS Science data Series 23b. *Institute of Geological and Nuclear Science client reports,* 2016**,** 39.

BACHE, F., MORTIMER, N., SUTHERLAND, R., COLLOT, J., ROUILLARD, P., STAGPOOLE, V. & NICOL, A. 2014. Seismic stratigraphic record of transition from Mesozoic subduction to continental breakup in the Zealandia sector of eastern Gondwana. *Gondwana Research,* 26**,** 1060-1078.

BACHE, F., STAGPOOLE, V. & SUTHERLAND, R. 2012a. Seismic stratigraphy of the Reinga Basin, NW New Zealand: tectonic and petroleum implications. *New Understanding of the Petroleum Systems of Continental Margins of the World***,** 221-22.

BACHE, F., SUTHERLAND, R., STAGPOOLE, V., HERZER, R., COLLOT, J. & ROUILLARD, P. 2012b. Stratigraphy of the southern Norfolk Ridge and the Reinga Basin: A record of initiation of Tonga–Kermadec–Northland subduction in the southwest Pacific. *Earth and Planetary Science Letters,* 321**,** 41-53.

BAUR, J., SUTHERLAND, R. & STERN, T. 2014. Anomalous passive subsidence of deep-water sedimentary basins: a prearc basin example, southern New Caledonia Trough and Taranaki Basin, New Zealand. *Basin Research,* 26**,** 242-268.

CANDE, S. C. & STOCK, J. M. 2004. Pacific—Antarctic—Australia motion and the formation of the Macquarie Plate. *Geophysical Journal International,* 157**,** 399-414.

CATUNEANU, O., ABREU, V., BHATTACHARYA, J., BLUM, M., DALRYMPLE, R., ERIKSSON, P., FIELDING, C. R., FISHER, W., GALLOWAY, W. & GIBLING, M. 2009. Towards the standardization of sequence stratigraphy. *Earth-Science Reviews,* 92**,** 1-33.

CATUNEANU, O., GALLOWAY, W. E., KENDALL, C. G. S. C., MIALL, A. D., POSAMENTIER, H. W., STRASSER, A. & TUCKER, M. E. 2011. Sequence stratigraphy: methodology and nomenclature. *Newsletters on stratigraphy,* 44**,** 173-245.

COLLOT, J., HERZER, R., LAFOY, Y. & GELI, L. 2009. Mesozoic history of the Fairway- Aotea Basin: Implications for the early stages of Gondwana fragmentation. *Geochemistry, Geophysics, Geosystems,* 10.

COOK, R. A., SUTHERLAND, R. & ZHU, H. 1999. *Cretaceous-Cenozoic geology and petroleum systems of the Great South Basin, New Zealand*, Institute of Geological & Nuclear Sciences.

COOPER, R. A., CRAMPTON, J. S., RAINE, J. I., GRADSTEIN, F. M., MORGANS, H. E., SADLER, P. M., STRONG, C. P., WAGHORN, D. & WILSON, G. J. 2001.

Quantitative biostratigraphy of the Taranaki Basin, New Zealand: a deterministic and probabilistic approach. *AAPG bulletin,* 85**,** 1469-1498.
CRAMPTON, J. S., MORTIMER, N., BLAND, K. J., STROGEN, D. P., SAGAR, M., HINES, B. R., KING, P. R. & SEEBECK, H. 2019. Cretaceous termination of subduction at the Zealandia margin of Gondwana: The view from the paleo-trench. *Gondwana Research,* 70**,** 222-242.
CROUGH, S. T. 1983. The correction for sediment loading on the seafloor. *Journal of Geophysical Research: Solid Earth,* 88**,** 6449-6454.
DAVY, B., HOERNLE, K. & WERNER, R. 2008. Hikurangi Plateau: Crustal structure, rifted formation, and Gondwana subduction history. *Geochemistry, Geophysics, Geosystems,* 9.
EXON, N., LAFOY, Y., HILL, P., DICKENS, G. & PECHER, I. 2007. Geology and petroleum potential of the Fairway Basin in the Tasman Sea. *Australian Journal of Earth Sciences,* 54**,** 629-645.
GAINA, C., MÜLLER, D. R., ROYER, J. Y., STOCK, J., HARDEBECK, J. & SYMONDS, P. 1998. The tectonic history of the Tasman Sea: a puzzle with 13 pieces. *Journal of Geophysical Research: Solid Earth,* 103**,** 12413-12433.
GRAHAME, J. Deepwater Taranaki Basin, New Zealand—New Interpretation and Modelling Results for Large Scale Neogene Channel and Fan Systems: Implications for Hydrocarbon Prospectivity. International Conference & Exhibition, 2015.
HAQ, B. U., HARDENBOL, J. & VAIL, P. R. 1987. Chronology of fluctuating sea levels since the Triassic. *Science,* 235**,** 1156-1167.
HAYWARD, B. W. 1984. Foraminiferal Biostratigraphy of Wainui-1 Offshore Well, West Taranaki - PPL 38049. *Ministry of Economic Development New Zealand Unpublished Petroleum Reports,* PR1057**,** 27.
HAYWARD, B. W. 1985. Foraminiferal biostratigraphy and paleobathymetry of Tane-1, Offshore Well, West Taranaki. *Ministry of Economic Development New Zealand Unpublished Petroleum Reports,* PR1131**,** 54.
HAYWARD, B. W. 1986. Foraminiferal biostratigraphy and paleobathymetry of Ariki-1 offshore well, North West Taranaki PPL 38048. *Ministry of Economic Development New Zealand Unpublished Petroleum Reports,* PR1175**,** 41.
HERZER, R. H. 1995. Seismic stratigraphy of a buried volcanic arc, Northland, New Zealand and implications for Neogene subduction. *Marine petroleum geology,* 12**,** 511-531.
HERZER, R. H., CHAPRONIERE, G., EDWARDS, A., HOLLIS, C., PELLETIER, B., RAINE, J., SCOTT, G., STAGPOOLE, V., STRONG, C. & SYMONDS, P. 1997. Seismic stratigraphy and structural history of the Reinga Basin and its margins, southern Norfolk Ridge system. *New Zealand Journal of Geology Geophysics,* 40**,** 425-451.
HIGGS, K., KING, P., RAINE, J., SYKES, R., BROWNE, G., CROUCH, E. & BAUR, J. 2012. Sequence stratigraphy and controls on reservoir sandstone distribution in an Eocene marginal marine-coastal plain fairway, Taranaki Basin, New Zealand. *Marine and petroleum geology,* 32**,** 110-137.
HOPCROFT, B. S. 2009. *Lithology and provenance of late Eocene-Oligocene sediments in eastern Taranaki Basin margin and implications for paleogeography.* The University of Waikato.
ISAAC, M. 1994. *Cretaceous and Cenozoic sedimentary basins of northland, New Zealand*, Institute of Geological & Nuclear Sciences.
ISHIZUKA, O., TANI, K., REAGAN, M. K., KANAYAMA, K., UMINO, S., HARIGANE, Y., SAKAMOTO, I., MIYAJIMA, Y., YUASA, M. & DUNKLEY, D. J. 2011. The

timescales of subduction initiation and subsequent evolution of an oceanic island arc. *Earth Planetary Science Letters,* 306**,** 229-240.
KENNETT, J. P. 1977. Cenozoic evolution of Antarctic glaciation, the circum- Antarctic Ocean, and their impact on global paleoceanography. *Journal of Geophysical Research: Solid Earth,* 82**,** 3843-3860.
KING, P. New Zealand's changing configuration in the last 100 million years: plate tectonics, basin development, and depositional setting. 2000 New Zealand Petroleum Conference Proceedings, 2000a. Crown Minerals, Ministry of Commerce Wellington, New Zealand.
KING, P. & THRASHER, G. 1996. *Cretaceous Cenozoic geology and petroleum systems of the Taranaki Basin, New Zealand*, Institute of Geological & Nuclear Sciences.
KING, P. R. 2000b. Tectonic reconstructions of New Zealand: 40 Ma to the present. *New Zealand Journal of Geology Geophysics,* 43**,** 611-638.
LAIRD, M. 1993. *Cretaceous continental rifts: New Zealand region,* Amsterdam.
LEASK, W. L. 1993. Brunner Coal Measures at Golden Bay, Nelson: An Eocene fluvial-estuarine deposit. *New Zealand journal of geology geophysics,* 36**,** 37-50.
MAGOON, L. B. & DOW, W. G. 1994. *The petroleum system: chapter 1: Part I. Introduction*.
MATTHEWS, K. J., SETON, M. & MÜLLER, R. D. 2012. A global-scale plate reorganization event at 105− 100 Ma. *Earth Planetary Science Letters,* 355**,** 283-298.
MCRAE, S. 1972. Glauconite. *Earth-Science Reviews,* 8**,** 397-440.
MILNE, A. & QUICK, R. 1999. Waka Nui-1 Welll Completion Report. PEP 38602. *Ministry of Economic Development New Zealand Unpublished Petroleum Reports,* PR2436**,** 922.
MITCHELL, J., MACKAY, K., NEIL, H., MACKAY, E., PALLENTIN, A. & NOTMAN, P. 2012. Undersea New Zealand, 1: 5,000,000. *NIWA chart, miscellaneous series*.
MITCHUM JR, R. & VAIL, P. 1977. Seismic stratigraphy and global changes of sea-level, part 7: stratigraphic interpretation of seismic reflection patterns in depositional sequences. Seismic Stratigraphy — Applications to Hydrocarbon Exploration. *AAPG Memoir,* 26**,** 135-144.
MITCHUM JR, R., VAIL, P. & THOMPSON III, S. 1977. Seismic stratigraphy and global changes of sea level: Part 2. The depositional sequence as a basic unit for stratigraphic analysis. Seismic Stratigraphy — Applications to Hydrocarbon Exploration. *AAPG Memoir,* 26**,** 53-62.
MORTIMER, N. 2004. New Zealand's geological foundations. *Gondwana Research,* 7**,** 261-272.
MORTIMER, N., CAMPBELL, H. J., TULLOCH, A. J., KING, P. R., STAGPOOLE, V. M., WOOD, R. A., RATTENBURY, M. S., SUTHERLAND, R., ADAMS, C. J. & COLLOT, J. 2017. Zealandia: Earth's hidden continent. *GSA Today,* 27**,** 27-35.
MORTIMER, N., GANS, P., MEFFRE, S., MARTIN, C., SETON, M., WILLIAMS, S., TURNBULL, R., QUILTY, P., MICKLETHWAITE, S. & TIMM, C. 2018. Regional volcanism of northern Zealandia: post-Gondwana break-up magmatism on an extended, submerged continent. *Geological Society, London, Special Publications,* 463**,** 199-226.
MORTIMER, N., RATTENBURY, M., KING, P., BLAND, K., BARRELL, D., BACHE, F., BEGG, J., CAMPBELL, H., COX, S. & CRAMPTON, J. 2014. High-level stratigraphic scheme for New Zealand rocks. *New Zealand Journal of Geology and Geophysics,* 57**,** 402-419.

MÜLLER, R., GOHL, K., CANDE, S., GONCHAROV, A. & GOLYNSKY, A. 2007. Eocene to Miocene geometry of the West Antarctic rift system. *Australian Journal of Earth Sciences,* 54**,** 1033-1045.

MUTTER, J. C., HEGARTY, K. A., CANDE, S. C. & WEISSEL, J. K. J. T. 1985. Breakup between Australia and Antarctica: a brief review in the light of new data. 114**,** 255-279.

NATHAN, S., ANDERSON, H. J., COOK, R. A., HERZER, R., HOSKINS, R., RAINE, J. & SMALE, D. 1986. *Cretaceous and Cenozoic sedimentary basins of the West Coast region, South Island, New Zealand*, Science Information Publishing Centre, DSIR, for the New Zealand Geological ….

NEAL, J. & ABREU, V. 2009. Sequence stratigraphy hierarchy and the accommodation succession method. *Geology,* 37**,** 779-782.

O'CONNOR, J. M., STEINBERGER, B., REGELOUS, M., KOPPERS, A. A., WIJBRANS, J. R., HAASE, K. M., STOFFERS, P., JOKAT, W. & GARBE- SCHÖNBERG, D. 2013. Constraints on past plate and mantle motion from new ages for the Hawaiian-Emperor Seamount Chain. *Geochemistry, Geophysics, Geosystems,* 14**,** 4564-4584.

ODIN, G. S. & MATTER, A. 1981. De glauconiarum origine. *Sedimentology,* 28**,** 611-641.

RAD, F. 2015. Romney-1 Well Completion Report. *Ministry of Economic Development New Zealand Unpublished Petroleum Reports,* PR4951**,** 980.

RAINE, J. I., BEU, A. G., BOYES, A. F., CAMPBELL, H., COOPER, R. A., CRAMPTON, J. S., CRUNDWELL, M. P., HOLLIS, C. J. & MORGANS, H. 2015. *Revised calibration of the New Zealand Geological Timescale: NTGT2015/1*, GNS Science Lower Hutt.

RAINE, J. I. & SCHIØLER, P. 2012. *Upper Cretaceous Biostratigraphy of Maui-4 and Tane-1 Wells, Taranaki Basin*, GNS Science.

SBPT 1977. Well Resume Tane-1 (Offshore). *Ministry of Economic Development New Zealand Unpublished Petroleum Reports,* PR698**,** 264.

SBPT 1982. Well Resume, Wainui. Taranaki offshore. PPL 38049. *Ministry of Economic Development New Zealand Unpublished Petroleum Reports,* PR869**,** 278.

SBPT 1984. Completion Report. Ariki-1. PPL 38048. *Ministry of Economic Development New Zealand Unpublished Petroleum Reports,* PR1038**,** 179.

SCHIØLER, P., POWELL, S. & REXILIUS, J. 2014. PEP 38451 Biostratigraphy of Romney-1 well (2370 - 4618 m), Deepwater Taranaki, New Zealand. *Ministry of Economic Development New Zealand Unpublished Petroleum Reports,* PR4935.

SKINNER, C. 2008. Assessment of Oil and Gas Reserves Discovered within the Taranaki Basin 1955-2000, and Potential Undiscovered Reserves. *In:* BUSHE, H. (ed.) *PESA Eastern Australasian Basins Symposium III.* Brisbane.

STAGPOOLE, V. 2011. Two-way time–depth relationship for Waka Nui-1 well to aid geological interpretations of the offshore northwestern New Zealand. *New Zealand journal of geology and geophysics,* 54**,** 341-346.

STAGPOOLE, V., FUNNELL, R., SCADDEN, P. & MILNER, M. 2007. Basin Modelling of PEP 38451, Deepwater Taranaki, New Zealand. *Ministry of Economic Development New Zealand Unpublished Petroleum Report,* PR3731**,** 43.

STAGPOOLE, V. & NICOL, A. 2008. Regional structure and kinematic history of a large subduction back thrust: Taranaki Fault, New Zealand. *Journal of Geophysical Research: Solid Earth,* 113.

STERN, T. & HOLT, W. 1994. Platform subsidence behind an active subduction zone. *Nature,* 368**,** 233.

STROGEN, D. P., BLAND, K. J., NICOL, A. & KING, P. R. 2014. Paleogeography of the Taranaki Basin region during the latest Eocene–Early Miocene and implications for

the ‘total drowning’of Zealandia. *New Zealand Journal of Geology and Geophysics,* 57**,** 110-127.

STROGEN, D. P., SEEBECK, H., NICOL, A. & KING, P. R. 2017. Two-phase Cretaceous–Paleocene rifting in the Taranaki Basin region, New Zealand; implications for Gondwana break-up. *Journal of the Geological Society,* 174**,** 929-946.

STRONG, C. P., MILDENHALL, D. C., RAINE, J. I., WILSON, G. J. & EDWARDS, A. R. 1999. Biostratigraphy of Waka Nui-1 Offshore Petroleum Well, Northland Basin, New Zealand. *Ministry of Economic Development New Zealand Unpublished Petroleum Reports,* PR2436**,** 922.

STRONG, C. P. & WILSON, G. J. 2002. Biostratigraphic reassessment (foraminiferal & palynology) of key western platform drillholes, Taranaki Basin. *Institute of Geological and Nuclear Science client reports,* 2002/105**,** 139.

SUTHERLAND, R. 1995. The Australia- Pacific boundary and Cenozoic plate motions in the SW Pacific: Some constraints from Geosat data. *Tectonics,* 14**,** 819-831.

SUTHERLAND, R. 1999. Basement geology and tectonic development of the greater New Zealand region: an interpretation from regional magnetic data. *Tectonophysics,* 308**,** 341-362.

SUTHERLAND, R. 2019. *Expedition 371 summary*.

SUTHERLAND, R., COLLOT, J., BACHE, F., HENRYS, S., BARKER, D., BROWNE, G., LAWRENCE, M., MORGANS, H., HOLLIS, C. & CLOWES, C. 2017. Widespread compression associated with Eocene Tonga-Kermadec subduction initiation. *Geology,* 45**,** 355-358.

SUTHERLAND, R., COLLOT, J., LAFOY, Y., LOGAN, G. A., HACKNEY, R., STAGPOOLE, V., URUSKI, C., HASHIMOTO, T., HIGGINS, K. & HERZER, R. H. 2010. Lithosphere delamination with foundering of lower crust and mantle caused permanent subsidence of New Caledonia Trough and transient uplift of Lord Howe Rise during Eocene and Oligocene initiation of Tonga- Kermadec subduction, western Pacific. *Tectonics,* 29.

SYKES, R. 2007. Review of Potential Source Rocks, PEP38451, Deepwater Taranaki, New Zealand: Correlatives and Analogues. *Ministry of Economic Development New Zealand Unpublished Petroleum Report,* PR3733**,** 60.

SYKES, R. 2008. Assessment of source rock quality in PEP 38618 and 38619, southern offshore Northland Basin. *GNS Science Consultancy Report,* 2008/192**,** 39.

TULLOCH, A., RAMEZANI, J., MORTIMER, N., MORTENSEN, J., VAN DEN BOGAARD, P. & MAAS, R. 2009. Cretaceous felsic volcanism in New Zealand and Lord Howe Rise (Zealandia) as a precursor to final Gondwana break-up. *Geological Society, London, Special Publications,* 321**,** 89-118.

URUSKI, C. 2007. PR3735: Seismic Interpretation Report. Deepwater Taranaki. Ministry of Economic Development New Zealand.

URUSKI, C. & WARBURTON, J. Sequence stratigraphy and facies prediction: PEP 38451, Deepwater Taranaki Basin. Proceedings of the 2010 New Zealand Petroleum Conference, Crown Minerals Unit, Wellington, 2010.

URUSKI, C. & WOOD, R. 1991. A new look at the New Caledonia Basin, an extension of the Taranaki Basin, offshore North Island, New Zealand. *Marine and petroleum geology,* 8**,** 379-391.

URUSKI, C. L. 2008. Deepwater Taranaki, New Zealand: structural development and petroleum potential. *Exploration geophysics,* 39**,** 94-107.

VAIL, P., MITCHUM, R. & THOMPSON III, S. 1977. Relative changes of sea level from coastal onlap. Seismic Stratigraphy–Application to Hydrocarbon Exploration. *AAPG Memoir,* 26**,** 63-81.

VAN MORKHOVEN, F. P., BERGGREN, W. A., EDWARDS, A. S. & OERTLI, H. 1986. *Cenozoic cosmopolitan deep-water benthic foraminifera*, Elf Aquitaine.

VAN WAGONER, J., MITCHUM JR, R., POSAMENTIER, H. & VAIL, P. 1987. Seismic stratigraphy interpretation using sequence stratigraphy: Part 2: Key definitions of sequence stratigraphy. *AAPG Bulletin*.

WOOD, R., LAMARCHE, G., HERZER, R., DELTEIL, J. & DAVY, B. 1996. Paleogene seafloor spreading in the southeast Tasman Sea. *Tectonics,* 15**,** 966-975.

8 Appendix 1 – New Zealand Geologic Timescale

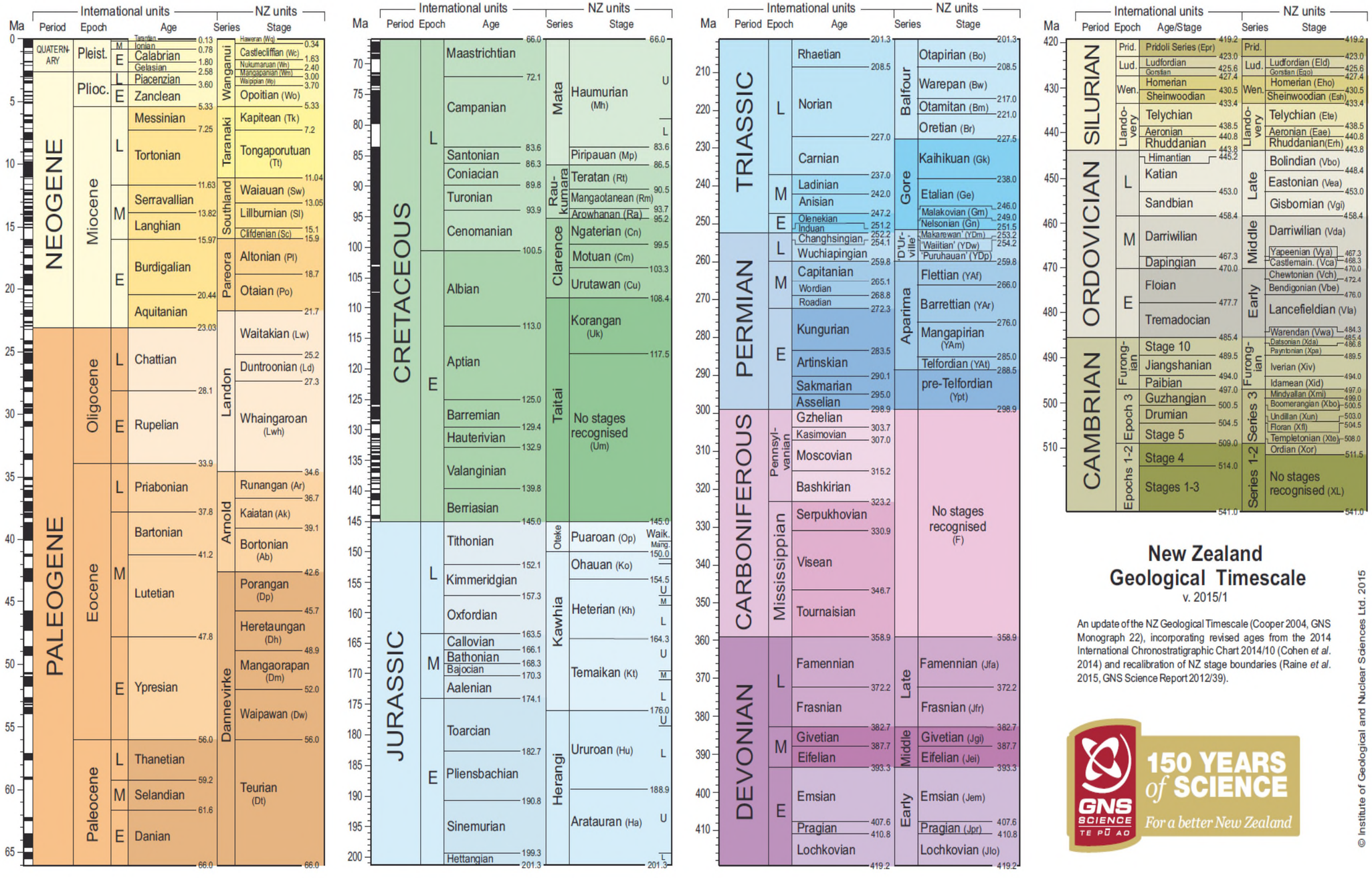

New Zealand Geological Timescale

v. 2015/1

An update of the NZ Geological Timescale (Cooper 2004, GNS Monograph 22), incorporating revised ages from the 2014 International Chronostratigraphic Chart 2014/10 (Cohen *et al.* 2014) and recalibration of NZ stage boundaries (Raine *et al.* 2015, GNS Science Report 2012/39).

150 YEARS of SCIENCE

For a better New Zealand